Examination of Diverse Physiological Functions of Mammalian Heme Oxygenases by Gene Targeting

by

Kenneth D. Poss

B.A. Biology
Carleton College, 1992

SUBMITTED TO THE DEPARTMENT OF BIOLOGY IN PARTIAL FULFILLMENT OF THE REQUIREMENTS FOR THE DEGREE OF

DOCTOR OF PHILOSOPHY IN BIOLOGY
AT THE
MASSACHUSETTS INSTITUTE OF TECHNOLOGY

FEBRUARY 1998

Signature of Author: _____
Department of Biology

Certified by: _____
Susumu Tonegawa
Professor of Biology
Thesis Supervisor

Accepted by: _____
Frank Solomon
Chairman
Biology Graduate Committee

Examination of Diverse Physiological Functions of Mammalian Heme Oxygenases by Gene Targeting

by

Kenneth D. Poss

Submitted to the Department of Biology
on October 3, 1997, in Partial Fulfillment of the
Requirements for the Degree of Doctor of Philosophy in
Biology

ABSTRACT

Several interesting physiological functions have been proposed for mammalian heme oxygenases (Hmox), which catabolize heme to yield biliverdin, carbon monoxide (CO), and free iron. CO, synthesized by the neuronal heme oxygenase-2 (Hmox2) isoform, is suspected to be a neuromodulator, while the stress-induced heme oxygenase-1 (Hmox1) isoform is thought to provide antioxidant protection during oxidative stress. It is also believed that both isoforms have important roles in iron metabolism. To define important biological duties of Hmox, gene targeting was employed to generate mice devoid of either Hmox1 or Hmox2, and various mutant physiological systems were assessed.

Results show that Hmox2 is not required for hippocampal long-term potentiation, and that CO is not likely a participant in this cellular model for memory formation. However, mice lacking Hmox2 have defects in an intestinal cGMP-synthesizing pathway, as well as in illeal relaxation. Furthermore, male *Hmox2* homozygous mutant mice have dysfunctional sexual behavior and ejaculatory physiology. Therefore, Hmox2 has important functions in these peripheral systems, possibly by generation of CO.

Results also indicate that the Hmox1 isoform is required for normal development, as approximately 80% of Hmox1-deficient mice expected from natural matings die during midgestation, likely due to placental defects. Surviving *Hmox1* homozygous mutant mice develop an iron metabolic disease, characterized by low levels of serum iron, causing microcytic anemia, with high levels of hepatic and renal non-heme iron, leading to oxidative stress and chronic inflammation. These findings suggest that adult iron metabolism in mammals requires heme catabolism by Hmox1 to release and recycle cellular iron into blood.

Finally, stress resistance in cells lacking Hmox1 was analyzed. Fibroblasts devoid of Hmox1 are hypersensitive to free radical generation and cytotoxicity when exposed to certain oxidants. Moreover, young adult Hmox1-deficient mice are vulnerable to hepatic damage and mortality in a murine model of sepsis. Therefore, Hmox1 appears to be important as an adaptive mechanism which protects against cellular damage caused by stress or disease. This finding has implications for the treatment of certain human conditions.

Thesis Supervisor: Susumu Tonegawa, Professor of Biology

ACKNOWLEDGMENTS AND ATTRIBUTIONS

I am grateful to the many collaborators at other universities with whom I have interacted over these four years in the Tonegawa laboratory. It was initially a frustrating realization to learn that in studying mammalian physiology, one must consult and rely on those who have expertise and experience. However, these relationships have proved educational and fruitful. Scientists as collaborators and colleagues that contributed in large ways to my thesis work include Tom O'Dell, to whose laboratory I attribute the electrophysiological work in Chapter 2, Solomon Snyder and Randa Zakhary, to whom I attribute the intellectual and technical analyses in Chapter 5, and Bud Burnett and Randy Nelson, to whose laboratories I attribute the majority of the technical work described in Chapter 6. Indeed, my technical contributions to Chapters 5 and 6 were only minor. I also thank Henk Vreman, who allowed my visit to his laboratory to learn some CO measurement techniques. Those were a hectic and emotional two weeks spent at Stanford, and I regret leaving those interesting results unfinished as I graduate. I have had a productive collaborative relationship with Phyllis Dennery, to whom I wish the best of luck in studying heme oxygenase. I also am grateful for my benefit from collaborations with Kazu Ishikawa and Jake Lusis.

I thank those who have assisted me in learning techniques and ideology along the way. This list begins with Alex Ebralidze, who influenced me as a gifted teacher and scientist. Ted Dawson was very helpful during my month at Johns Hopkins. The advice of Bill Dove had a significant impact on my turn in interest toward mammalian genetics. Mark Fleming helped to walk me through yet another new field, namely iron metabolism. I learned a great deal about histopathology from discussions with Kim Mercer, Denise Crowley, and Rod Bronson. I thank my thesis committee including Monty Krieger, who pointed out my weakness in knowledge of physiology and helped me enjoy its study, and Rudy Jaenisch, for their efforts in steering me toward interesting problems and away from dead ends. I am also grateful to Nancy Andrews, David Housman, and Richard Hynes for their generous efforts in critique of my thesis work as members of my thesis defense committee.

I must acknowledge Tonegawa laboratory members for their help in my completion of this thesis research. I have benefitted greatly from relationships with members of the laboratory over the years. Those who have assisted me through discussion or technical advice include other students in the lab such as Tom McHugh, David Gerber, Joe Delaney, and Heather Hinds, as well as post-doctoral fellows such as Maz Hasan, Matt Anderson, Atsu Aiba, Suzanna Marusic-Galesic, and Juan Lafaille. I also thank those

graduate students in my entering class, who have been good friends with similar objectives, including Tina Yoon, Andrew Diener, Lawren Wu, and Letty Vega. I especially thank my advisor Susumu Tonegawa for several aspects of my training. The independence I had was tremendous. Because of this, I learned to self-teach, and how to be responsible in all aspects of science. I am also thankful for his generosity in allowing excursions to various laboratories and conferences in order to learn techniques, assimilate new information, or attempt to generate data.

Lastly, I acknowledge those who helped me get through to this stage. John Tymoczko at Carleton gave me my first opportunity to do research, and was a fantastic mentor at a top teaching school. My family, especially my parents, have always shown wonderful support and enthusiasm for my successes, and have shared the distress with me during failures. My marriage has brought me the gift of my wife's parents and family, so that I feel doubly buttressed. Alexis, my wife, receives my final note of gratitude. Her love and dedication, and her enthusiastic support for my career aspirations in parallel with her own, guide me toward lofty goals, and yet remind me of what truly belies my happiness.

TABLE OF CONTENTS PAGE

Chapter 1

Introduction

I began my thesis work with the objective of deepening the understanding of molecular mechanisms of memory formation by defining the putative role of carbon monoxide synthesized by the heme-degrading enzyme heme oxygenase. Later, my focus shifted to the study of how mammalian cells might utilize heme oxygenase in protection against damage caused by disease. Nevertheless, since heme oxygenase was discovered in attempts to unravel biochemical pathways of heme catabolism, the introduction to this thesis begins with a brief description of mammalian iron and heme metabolism, and how heme oxygenase is thought to participate. In part II, I describe the evolution of the idea that the carbon monoxide byproduct of heme oxygenase functions as a physiological messenger, and list evidence supporting its validity. In part III, experimental findings that suggest a protective role for heme oxygenase during cellular stress are outlined. The final part of this introduction explains the rationale for utilizing gene targeting techniques to approach my specific aims.

I. Iron Metabolism, Heme, and Heme Oxygenase

The discovery of heme oxygenase, an enzymatic system that degrades heme and releases as products the bile pigment biliverdin, the gas carbon monoxide, and unbound ferrous iron, was born from attempts to perceive how humans metabolize iron. This was and still is an important issue, since throughout the world, many millions are stricken with disorders of iron metabolism. The majority of these cases stem from the inability to retrieve adequate amounts of iron from available resources, causing an often dehabilitating anemia. In addition, the anemia that often accompanies and complicates chronic inflammatory diseases is partially due to reductions in accessible iron (1). Indeed, iron is an essential element to all life forms, contributing not only to hemoglobin synthesis and erythropoiesis, but also to processes such as detoxification and energy production, as a necessary cofactor or catalyst for hundreds of enzymatic reactions. A paradoxical corollary is that this crucial element is potently toxic when present in excess amounts. Iron is an oxidant that mediates production of deleterious oxygen free radicals by reaction with other physiological oxidants (2). Those who receive frequent blood

transfusions often experience iron overloading, as do those who inherit hemochromatosis, a disease of multiorgan pathology resulting from an unrelenting absorption and storage of iron that saturates the body. Hemochromatosis is a recessive disorder extremely common in the Caucasian population, affecting approximately 1 in 200 people (3). Furthermore, Friedrich's Ataxia, which affects approximately 1 in 50,000 of European descent making it the most commonly inherited ataxia, was recently proposed to result from iron loading within mitochondria (4). Despite the prevalence and disturbing consequences of these and other iron metabolism disorders, we know surprisingly little about how iron homeostasis occurs at the molecular and cellular levels, or at the level of the whole organism.

Certain molecular players in iron metabolism have been identified. Most researchers believe that extracellular iron is rarely unbound physiologically, but is carried between sites of absorption, storage, and utilization by transferrin, which is received and taken up by cells presenting transferrin receptors. Inside cells, iron is immediately utilized for processes such as heme synthesis, or it is shuttled to ferritin, which is a multi-subunit protein capable of storing 4500 atoms of iron (5). The mechanisms by which iron is trafficked after cellular uptake are not well-understood. An iron transport system to assist inter- or intracellular manipulation of iron has long remained elusive to researchers, although recently, two groups provided strong evidence that the product of the *Nramp2* gene can transfer iron and other metals through cellular membranes (6, 7).

Logically, since reductions or increases in cellular iron levels can have such extreme pathological effects, mammalian iron metabolism must normally be a tightly regulated process. An elegant regulatory mechanism that helps to maintain appropriate levels of cellular iron involves the iron-sensing iron regulatory proteins. Specifically, these proteins bind to iron-regulatory elements contained within the mRNAs of gene products that contribute to cellular iron metabolism (8). For instance, when cellular iron is low, transferrin receptor expression is increased to allow uptake of iron, while further ferritin expression is halted to dissuade storage (9, 10).

The amounts of iron taken up by cells, relegated for immediate utilization, or stored within ferritin are also affected by the total levels of iron within the organism. This is determined in part by the amount of iron in the available diet. Dietary iron is absorbed through the intestine and into the blood as iron salts by some sort of transport system, likely involving *Nramp2* (6, 7), or it can enter in the hydrophobic form of heme. Humans normally absorb about 1 mg of iron daily, during which time an approximately equal amount is eliminated in sweat, through bleeding such as menstruation in females, and in urine and feces (5). There appear to be regulatory mechanisms which assess the iron

status of an organism and regulate absorption and distribution of iron accordingly. For instance, intestinal absorption mechanisms are facilitated in iron-deplete mammals, and they are downregulated in overloaded animals. In addition, iron stored in tissues such as muscle and liver can be recruited when bone marrow levels are compromised (11-13). However, little is known how this homeostatic modulation of iron absorption and utilization is achieved.

Remarkably, iron absorbed through the intestine contributes a paltry 1-3% to total body daily needs. In fact, the majority of accessible iron is reutilized, or recycled, from existing body stores of approximately 4 g, of which 0.2-0.3% is bound to transferrin, 20-25% is stored within ferritin, and 70-75% is contained as heme primarily within hemoglobin or myoglobin (14). From these numbers, it is clear that metabolism of heme has a significant effect on the iron status of mammals, and it is logical that the body must intertwine mechanisms that maintain levels of nonheme iron with those that regulate heme synthesis and degradation.

The term "heme" refers to a complex of four nitrogen atoms of a cyclic tetrapyrrole, or porphyrin, bound to a single ferrous ion. Heme is also known as iron protoporphyrin, as several other metals may occupy the center of a porphyrin ring. As perhaps the most biologically active form of iron, heme acts as a cofactor in a large number of enzymes, often for accepting electrons, such as in oxidative phosphorylation. or for binding oxygen, as done by hemoglobin. There are eight enzymes involved in the synthesis of heme, and they are located cytosolically or on the mitochondrial membrane (15). All of these enzymes have been cloned, and the pathway by which heme is constructed is illustrated in Fig. 1. The enzyme 5-aminolevulinic acid synthase (ALAS) catalyzes the initial condensation of the eight molecules of succinyl CoA and eight molecules of glycine necessary to form one molecule of heme. The final step in this pathway is catalyzed by ferrochetalase, which inserts one ferrous ion into the pocket of the porphyrin ring. Disturbances in this pathway have profound effects, as mutations in genes encoding heme biosynthetic enzymes lead to the accumulation of porphyrin products characteristic of diseases known as porphyrias. Some clinical symptoms in porphyric patients are high levels of urine porphyrins, photosensitivity, siderosis, abdominal pain, as well as various neuropathies (16).

Regulation of heme biosynthesis is mainly targeted at ALAS, which catalyzes its rate-limiting step. There is evidence that the end-product heme can inhibit ALAS activity by mechanisms such as transcriptional silencing and even direct inhibition of enzymatic activity (15). In addition, one *ALAS* gene contains an iron regulatory element positioned

to mediate reductions in translation of ALAS when iron availability is low, indicating a tight synergism between iron levels and heme levels (17).

Although the study of heme synthesis contributes to our perception of how mammals regulate iron levels, information concerning the catabolism of heme is especially fruitful, since iron released from cellular heme is eventually recycled into the blood. In 1934, the ubiquitous bile pigments biliverdin and bilirubin were shown to be degradatory products of heme (18). Eighteen years later, Sjostrand demonstrated that carbon monoxide (CO) is also derived from heme (19). This metabolic pathway was hinted at by the measurement of end products of radiolabeled heme or erythrocytes administered to live animals. In 1968, the enzymatic activity responsible for the conversion of heme to biliverdin, CO, and free iron was isolated by Tenhunen and colleagues (20). They showed that this activity was largely microsomal, required oxygen and NADPH in addition to the heme substrate, and was inhibited by CO. The partially purified activity, found in all major organs examined, was termed "microsomal heme oxygenase" (Hmox). Further purification of Hmox activity from swine splenic microsomes and from rat hepatic microsomes led to discoveries of a 32 kD protein that catalyzes heme degradation (21, 22). The latter study was aided by the fact that hepatic Hmox activity was strongly induced by injection of animals with cobalt chloride. Because it was later shown that Hmox activity observed in testes and brain is not inducible, it was hypothesized that there may be at least two distinct sources of Hmox activity. This was subsequently confirmed as a 36 kD Hmox isoform refractory to metals was purified from rat testes microsomal fractions (23, 24). Molecular cloning revealed that separate genes encode the two isoforms; the inducible isoform was termed Hmox1, and the non-inducible isoform named Hmox2 (25, 26). Hmox1 and Hmox2 both have a C-terminal membrane spanning domain and are thought to exist primarily on the endoplasmic reticulum (27).

The multistep biochemistry of the Hmox reaction is indicated in Fig. 2. Hmox first binds heme and accepts an electron from the NADPH-cytochrome c (P-450) reductase, after which a molecule of oxygen binds to the heme group. This α-*meso*-hydroxyheme intermediate then undergoes oxygen-dependent elimination of the hydroxylated α-*meso*-carbon as CO, while verdoheme is concomitantly formed. A final electron donation converts this complex to ferrous iron and biliverdin (29, 30). In effect, heme acts as both a substrate and a prosthetic group for Hmox. The two different Hmox isoforms both utilize this mechanism, despite having a relatively low homology of 40-45% at the amino acid level (31). Mutagenesis studies have indicated that a conserved histidine site corresponding to Hmox1 residue number 25 and Hmox2 residue 45 is responsible for

enzymatic heme-binding, while a highly conserved 24-amino acid region termed the Hmox signature region appears to contribute to enzymatic stability (32, 33).

An obvious dissimilarity between Hmox1 and Hmox2 is their representation in mammalian tissues. Hmox1 is highly represented in the spleen and to a lesser extent in the liver, but its activity is negligible in other major organs under normal conditions. In contrast, Hmox2 is expressed in most major organs, with greatest representation in the brain and testes (34). At the cellular level, Hmox1 is the predominant isoform in macrophages, while Hmox2 nearly exclusively represents neurons. As alluded to above, the regulation of expression of each Hmox isoform is even more disparate. Hmox1 is a highly inducible protein and is also referred to as the 32 kD heat shock protein or Hsp32. In fact, upregulation of Hmox1, observed in vivo and in vitro, is considered to be the strongest and most consistent cellular response to stress known. For instance, Hmox1 expression is induced not only by metals such as cobalt and cadmium (35, 36), but by other chemicals such as the Hmox substrate hemin, oxidized lipoproteins, inflammatory cytokines such as TNFα and IL-1, as well as hydrogen peroxide (H_2O_2) and nitric oxide (NO; ref. 37-41). Several experimental conditions also incite Hmox1 expression, including hyperthermia, ultraviolet light, visible light, hypoxia, and hyperoxia (40, 42-45) Furthermore, Hmox1 is upregulated during trauma and stress due to disease, such as during hemorrhage, endotoxemia, or ischemia in rodents, and during Alzheimer pathology in humans (46-49). This cellular response of Hmox1 induction has been observed in all cell types tested, and occurs at the transcriptional level, as the *Hmox1* gene contains a concentrated sequence of stress-inducible promoter regions. To date, activator protein-1 sites, CCAAT/enhancer binding protein sites, phorbol ester response elements, heme response elements, and antioxidant response elements have been identified in the region 5' of *Hmox1* coding sequence (50). Hmox2, in contrast, is refractory to upregulation by stress, although glucocorticoids do transcriptionally induce Hmox2 expression (51). In addition, no traditional second messenger systems appear to modulate either Hmox1 or Hmox2 activity post-translationally.

Those initially studying Hmox proposed that it was the primary mammalian catalyst of heme degradation. Therefore, it would concurrently be responsible for mobilizing the majority of iron reutilized in mammals. However, examination of endogenous heme degradation by Bizelle and Guzelian indicated that less than 50% of hepatic heme yields byproducts of Hmox activity (52). Experiments by others have also pointed out that heme is likely metabolized through other enzymatic pathways in addition to Hmox (53, 54). Numerous activities that can degrade heme and yield products other than CO or biliverdin have since been discovered. These include microsomal NADPH-dependent

cytochrome P-450 reductase, cytosolic xanthine oxidase, and a mitochondrial heme-degrading activity not fully characterized (55). Indeed, prior to the initiation of my thesis work, it was unclear which mechanisms of heme degradation were prominent in mammals, and whether these pathways shuttled heme iron to different inter- or intracellular destinations. Therefore, an important issue remained to be conclusively addressed; namely, how, and to what extent is the crucial reutilization component of mammalian iron homeostasis dependent on the activity of heme oxygenase isoforms.

II. The Hypothesis That Carbon Monoxide Is A Physiological Signaling Molecule

Researchers have not only questioned the extent to which Hmox is responsible for the reutilization component of iron homeostasis, but have wondered whether Hmox isoforms have physiological roles independent of heme and iron metabolism "housekeeping." For example, cerebral and peripheral neurons express high levels of Hmox2 but do not have hemolytic capabilities, so could Hmox2 activity somehow affect neuron-specific functions? Interestingly, measurements of mammalian CO production have indicated that Hmox is likely the major generator of CO in vivo, and in 1991, Marks and colleagues suggested that this CO product could potentially support biological activities (56).

The notion that CO might be a nontraditional gaseous messenger is derived by analogy with NO, produced by nitric oxide synthase (Nos) in the conversion of arginine to citrulline. It has been recognized for 10 years that NO participates in important biological processes (57). There are three Nos isoforms that generate NO, and they are encoded by separate genes (58). One isoform is inducible Nos, which is transcriptionally activated by inflammatory cytokines in phagocytic cells. NO along with H_2O_2 and superoxide are generated during phagocytic respiratory bursts, which help destroy captured bacterial pathogens (59). A second isoform is endothelial Nos, which is non-inducible but requires Ca^{2+} for activity, and is found primarily in vascular endothelial cells. NO (once termed EDRF for endothelium-derived relaxing factor) stimulates soluble guanylyl cyclase (sGC) in smooth muscle, enhancing Ca^{2+} influx and causing vasorelaxation (57, 60, 61). A third type of Nos is neuronal Nos, which is another Ca^{2+}-dependent, non-inducible isoform expressed mainly in selected neurons. Evidence was recently obtained supporting roles for neuronally-derived NO in the modulation of synaptic activity, such as that which constitutes long-term depression, a cellular model for cerebellar-based memory formation, as well as that which mediates peripheral systems such as penile erection and intestinal relaxation (62-64). That a simple, gaseous, and even toxic molecule such as NO could act as a messenger molecule has introduced a

new perception of signal transduction, since the membrane-permeable nature of NO allows it to affect signal transduction in the cells which produce it, as well as in adjacent cells. In total, thousands of studies published in the last 10 years have revealed new information about numerous physiological systems and the participation of NO.

Several similarities exist between NO and CO. First and foremost, CO is a simple, membrane-permeable gas structurally akin to NO and also notoriously toxic. Second, like NO, CO is generated in neurons, in this case by the Hmox2 isoform of Hmox. Third, CO stimulates sGC, the second messenger system through which NO predominantly acts, albeit with several-fold lower efficacy than NO in vitro (65, 66). With these similarities noted, it became important to determine whether the study of Hmox-generated CO may also lend insights into biological systems.

Therefore, pharmacology using an arsenal of direct carbon monoxide application to supplement experiments with heme oxygenase inhibitors was utilized in attempts to implicate roles for Hmox and CO. Verma et al. noted in 1992 that *Hmox2* mRNA expression shows striking cerebral colocalization with *sGC* mRNA. They also found that inhibition of Hmox in cultured olfactory neurons reduces odorant-stimulated cGMP generation, while CO application has the opposite effect (67). Results analogous to these followed, reported after the initiation of this thesis work, indicating that CO may affect the activity of several physiological systems in addition to olfaction. For instance, researchers showed that CO might have a role in controlling activity of cerebellar Purkinje cells, by mediating long-term depression or by modulating membrane potential through regulation of the Na^+/K^+ ATPase (68, 69). Furthermore, others have found supportive evidence for Hmox2 and CO in mediating carotid body chemoreception, intestinal smooth muscle relaxation, anal sphincter relaxation, and regulation of vascular tension (70-73). That such a variety of systems might utilize CO hinted that this gas may even approach the versatility of NO.

An especially interesting system thought to involve NO and/or CO is that of long-term potentiation (LTP) in the hippocampus, which is the best-recognized cellular model for certain types of hippocampal-dependent memory formation. LTP is a phenomenon whereby synaptic transmission between the CA1 and CA3 hippocampal neurons is upregulated and adjusted to maintain that high level of activity. It can be induced in vitro or vivo by a strong stimulus called a tetanus applied to the CA3 cells (74). This long-term change in synaptic activity is postulated to be a mechanism whereby neurons can form or store memories. As diagrammed in Fig. 3 and explained in greater detail in Chapter 2 of this thesis paper, diffusible messengers synthesized postsynaptically may be necessary in the molecular scheme of LTP for enhancing neurotransmitter release in a

potentiated synapse. Because CO and NO are gases synthesized in CA1 neurons, and since presynaptic cGMP levels are thought to modulate transmitter release and LTP (75), both Hmox2 and nNos have been studied intensely as possible generators of the hypothesized "retrograde messenger" required for LTP (Fig. 3). Indeed, several groups have found evidence that Nos activity is required for LTP, while others using either Hmox inhibitors or CO application have implicated CO generation in LTP (76-79).

Notwithstanding, studies investigating roles of Hmox and CO have also been interpreted cautiously, since pharmacological inhibitors utilized therein have demonstrated conspicuous non-specificity. Metalloporphyrins containing non-iron metals such as zinc, tin, or manganese have been used to competively inhibit Hmox from binding and catabolizing heme, but also have the potential to block any heme-containing protein. Two very relevant heme-containing enzymes shown to be inhibited by metalloporphyrins are sGC and Nos, albeit less effectively than Hmox in vitro (80, 81). Clearly, it is difficult to attribute function to Hmox-generated CO if the Hmox inhibitor has some effects on putative downstream or parallel pathway enzymes. Therefore, the obligatory experiment at this juncture was to confirm the relevance of the encouraging pharmacological data which supported the roles of CO in biological phenomena such as hippocampal LTP, using approaches that did not involve such questionable reagents.

III. Possible Functions Of Heme Oxygenase In Stressed Cells

Another characteristic of Hmox enzymes that has interested researchers is the transcriptional regulation of Hmox1. The numerous conditions of stress described in Part I that induce Hmox1 expression are similar in that they contribute to increasing the amount of cellular oxygen free radicals, thereby resulting in a prooxidant state, or "oxidative stress". In addition to environmental sources of oxidative stress, oxidants such as superoxide, H_2O_2, and NO originate endogenously by several mechanisms (82). These oxidants decompose to form hydroxyl radicals (OH·), which leave a trail of oxidative modifications in cellular lipids, proteins, and nucleic acids, due to their high reactivity.

To counter prooxidants before cell viability is endangered, there exists an extensive repetoire of specific and general antioxidant defense systems. For example, superoxide dismutase enzymes and catalases specifically deplete superoxide and H_2O_2, respectively, reducing the cellular potential for ·OH formation. General antioxidants such as ascorbate, α-tocopherol, and carotenoids are obtained from the diet and stabilize reactive radical electrons. Furthermore, systems are present to destroy oxidized lipids and proteins, and to repair oxidized DNA (82). Also thought to protect cells from oxidative damage are the

stress-induced heat shock proteins (Hsp), many of which apparently function to prevent accumulation of damaged or misfolded proteins (83). When any of these antioxidant functions are disabled, ·OH and associated macromolecular modifications can rapidly accrue, destroying vulnerable cell populations. The inability to control massive cellular production of oxygen free radicals is thought to underly the etiologies of numerous human conditions, including ischemia, atherosclerosis, rheumatoid arthritis, several neuromuscular and neurodegenerative disorders, and the normal processes of aging (84, 85). Therefore, progress in understanding how cells defend themselves during stress brings immense clinical implications.

By analogy to the induction of Hsp during stress, many have proposed that induction of Hmox1 may be an adaptive mechanism that protects stressed cells. Different researchers have suggested several mechanisms whereby upregulation of Hmox1 could prevent potential oxidative damage. First, Hmox depletes heme, a membrane-permeable form of iron that could potentially act as a catalyst in ·OH production (84, 86, 87). Second, production of biliverdin by Hmox1 may be beneficial since it is immediately converted in vivo to the free radical scavenger, bilirubin (88). Third, some think that Hmox activity increases intracellular iron during stress, thereby leading to protective upregulation of the iron-binding protein ferritin (89, 90). Fourth, some have suggested that the regulation of vascular tension by Hmox1-generated CO might reduce hypoxic stress (73, 91).

Consistent with the hypothesis that Hmox1 confers a protective role is the fact that resistance of cells to oxidative challenges often correlates with the level of Hmox1 expression (45, 86, 90). In fact, pretreatment in vitro or in vivo with hemoglobin both upregulates Hmox1 and affords subsequent protection in certain in vivo and in vitro experimental stress paradigms, such as endotoxemia, rhabdomyolysis, and oxidized LDL-mediated toxicity in cultured vascular cells (92-94). Conversely, the addition of Hmox inhibitors can increase sensitivity to stress paradigms (93, 94). However, problems in interpreting these experiments are that this stress protection cannot be solely attributed to Hmox1 upregulation, and that many of the metalloporphryins used to block Hmox can also generate free radicals (95). In circumventing these issues, recent studies have indicated that cells transfected with *Hmox1* cDNA show slight resistance to certain in vitro stress paradigms (45, 86). However, some groups have insisted that upregulation of Hmox1 does not affect stress resistance (96), while still others have suggested that Hmox1 activity may facilitate increases in intracellular iron (itself, an oxidant, as mentioned above) that ultimately increase oxidative stress (97). Therefore, which role, if

any, Hmox1 has during stress initiated in many disease states remained to be elucidated at the initiation of my thesis research.

IV. Specific Objectives Of This Thesis Work

As described in previous sections of this introduction, my feeling was that the study of Hmox could provide insight into several interesting and important aspects of mammalian physiology and pathology. My experimental strategy involved supplementing a genetic approach to those approaches previously taken to implicate functions for Hmox. In 1993 and 1994, I utilized conventional gene targeting techniques to generate mice containing homozygous null mutations in *Hmox1* and *Hmox2* genes.

Historically, the advent of gene targeting was a key technological breakthrough for the study of mammalian biology. A strategy using homologous recombination in totipotent embryonic stem cells was developed in 1988, so that mice containing experimentally-designed mutations targeted at mammalian genes of interest could be created (98, 99). This reverse genetics approach has since been a boon to several fields of mammalian biology. Perhaps foremost, this approach allows the creation of mouse models of inherited human diseases. Mouse strains have been constructed containing disruptions in murine homologues of human disease genes such as those mutated in cystic fibrosis, familial hypercholesterolemia, certain cancers, fragile X syndrome, and familial hypertrophic cardiomyopathy, among others (100-105). Gene targeting has been crucial for basic research fields as well. The availability of null mutants allows researchers to ascribe temporal and regional requirements for gene products implicated in contributions to development (106-109). In addition, the field of immunology has benefitted from the availability of strains with mutations causing deficiencies in certain immune cell lineages (110, 111). Furthermore, taking advantage of gene targeting in a then unique manner, Silva and colleagues indicated in 1992 how engineered mouse mutants could be used as models toward establishing correlative relationships between cellular electrophysiological phenomena and estabished animal behaviorial paradigms. In that study, mice lacking the alpha subtype of calcium/calmodulin-dependent protein kinase II demonstrated deficits in both hippocampal long-term potentiation and performance in a spatial memory task (112, 113). Numerous similar examinations of the contributions of other gene products to physiology and behavior followed this study (114-118). More recently, gene targeting protocols have been refined such that tissue-specific and temporally-induced mutations may be implemented (119-121).

Armed with mice lacking either of the Hmox isoforms, I first hoped to ascertain whether selected murine physiological phenomena require Hmox2 as a generator of CO.

Initially, as I describe in Chapter 2, I utilized the Hmox2-deficient animals to examine the idea that Hmox-generated CO acts as the postulated retrograde messenger in hippocampal long-term potentiation. This approach circumvents historical difficulties with pharmacological reagents used to block Hmox activity, and it allows correlations between physiological and behavioral phenotypes in mutant animals. Mice lacking functional Hmox2 were also useful for studying whether peripheral neurophysiological systems require the CO byproduct. Chapter 5 and 6 describe the investigation of intestinal relaxation and male ejaculatory function, respectively, in these mutant animals.

Another objective of mine was to examine the extent to which adult iron metabolism requires the Hmox isoforms. Chapter 3 describes the generation of Hmox1-deficient mice, the developmental requirements for Hmox1, as well the iron metabolic consequences in adult mice that do not express functional Hmox1.

Finally, I wished to examine whether cells utilize Hmox1 to protect against oxidative damage induced by stress, such as that during disease. Chapter 4 describes the responses of cells from mice lacking functional Hmox1 to in vitro or in vivo oxidative challenges. This approach of challenging mammalian cells potentially defective in stress defense is analogous to experiments using bacterial or yeast cells, where gene products important for stress resistance have been identified by mutagenesis and the appropriate selection or screening (122, 123).

The concluding chapter of my thesis constitutes an assessment of how the availability of mice lacking either Hmox isoform has contributed to the understanding of various physiological systems. In addition, I describe how findings detailed within these chapters may be further expounded upon in subsequent analyses.

References

1. Means, R. T. & Krantz, S. B. (1992). *Blood* **80**, 1639-1647.
2. Halliwell, B. & Gutteridge, J. M. C. (1990). *Meth. Enzymol.* **186**, 1-85.
3. Feder, J. N., Gnirke, A., Thomas, W., Tsuchihashi, Z., Ruddy, D. A. et al. (1996). *Nature Genet.* **13**, 399-408.
4. Babcock, M., de Silva, D., Oaks, R., Davis-Kaplan, S., Jiralerspong, S., Montermini, L., Pandolfo, M. & Kaplan, J. (1997). *Science* **276**, 1709-1712.
5. Bothwell, T. H., Charlton, R. W. & Motulsky, A. G. (1995) in *The Metabolic and Molecular Bases of Inherited Disease*, eds. Scriver, C. R., Beaudet, A. L., Sly, W. S. & Valle, D. (McGraw-Hill, New York), pp. 2237-2269.
6. Fleming, M. D., Trenor, C. C., Su, M. A., Foernzler, D., Beier, D. R., Dietrich, W. D. & Andrews, N. C. (1997). *Nature Genet.* **16**, 383-386.
7. Gunshin, H., Mackenzie, B., Berger, U. V., Gunshin, Y., Romero, M. R., Boron, W. F., Nussberger, S., Gollan, J. L., Hediger, M. A. (1997). *Nature* **388**, 482-488.
8. Hentze, M. W. & Kuhn, L. C. (1996). *Proc. Natl. Acad. Sci. USA* **93**, 8175-8182.
9. Casey, J. L., Hentze, M. W., Koeller, D. M., Caughman, S. W., Rouault, T. A., Klausner, R. D. & Harford, J. B. (1988). *Science* **240**, 924-928.
10. Theil, E. C. (1990). *J. Biol. Chem.* **265**, 4771-4774.
11. Sorensen, E. W. (1965). *Acta Med. Scand.* **178**, 385-392.
12. Oates, P. S. & Morgan, E. H. (1996). *Am. J. Physiol.* **270**, G826-G832.
13. Dallman, P. R., Refino, C. & Yland, M. J. (1982). *Am. J. Clin. Nutr.* **35**, 671-677.
14. Bacon, B. R. & Tavill, A. S. (1996) in *Hepatology. A Textbook of Liver Disease*, eds. Zakim, D. & Boyer, T. D. (Saunders, Philadelphia), pp. 1439-1472.
15. Ponka, P. (1997). *Blood* **89**, 1-25.
16. Kappas, A., Sassa, S., Galbraith, R. A. & Nordmann, Y. (1989) in *The Metabolic and Basis of Inherited Disease*, eds. Scriver, C. R., Beaudet, A. L., Sly, W. S. & Valle, D. (McGraw-Hill, New York), pp. 1305-1365.
17. Cox, T. C., Bawden, M. J., Martin, A. & May, B. K. (1991). *EMBO J.* **10**, 1891-1902.
18. Lemberg, R. (1934). *Biochem. J.* **29**, 1322-1332.
19. Sjostrand, T. (1952). *Acta Phys. Scand.* **26**, 334-343.
20. Tenhunen, R., Marver, H. S. & Schmid, R. (1968). *Proc. Natl. Acad. Sci. USA* **61**, 748-755.
21. Yoshida, T. & Kikuchi, G. (1977). *J. Biochem.* **81**, 265-268.
22. Yoshida, T. & Kikuchi, G. (1978). *J. Biol. Chem.* **254**, 4487-4491.
23. Maines, M. D., Trakshel, G. M. & Kutty, R. K. (1986). *J. Biol. Chem.* **261**, 411-419.
24. Trakshel, G. M., Kutty, R. K. & Maines, M. D. (1986). *J. Biol. Chem.* **261**, 11131-11137.
25. Shibahara, S., Muller, R., Taguchi, H. & Yoshida, T. (1985). *Proc. Natl. Acad. Sci. USA* **82**, 7865-7869.
26. Rotenberg, M. O. & Maines, M. D. (1990). *J. Biol. Chem.* **265**, 7501-7506.
27. Shibahara, S., Yoshida, T. & Kikuchi, G. (1980). *J. Biochem.* **88**, 45-50.
28. Torpey, J. & Ortiz de Montallano, P. R. (1996). *J. Biol. Chem.* **271**, 26067-26073.
29. Yoshida, T. & Kikuchi, G. (1978). *J. Biol. Chem.* **253**, 4230-4236.
30. Yoshida, T., Noguchi, M. & Kikuchi, G. (1980). *J. Biol. Chem.* **255**, 4418-4420.
31. Rotenberg, M. O. & Maines, M. D. (1991). *Arch. Biochem. Biophys.* **290**, 336-344.

32. Ito-Maki, M., Ishikawa, K., Matera, K. M., Sato, M., Ikeda-Saito & Yoshida, T. (1995). *Arch. Biochem. Biophys.* **317**, 253-258.
33. Matera, K. M., Zhou, H., Migita, C. T., Hobert, S. E., Ishikawa, K., Katakura, K., Maeshima, H., Yoshida, T. & Ikeda-Saito, M. (1997). *Biochem.* **36**, 4909-4915.
34. Maines, M. D. (1988). *FASEB J.* **2**, 2557-2568.
35. Maines, M. D. & Kappas, A. (1974). *Proc. Natl. Acad. Sci. USA* **71**, 4293-4297.
36. Krasny, H. C. & Holbrook, D. J. (1977). *Mol. Pharmacol.* **13**, 759-765.
37. Shibahara, S., Yoshida, T. & Kikuchi, G. (1978). *Arch. Biochem. Biophys.* **188**, 243-250.
38. Siow, R. C., Ishii, T., Taketani, S., Leske, D. S., Sweiry, J. H., Pearson, J. D., Bannai, S., & Mann, G. E. (1995). *FEBS Lett.* **368**, 239-242.
39. Rizzardini, M., Terao, M., Falciani, F. & Cantoni, L. (1993), *Biochem. J.* **290**, 343-347.
40. Keyse, S. M. & Tyrrell, R. M. (1989). *Proc. Natl. Acad. Sci. USA* **86**, 99-103.
41. Durante, W., Kroll, M. H., Christodoulides, N., Peyton, K. J. & Schafer, A. I. (1997). *Circ. Res.* **80**, 557-564.
42. Ewing, J. F. & Maines, M. D. (1991). *Proc. Natl. Acad. Sci. USA* **88**, 5364-5368.
43. Kutty, R. K., Kutty, G., Wiggert, B., Chader, G. J., Darrow, R. M., & Organisciak, D. T. (1995). *Proc. Natl. Acad. Sci. USA* **92**, 1177-1181.
44. Murphy, B. J., Laderoute, K. R., Short, S. M. & Sutherland, R. M. (1991). *Br. J. Cancer* **64**, 69-73.
45. Dennery, P. A., Sridhar, K. J., Lee, C. S., Wong, H. E., Shokoohi, V., Rodgers, P. A. & Spitz, D. R. (1997). *J. Biol. Chem.* **272**, 14937-14942.
46. Matz, P. G., Massa, S. M., Weinstein, P. R., Turner, C., Panter, S. S. & Sharp, F. R. (1996). *J. Neurosurg.* **85**, 892-900.
47. Rizzardini, M., Carelli, M., Cabello Porras, M. R. & Cantoni, L. (1994). *Biochem. J.* **304**, 477-483.
48. Takeda, A., Onododera, H., Sugimoto, A., Itoyama, Y., Kogure, K. & Shibahara, S. (1994). *Brain Res.* **666**, 120-124.
49. Yan, S. D., Chen, X., Fu, J., Chen, M., Zhu, H., Roher, A., Slattery, T., Zhao, L., Nagashima, M., Morser, J., Migheli, A., Nawroth, P., Stern, D., & Schmidt, A. M. (1996). *Nature* **382**, 685-691.
50. Inamdar, N. M., Ahn, Y. I. & Alam, J. (1996). *Biochem. Biophys. Res. Commun.* **221**, 570-576.
51. Weber, C. M., Benay, C. E. & Maines, M. D. (1994). *J. Neurochem.* **63**, 953-962.
52. Bissell, D. M. & Guzelian, P. S. (1980). *J. Clin. Invest.* **65**, 1135-1140.
53. Pimstone, N. R., Tenhunen, R., Seitz, P. T., Marver, H. S. & Schmid, R. (1971). *J. Exp. Med.* **133**, 1264-1281.
54. Drummond, G. S. & Kappas, A. (1984). *J. Clin. Invest.* **74**, 142-149.
55. Maines, M. D. (1997). *Annu. Rev. Pharmacol. Toxicol.* **37**, 517-554.
56. Marks, G. S., Brien, J. F., Nakatsu, K. & McLaughlin, B. E. (1991). *Trends Pharmacol. Sci.* **12**, 185-188.
57. Ignarro, L. J., Buga, G. M., Wood, K. S., Byrns, R. E. & Chaudhuri, G. (1987). *Proc. Natl. Acad. Sci. USA* **84**, 9265-9269.
58. Jaffrey, S. R. & Snyder, S. H. (1995). *Ann. Rev. Dev. Biol.* **11**, 417-440.Gerzer,
59. Liew, F. Y., Millott, S., Parkinson, C., Palmer, R. M. & Moncada, S. (1990). *J. Immunol.* **144**, 4794-4797.
60. Ignarro, L. J., Byrns, R. E., Buga, G. M. & Wood, K. S. (1987). *Circ. Res.* **61**, 866-879.
61. Ischiropoulos, H., Zhu, L. & Beckman, J. S. (1992). *Arch. Biochem. Biophys.* **298**, 446-451.
62. Lev-Ram, V., Jiang, T., Wood, J., Lawrence, D. S. & Tsien, R. Y. (1997). *Neuron* **18**, 1025-1038.

63. Burnett, A. L., Lowenstein, C. J., Bredt, D. S., Chang, T. S. K. & Snyder, S. H. (1992). *Science* **257**, 401-403.
64. Stark, M. E., Bauer, A. J. & Szurszewski, J. H. (1991). *J. Physiol.* **444**, 743-761.
65. Ignarro, L. J. (1989). *Sem. Hematol.* **26**, 63-76.
66. Brune, B., Schmidt, K. U. & Ullrich, V. (1990). *Eur. J. Biochem.* **192**, 683-688.
67. Verma, A., Hirsch, D. J., Glatt, C. E., Ronnett, G. V. & Snyder, S. H. (1993). *Science* **259**, 381-384.
68. Lev-Ram, V., Makings, L. R., Keitz, P. F., Kao, J. P. & Tsien, R. Y. (1995). *Neuron* **15**, 407-415.
69. Nathanson, J. A., Scavone, C., Scanlon, C. & McKee, M. (1995). *Neuron* **14**, 781-794.
70. Prabhakar, N. R., Dinerman, J. L., Agani, F. H. & Snyder, S. H. (1995). *Proc. Natl. Acad. Sci. USA* **92**, 1994-1997.
71. Farrugia, G., Irons, W. A., Rae, J. L., Sarr, M. G. & Szurszewski, J. H. (1993). *Am. J. Physiol.* **264**, G1184-G1189.
72. Rattan, S. & Chakder, S. (1993). *Am. J. Physiol.* **265**, G799-G804.
73. Zakhary, R., Gaine, S. P., Dinerman, J. L., Ruat, M., Flavahan, N. A., & Snyder, S. H. (1996). *Proc. Natl. Acad. Sci. USA* **93**, 795-798.
74. Bliss, T. V. P. & Lomo, T. (1973). *J. Physiol.* **232**, 331-356.
75. Zhuo, M., Hu, Y., Schultz, C., Kandel, E. R. & Hawkins, R. D. (1994). *Nature* **368**, 635-639.
76. O'Dell, T. J., Hawkins, R. D., Kandel, E. R. & Arancio, O. (1991). *Proc. Natl. Acad. Sci. USA* **88**, 11285-11289.
77. Arancio, O., Kiebler, M., Lee, C. J., Lev-Ram, V., Tsien, R. Y., Kandel, E. R. & Hawkins, R. D. (1996). *Cell* 87, 1025-1035.67.
78. Stevens, C. F. & Wang, Y. (1993). *Nature* **364**, 147-149.
79. Zhuo, M., Small, S. A., Kandel, E. R. & Hawkins, R. D. (1993). *Science* **260**, 1946-1950.
80. Ignarro, L. J., Ballot, B. & Wood, K. S. (1984). *J. Biol. Chem.* **259**, 6201-6207.
81. Meffert, M. K., Haley, J. E., Schuman, E. M., Schulman, H. & Madison, D. V. (1994). *Neuron* **13**, 1225-1233.
82. Ames, B, N., Shigenaga, M. K. & Hagen, T. M. (1993). *Proc. Natl. Acad. Sci. USA* **90**, 7915-7922.
83. Parsell, D. A. & Lindquist, S. (1993). *Annu. Rev. Genet.* **27**, 437-496.
84. Halliwell, B. & Gutteridge, J. M. C. (1990). *Meth. Enzymol.* **186**, 1-85.
85. Coyle, J. T. & Puttfarcken, P. (1993). *Science* **262**, 689-695.
86. Abraham, N. G., Lavrovsky, Y., Schwartzman, M. L., Stoltz, R. A., Levere, R. D., Gerritsen, M. E., Shibahara, S. & Kappas, A. (1995). *Proc. Natl. Acad. Sci. USA* **92**, 6798-6802.
87. Hunt, R. C., Handy, I. & Smith, A. (1996). *J. Cell. Physiol.* **168**, 81-86.
88. Stocker, R., Yamamoto, Y., McDonagh, A. F., Glazer, A. N. & Ames, B. N. (1987). *Science* **235**, 1043-1046.
89. Eisenstein, R. S., Garcia-Mayol, D., Pettingell, W. & Munro, H. N. (1991). *Proc. Natl. Acad. Sci. USA* **88**, 688-692.
90. Vile, G. F., Basu-Modak, S., Waltner, C. & Tyrrell, R. M. (1994). *Proc. Natl. Acad. Sci. USA* **91**, 2607-2610.
91. Agarwal, A., Kim, Y., Matas, A., Alam, J. & Nath, K. A. (1996). *Transplantation* **61**, 93-98.
92. Otterbein, L., Sylvester, S. L. & Choi, A. M. (1995). *Am. J. Respir. Cell. Mol. Biol.* **13**, 595-601.
93. Nath, K. A., Balla, G., Vercellotti, G. M., Balla, J., Jacob, H. S., Levitt, M. D., & Rosenberg, M. E. (1992). *J. Clin. Invest.* **90**, 267-270.

94. Ishikawa, K., Navab, M., Leitinger, N., Fogelman, A. M. & Lusis, A. J. (1997). J. Clin. Invest. (in press).
95. Dennery, P. A., Hreman, H. J., Rodgers, P. A. & Stevenson, D. K. (1993). *Pediatr. Res.* **33**, 87-91.
96. Nutter, L. M., Sierra, E. E. & Ngo, E. O. (1994). *J. Lab. Clin. Med.* **123**, 506-514.
97. Van Lenten, B. J., Prieve, J., Navab, M., Hama, S., Lusis, A. J., & Fogelman, A. M. (1995). *J. Clin. Invest.* **95**, 2104-2110.
98. Mansour, S. L., Thomas, K. R. & Capecchi, M. R. (1988). *Nature* **336**, 348-352.
99. Capecchi, M. R. (1994). *Sci. Am.* **270**, 52-59.
100. Clarke, L. L., Grubb, B. R., Gabriel, S. E., Smithies, O., Koller, B. H. & Boucher, R. C. (1992). *Science* **257**, 1125-1128.
101. Ishibashi, S., Brown, M. S., Goldstein, J. L., Gerard, R. D., Hammer, R. E. & Herz, J. (1993). *J. Clin. Invest.* **92**, 883-893.
102. Jacks, T., Fazeli, A., Schmitt, E. M., Bronson, R. T., Goodell, M. A. & Weinberg, R. A. (1992). *Nature* **359**, 295-300.
103. Kemp, C. J., Donehower, L. A., Bradley, A. & Balmain, A. (1993). *Cell* **74**, 813-822.
104. Dutch-Beligian Fragile X Consortium. (1994). *Cell* **78**, 23-33.
105. Geisterfer-Lowrance, A. A., Christe, M., Conner, D. A., Ingwall, J. S., Schoen, F. J., Seidman, C., and Seidman, J. G. (1996). *Science* **272**, 731-734.
106. Lee, K. F., Simon, H., Chen, H., Bates, B., Hung, M. C. & Hauser, C. (1995). *Nature* **378**, 394-398.
107. Chiang, C., Litingtung, Y., Lee, E., Young, K. E., Corden, J. L., Westphal, H. & Beachy, P. A. (1996). *Nature* **383**, 407-413.
108. Blendy, J. A., Kaestner, K. H., Weinbauer, G. F., Nieschlag, E. & Schutz, G. (1996). *Nature* **380**, 162-165.
109. Wong, P. C., Zheng, H., Chen, H., Becher, M. W., Sirinathsinghji, D. J., Trumbauer, M. E., Chen, H. Y., Price, D. L., Van der Ploeg, L. H. & Sisodia, S. S. (1997). *Nature* **387**, 288-292.
110. Mombaerts, P., Iacomini, J., Johnson, R. S., Herrup, K., Tonegawa, S. & Papaioannou, V. E. (1992). *Cell* **68**, 869-877.
111. Itohara, S., Mombaerts, P., Lafaille, J., Iacomini, J., Nelson, A., Clarke, A. R., Hooper, M. L., Farr, A. & Tonegawa, S. (1993). *Cell* **72**, 337-348.
112. Silva, A. J., Stevens, C. F., Tonegawa, S. & Wang, Y. (1992). *Science* **257**, 201-206.
113. Silva, A. J., Paylor, R., Wehner, J. M. & Tonegawa, S. (1992). *Science* **257**, 206-211.
114. Grant, S. G., O'Dell, T. J., Karl, K. A., Stein, P. L., Soriano, P. & Kandel, E. R. (1992). Science 258, 1903-1910.
115. Xu, M., Hu, X. T., Cooper, D. C., Moratalla, R., Graybiel, A. M., White, F. J. & Tonegawa, S. (1994). *Cell* **79**, 945-955.
116. Saudou, F., Amara, D. A., Dierich, A., LeMeur, M., Ramboz, S., Segu, L., Buhot, M. C. & Hen, R. (1994). *Science* **265**, 1875-1878.
117. Aiba, A., Kano, M., Chen, C., Stanton, M. E., Fox, G. D., Herrup, K., Zwingman, T. A. & Tonegawa, S. (1994). *Cell* **79**, 377-388.
118. Huang, Y. Y., Kandel, E. R., Varshavsky, L., Brandon, E. P., Qi, M., Idzerda, R. L., McKnight, G. S. & Bourtchouladze, R. (1995). *Cell* **83**, 1211-1222.
119. Kuhn, R., Schwenk, F., Aguet, M. & Rajewsky, K. (1995). *Science* **269**, 1427-1429.
120. Rajewsky, K., Gu, H., Kuhn, R., Betz, U. A., Muller, W., Roes, J. & Schwenk, F. (1996). *J. Clin. Invest.* **98**, 600-603.
121. Tsien, J. Z., Chen, D. F., Gerber, D., Tom, C., Mercer, E. H., Anderson, D. J., Mayford, M., Kandel, E. R. & Tonegawa, S. (1996). *Cell* **87**, 1317-1326.

122. Christman, M. F., Morgan, R. W., Jacobson, F. S. & Ames, B. N. (1985). Cell 41, 753-762.
123. Kennedy, B. K., Austriaco, N. R., Zhang, J. & Guarente, L. (1995). Cell 80, 485-486.

Fig. 1. The heme biosynthetic pathway. Subcellular distribution of enzymes and intermediates in the synthesis of heme is shown. ALA, 5-aminolevulinic acid; PBG, pophobilinogen; Uro'gen, uroporphyrinogen; Copro'gen, coproporphyrinogen; Proto'gen, protoporphyrinogen; A, $-(CH_2)_2\cdot COOH$; M, $-CH_3$; P, $-CH_2\cdot COOH$; V, $-CH=CH_2$. Diagram is taken from ref. #16.

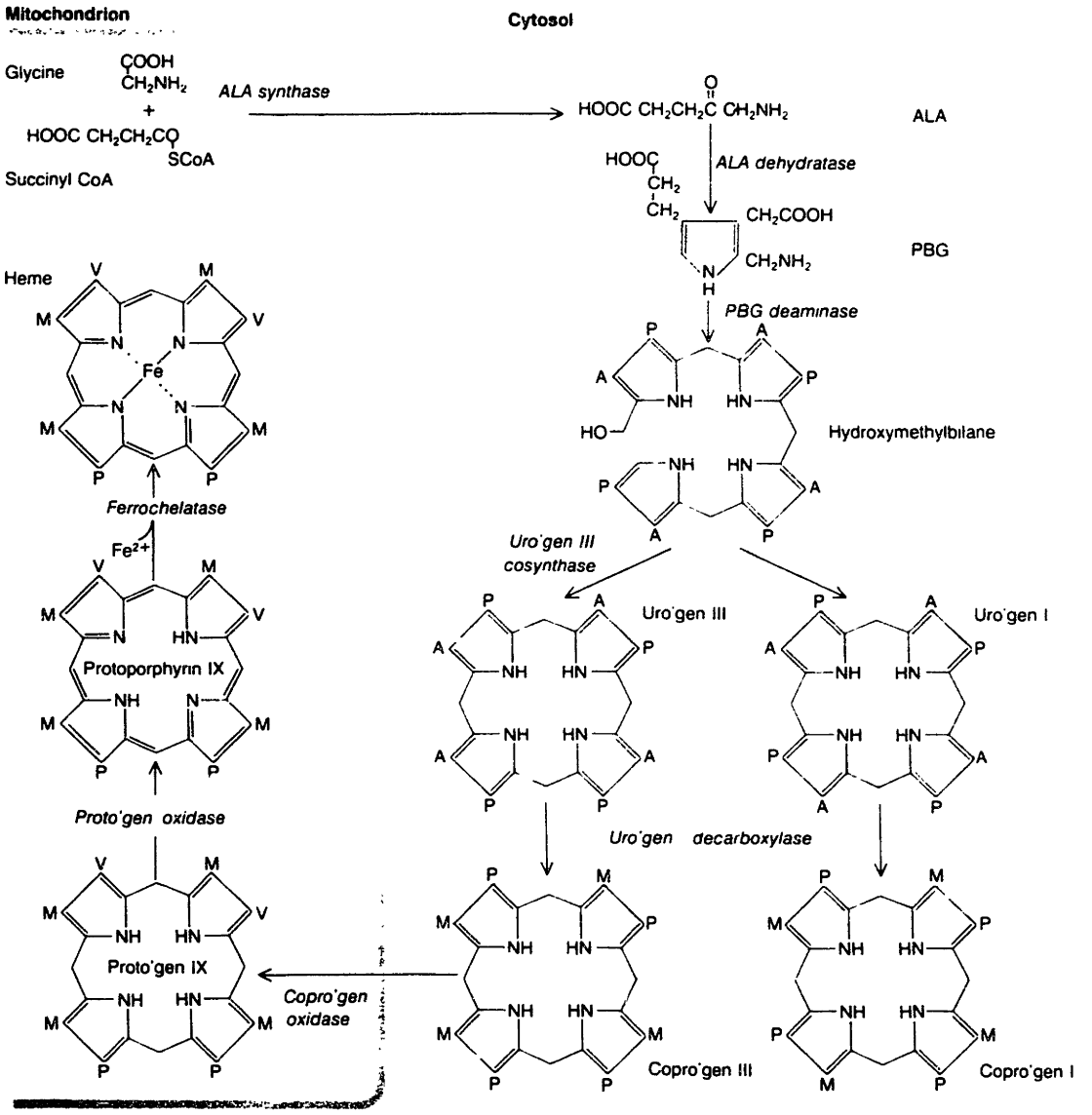
Mitochondrion
Cytosol
Glycine
Succinyl CoA
ALA synthase
ALA
ALA dehydratase
PBG
PBG deaminase
Hydroxymethylbilane
Heme
Ferrochelatase
Fe2+
Protoporphyrin IX
Uro'gen III cosynthase
Uro'gen III
Uro'gen I
Proto'gen oxidase
Uro'gen decarboxylase
Proto'gen IX
Copro'gen oxidase
Copro'gen III
Copro'gen I

Fig. 2. Intermediates in the reaction catalyzed by heme oxygenase. Me, $-CH_3$; P, $-CH_2 \cdot COOH$; V, $-CH=CH_2$. Diagram is taken from ref. #28.

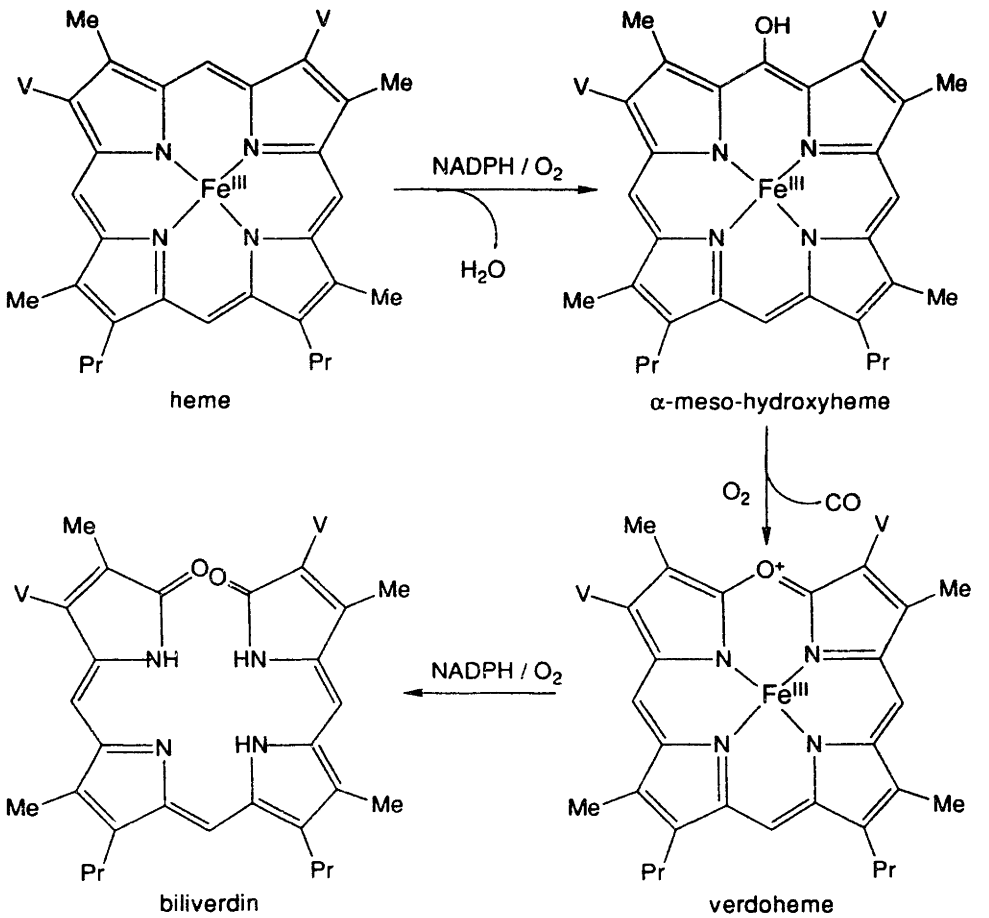
Me
V
Me
V
N
N
Fe^{III}
N
N
Me
Me
Pr
Pr
heme
NADPH / O_2
H_2O
Me
OH
V
V
Me
N
N
Fe^{III}
N
N
Me
Me
Pr
Pr
α-meso-hydroxyheme
O_2
CO
Me
V
V
Me
O$^+$
N
N
Fe^{III}
N
N
Me
Me
Pr
Pr
verdoheme
NADPH / O_2
Me
V
V
Me
O
O
NH
HN
N
HN
Me
Me
Pr
Pr
biliverdin

Fig. 3. Candidate molecular mechanism for LTP. A, Before tetanic stimulation, glutamatergic neurotransmission occurs through the AMPA subtype of glutamate receptor, resulting in a baseline synaptic response (far right). B, When a tetanus is given to the presynaptic terminal (left), sufficient depolarization results in the release of a Mg^{2+} block from the NMDA subtype of glutamate receptor, and an influx of Ca^{2+}. This postsynaptic increase in intracellular Ca^{2+} is thought to lead to activation of protein kinases important for maintaining LTP. C, A synapse expressing LTP displays increased synaptic activity. This is in part due to an enhanced response by AMPA receptors, perhaps after modification by activated kinases. Also, presynaptic transmitter release is stimulated, perhaps due to increased kinase activity in the presynaptic terminal. Since LTP is induced postsynaptically as in (B), but is expressed in part presynaptically, a retrograde messenger such as NO or CO is believed to diffuse from its postsynaptic site of synthesis to the presynaptic site of action. AMPA, 2-amino-3-hydroxy-5-methylisoxazole-4-proprionic acid; NMDA, N-methyl-D-aspartate; CaMKII, calcium/calmodulin-dependent protein kinase II; PKC, protein kinase C; PKA, protein kinase A.

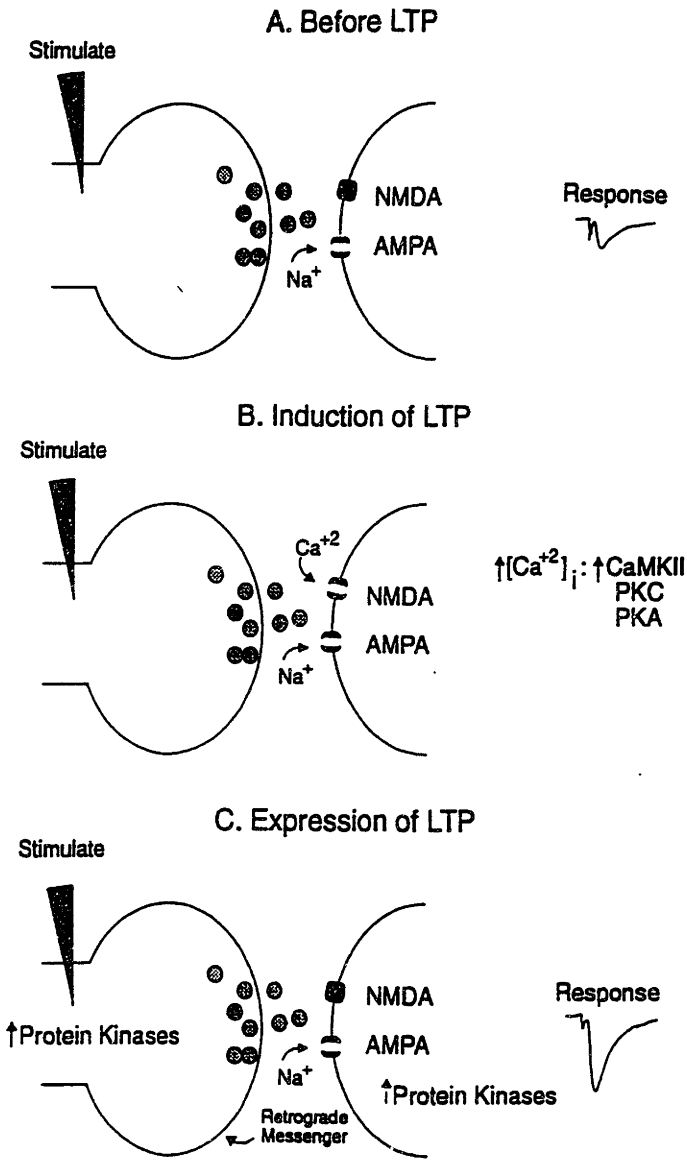
A. Before LTP
Stimulate
NMDA
AMPA
Na+
Response
B. Induction of LTP
Stimulate
Ca+2
NMDA
AMPA
Na+
↑[Ca+2]i: ↑CaMKII
PKC
PKA
C. Expression of LTP
Stimulate
↑Protein Kinases
NMDA
AMPA
Na+
↑Protein Kinases
Retrograde Messenger
Response

Chapter 2

Hippocampal Long-Term Potentiation Is Normal In Heme Oxygenase-2-Deficient Mice

Note: This chapter is adapted from a manuscript published in *Neuron* **15**, pp. 867-873, by the authors Kenneth D. Poss, * Mark J. Thomas, † Alexander K. Ebralidze, * Thomas J. O'Dell, † and Susumu Tonegawa. *

*Howard Hughes Medical Institute and Center for Learning and Memory
Department of Biology
Massachusetts Institute of Technology
Cambridge, Massachusetts 02139
†Department of Physiology and Interdepartmental Graduate Program in Neuroscience
University of California School of Medicine
Los Angeles, California 90024

Summary

We have generated mice deficient in heme oxygenase-2 (Hmox2), the major cerebral isoform of Hmox, in order to assess the potential role of carbon monoxide as a retrograde messenger in hippocampal long-term potentiation (LTP). Cerebral Hmox catalytic activity was markedly reduced in the *Hmox2*$^{-/-}$ mice, yet no differences were found between wild-type and *Hmox2*$^{-/-}$ mice in gross neuroanatomical structure, in basal hippocampal synaptic transmission, or in the amount of potentiation produced by various LTP induction protocols. Furthermore, zinc protoporphyrin IX, an inhibitor of Hmox, had nearly identical inhibitory effects on LTP in wild-type and *Hmox2*$^{-/-}$ hippocampal slices. Our data indicate that carbon monoxide produced endogenously by Hmox is unlikely to be a neuromodulator required for LTP in the hippocampus .

Introduction

Long-term potentiation (LTP) is experimentally defined as a long-lasting enhancement of synaptic transmission that results from a strong high frequency presynaptic stimulus (1), or a low frequency presynaptic stimulus paired with postsynaptic depolarization (2). It is well-established by pharmacological studies that postsynaptic activation of the NMDA subtype of glutamate receptor and subsequent Ca^{2+} influx are required for the induction of LTP (3). In contrast, whether the expression of LTP occurs at either the pre- or postsynaptic site, or both, is still controversial (4-6). An example of a presynaptic cellular change underlying LTP would be an increase in glutamate release, while a postsynaptic modification might involve an augmentation in postsynaptic responses to released transmitter. If there is indeed such a presynaptic component, there must correspondingly be some messenger which is synthesized postsynaptically, but is released and has the ability to signal to the presynaptic terminal. The membrane-permeable molecule nitric oxide (NO), generated by nitric oxide synthase (Nos), is a candidate for this retrograde signal. Inhibitors of Nos can block hippocampal LTP. Also, hemoglobin, a molecule which binds NO and is confined to the extracellular space, will block LTP when added to hippocampal slices (7, 8). However, it has been difficult to conclusively determine a retrograde messenger role for NO in LTP, since Nos inhibitors are only effective in reducing LTP under certain experimental conditions (9), and LTP is normal in mice lacking a functional neuronal *Nos* gene (10).

Another candidate for the retrograde messenger is carbon monoxide (CO), which was initially investigated for neuromodulatory function because of its chemical similarities with NO. The sole enzyme known to stoichiometrically produce CO is microsomal heme oxygenase (Hmox), which metabolizes heme groups yielding biliverdin, free iron, and CO (11). Separate genes encode two isoforms of Hmox. One of these isoforms, Hmox2, is highly expressed throughout the brain, including hippocampal CA1 pyramidal cells (12). The other isoform, Hmox1, is expressed mainly in peripheral organs and is detected only in scattered neurons of the central nervous system (13, 14). Although relatively little is known about the neuromodulatory role of CO, there is evidence which suggests that CO may participate in olfactory response (12), smooth muscle relaxation (15, 16), and modulation of Purkinje cell excitability (17). Recently, CO has been considered a candidate retrograde messenger in the hippocampus, based on experiments showing that metalloporphyrin inhibitors of Hmox, such as zinc protoporphyrin IX (ZnPP), are capable of blocking the induction and/or maintenance of LTP in hippocampal slices (18, 19). The ability of hemoglobin to inhibit LTP is consistent with this hypothesis, since hemoglobin sequesters CO in addition to NO. Moreover, CO application paired with weak tetanic

stimulation can cause an enhancement of synaptic transmission in hippocampal slices which resembles LTP (19). Pharmacological evidence indicating that cGMP generation may be necessary for CA1 region LTP (20) is also in agreement with a retrograde messenger role for CO, since, like NO, CO can potently activate soluble guanylyl cyclase (sGC) by binding to the heme group contained in the enzyme (21, 22).

There remain significant challenges to the notion that CO participates in LTP. Metalloporphyrins may have inhibitory effects on Hmox-independent activities important for LTP. Such studies have documented direct attenuation by ZnPP of sGC and NOS activity (23, 24), suggesting certain limitations in using such metalloporphyrins as reagents for investigating Hmox function. CO itself is a relatively stable molecule, in contrast with NO; this would appear to make temporally- and locally-controlled presynaptic activation more difficult. Finally, since Hmox has not yet been found to be directly regulated by Ca^{2+} or any other components of the signal transduction pathway thought to be responsible for LTP, it is unclear how CO production could be coupled to changes in Ca^{2+} levels that are integral for the postsynaptic induction of LTP. However, Nathanson et al. did report increases in CO production from cerebellar slices following glutamate application (17).

To further address the role of CO as a signaling molecule in LTP or in other systems for which CO participation has been implicated, we have used gene targeting techniques to generate mice devoid of functional Hmox2. In this study, these mice were used to examine hippocampal synaptic transmission and LTP.

Methods and Materials

Hmox2 Targeting Vector

The published rat *Hmox2* cDNA sequence (25) was utilized for synthesis of primers toward generating a mouse DNA probe by PCR amplification. This probe contained sequence corresponding to the final 68 amino acids of rat Hmox2 protein. It was used to screen a lambda EMBL3 library containing mouse 129/Sv strain genomic fragments, from which the *Hmox2* gene was obtained. A 4.5 kb XbaI fragment and a 4.0 kb EcoRI-SpeI fragment were used as 5' and 3' arms of the construct, surrounding a 1.8 kb *pgk-neo* fragment in pBluescript KS^+. The construct was designed to remove a 3.5 kb XbaI-EcoRI fragment of mouse DNA containing intron sequences and coding sequence corresponding to rat Hmox2 amino acids 67-315.

Targeting Experiments and Generation of *Hmox2* Mutant Mice

D3 ES cells derived from 129/Sv mice were grown on mitotically-inactivated embryonic fibroblast feeder cells and electroporated with 50 μg of the NotI-linearized construct

using a Bio-Rad Gene Pulser (800 V and 3 μF settings). G418 at 200 μg/ml was applied 24 hours later as selection for transfectants, and G418-resistant colonies were isolated on days 7 and 8 of selection. Genomic DNA for EcoRV restriction digests was isolated from approximately 300 colonies grown in 24-well plates. Southern blotting and hybridization with the 5' external 0.8 kb probe or the 3' external 2.0 kb probe (shown in Figure 1A) revealed 24 homologous recombinants. Six corresponding ES clones were used for injection into C57BL/6 blastocysts. Chimeric mice were generated as described (26). Pseudopregnant C57BL/6 x DBA/2 (F1 generation) were used as blastocyst recipients. Mice heterozygous for the mutation were obtained by mating male chimeras with C57BL/6 females; these heterozygous mice were intercrossed to produce homozygous *Hmox2* mutants. Genotypes of mice were determined by Southern analysis of progeny tail DNA, as mentioned above (see Figure 1B). For all experments, C57BL/6 x 129/Sv wild type and mutant mice were used.

RNA Analysis

Total RNA was isolated from brain by guanidine thiocyanate denaturation and cesium chloride gradient ultracentrifugation. Approximately 30 μg of RNA was electrophoresed in the presence of formaldehyde, Northern blotted onto Hybond-N nylon membrane (Amersham), and hybridized with the DNA probe used for isolating the *Hmox2* genomic sequence. Afterwards, blots were hybridized with a human *B-actin* cDNA probe to control for amounts loaded.

Hmox Enzymatic Activity

Pooled brains, spleens, or testes from wild type or mutant mice were homogenized in 100 mM phosphate buffer pH 7.4, and the 10,000 x g supernatant was immediately used for Hmox assays. Reactions with wild type and mutant homogenates were set up in parallel. All experiments were performed under dim lighting. Reactions (3 ml) contained 3-5 mg of protein, 20 μM hemin, and 0.05% BSA in 100 mM phosphate buffer pH 7.4. 300 nmoles NADPH was added to initiate reactions; those without NADPH were considered to have zero activity. After 20 min at 37 ^{o}C, reactions were stopped on ice and added to spectrophotometer cuvettes. Bilirubin production was calculated using the difference in absorbance between 468 and 520 nm. Bilirubin and hemin solutions were prepared as described (27).

Electrophysiology

Thick (400 μM) transverse slices of mouse hippocampus prepared using standard techniques were maintained in an interface type recording chamber perfused (1-3 mL/min) with an oxygenated (95% O_2/5% CO_2) mouse artificial cerebrospinal fluid (ACSF - 124 mM NaCl, 4.4 mM KCl, 25 mM Na_2HCO_3, 1.0 mM $NaPO_4$, 1.2 mM

$MgSO_4$, 2.0 mM $CaCl_2$, and 10 mM glucose). All experiments were done at 30-31 °C. Male mice six to eight weeks old were used, and data collection and analysis were done in a blind fashion.

EPSPs elicited by stimulation of the Schaffer collateral/commisural fibers in CA1 were evoked using a bipolar nichrome wire stimulating electrode (stimulation rate = 0.02 Hz, 0.01-0.02 ms duration pulses) and were recorded using glass microelectrodes (5-15 Mohms, filled with ACSF) placed in stratum radiatum of the CA1 region of the hippocampus. A stimulation intensity sufficient to elicit field EPSPs that were approximately 50% of the maximal response was used throughout the experiment. In experiments examining the effects of ZnPP on LTP, Na_2PO_4 was omitted from the ACSF, and $MgCl_2$ was substituted for $MgSO_4$ (see Meffert et al., 1994). ZnPP (Research Biochemicals, Inc.) was first dissolved in 100% DMSO and then diluted into aqueous base (0.002 N NaOH) prior to a final dilution into ACSF to give 15 μM ZnPP (final DMSO concentration was 0.05%).

Intracellular EPSPs were recorded from individual CA1 pyramidal cells using high resistance (60-120 Mohms) glass microelectrodes filled with 2.0 M CsCl. In these experiments, EPSPs were evoked every 15 s and the ACSF contained 100 μM picrotoxin to block inhibitory synaptic transmission. To prevent spontaneous and evoked bursting, the CA3 region of the slice was removed and the concentrations of $CaCl_2$ and $MgSO_4$ were elevated to 4.0 mM each. LTP was induced by pairing 40 EPSPs (evoked at 1 Hz) with depolarization of the postsynaptic membrane potential to approximately -20 mV. Only cells with resting membrane potentials more negative than -60 mV and input resistances larger than 40 Mohms (measure with 0.2-0.3 nA hyperpolarizing current injections) were used. In these experiments cells were hyperpolarized to between -80 and -90 mV by injecting hyperpolarizing current through the electrode to prevent potentiated EPSPs from eliciting action potentials. There were no differences between wild-type and mutants in either resting membrane potentials (wild type: -65.7± 3.5 mV (mean ± SEM, N = 4 mice, 8 cells; mutant: -65.1 ± 4.0 mV, N = 5 mice, 9 cells) or input resistances (wild type: 68.1 ± 19.6 Mohms; mutant: 63.9 ± 14.7 Mohms).

Results

Generation of *Hmox2* Homozygous Mutant Mice

The *Hmox2* targeting construct replaces a region of murine *Hmox2* sequence which corresponds to rat *Hmox2* exons 4 and 5 (28) with a neomycin resistance cassette containing a *pgk* promoter (Fig. 1A). This mutation removes approximately 80% of the coding sequence, including the putative membrane-spanning region. Following

transfection of this construct into ES cells and G418 selection, Southern analysis was used to verify homologous recombination events. Approximately 8% of transfectants contained a targeted *Hmox2* locus. Six male chimeras with the capacity to transmit the targeted allele through the germline were obtained via blastocyst injection of two of these positive clones. Matings between heterozygous mice yielded expected Mendelian ratios; these offspring were typed using Southern blots (Fig. 1B).

The absence of *Hmox2* gene expression in homozygous mutant mice (referred to hereafter as *Hmox2*$^{-/-}$ mice) was confirmed by Northern blot analysis using adult brain RNA. A single band of approximately 1.8 kb was present in blots of wild type RNA, while missing from those of RNA from mutants (Fig. 1C). Hmox enzymatic assays revealed a lack of activity, measured indirectly by bilirubin production, in brains of *Hmox2*$^{-/-}$ mice (Fig. 1D). Although the assay used was not sensitive enough to detect very low levels of Hmox activity, this result confirms a previous report which found minimal cerebral contribution from the Hmox1 isoform (29). RNA analysis further indicated no upregulation of *Hmox1* mRNA in *Hmox2*$^{-/-}$ brains (data not shown). Hmox activity was clearly reduced in the testes of *Hmox2*$^{-/-}$ mice compared to wild-type mice, while the reduction was less pronounced in the *Hmox2*$^{-/-}$ spleens (Fig. 1D). These data are also consistent with previous work describing the contributions of each isoform to total Hmox activity in these tissues (30, 31).

Behavior and Anatomy of *Hmox2*$^{-/-}$ Mice

Hmox2-deficient mice are morphologically indistinguishable from their wild-type littermates throughout development and adulthood. *Hmox2*$^{-/-}$ mice are fertile and survive normally up to at least one year. They appear to have typical feeding and grooming behavior, gait, and circadian rhythms. Histological examination of *Hmox2*$^{-/-}$ brains at a gross level revealed no neuroanatomical differences from those of wild-type mice (data not shown). Several tissues other than brain were also examined histologically, but unveiled no mutation-linked abnormalities (data not shown). Additionally, no significant differences in major hematological parameters were noted between wild-type and *Hmox2*$^{-/-}$ mice, including carboxyhemoglobin levels (data not shown).

Hippocampal Synaptic Transmission and LTP

In hippocampal slices from wild-type and *Hmox2*$^{-/-}$ mice, we measured excitatory synaptic transmission in the CA1 region following Schaffer collateral stimulation. There was no significant difference seen in maximal field excitatory postsynaptic potentials (EPSPs; wild-type (mean ± SEM): 8.98 ± 0.27 mV (n = 10 mice, 59 slices); *Hmox2*$^{-/-}$: 9.25 ± 0.30 mV (n = 10 mice, 64 slices); $t(18) = 0.271$, not significant). We next

analyzed paired-pulse facilitation, which is a short-lasting, presynaptic form of synaptic plasticity characterized by an enhanced response to the second of a pair of stimulation pulses delivered in rapid succession. Paired-pulse facilitation was similar in wild-type and *Hmox2*$^{-/-}$ mice over a range of 20-200 ms interstimulus intervals (n = 6 mice, 11 slices analyzed from each group; data not shown). Together, these results suggest that there is no gross irregularity of basal synaptic function in the *Hmox2*$^{-/-}$ hippocampi, and are consistent with reports showing that inhibitors of Hmox had no effect on baseline hippocampal synaptic transmission (18, 19, 24).

We used several different protocols to induce LTP in slices from wild-type and *Hmox2*$^{-/-}$ animals. A high frequency tetanus protocol (2 trains of 100 Hz/1s duration) was initially used to induce a strong potentiation in hippocampal slices. There was no significant difference between the average LTP induced in wild-type slices (188.2% ± 7.1% of pre-tetanus baseline, measured at 60 min post-tetanus; n = 6 mice, 13 slices) and that from *Hmox2*$^{-/-}$ slices (Fig. 2A; 212.0% ± 14.7%; n = 6 mice, 13 slices; $t(10) = 1.461$, not significant). It remained possible that the tetanic stimulus used in these experiments was too powerful to allow for the detection of any subtle LTP differences between the two groups of mice. Therefore, we attempted to determine a protocol which might induce LTP in wild-type mice, yet does not meet the threshold for LTP production in *Hmox2*$^{-/-}$ slices. Protocols using 20 Hz, 10 Hz, or 5 Hz stimulation each produced a long-lasting potentiation in our experiments. Fig. 2B-D indicate that these weaker protocols did not reveal any significant differences in average LTP values between wild type and *Hmox2*$^{-/-}$ slices. From wild-type slices, protocols of 20 Hz, 10 Hz, and 5 Hz yielded LTP of 225.1% ± 13.3% (n = 4 mice, 10 slices), 154.8% ± 17.0% (n = 4 mice, 9 slices), and 115.2% ± 9.6% (n = 6 mice, 15 slices), respectively. *Hmox2*$^{-/-}$ slices had corresponding LTP values of 228.7% ± 16.3% (n = 4 mice, 9 slices; $t(6) = 0.173$, not significant), 164.2% ± 11.3% (n = 5 mice, 12 slices; $t(7) = 0.463$, not significant), and 125.2% ± 8.4% (n = 5 mice, 14 slices; $t(9) = 0.789$, not significant).

Finally, we measured CA1 LTP induced by presynaptic low frequency stimulation paired with intracellular postsynaptic depolarization (see Experimental Procedures). Similar LTP values were obtained from wild-type and *Hmox2*$^{-/-}$ slices using this type of analysis as well (Fig. 3; wild type: 274.3% ± 21.5%, n = 4 mice, 8 cells; *Hmox2*$^{-/-}$: 279.6% ± 47.4%, n = 5 mice, 9 cells; $t(7) = 0.095$, not significant). In summary, we observed normal amounts of LTP in *Hmox2*$^{-/-}$ slices through use of a variety of LTP induction protocols, indicating that CO production by Hmox2 is not required for LTP in the CA1 hippocampal region. On the contrary, the *Hmox2*$^{-/-}$ LTP values were higher

than wild-type values for each protocol used, though never by a statistically significant margin.

Effects of Hmox Inhibitor

Our results demonstrating essentially normal LTP in *Hmox2*$^{-/-}$ mice do not support the findings of previous pharmacological studies, which indicated disruption of LTP by Hmox inhibitors (18, 19). To begin to address this issue, we tested the effects of 15 μM ZnPP on the induction of LTP using a single train of 100 Hz (1 s duration) in slices from wild-type and *Hmox2*$^{-/-}$ mice. In wild-type slices, ZnPP application resulted in a significant reduction of LTP (Fig. 4A; control potentiation: 196.7%± 26.3%, n = 5 mice, 11 slices; ZnPP treatment: 122.9% ± 8.1%, n = 5 mice, 11 slices; $t(4) = 3.803$, $p < 0.05$). Fig. 4B indicates that 15 μM ZnPP had very similar effects on LTP in *Hmox2*$^{-/-}$ animals (control: 191.6% ± 19.3%, n = 5 mice, 10 slices; ZnPP: 123.7% ± 12.5%, n = 4 mice, 8 slices; $t(7) = 2.77$, $p < 0.025$). In fact, there were no significant differences between wild-type and *Hmox2*$^{-/-}$ mice in either control LTP or ZnPP-affected LTP (control: $t(8) = 0.155$, not significant; ZnPP-treated: $t(7) = 0.058$, not significant). Thus, even though the major cerebral isoform of Hmox was absent from *Hmox2*$^{-/-}$ hippocampal slices, ZnPP was able to block LTP to the same extent as in wild-type slices.

Discussion

CO, a product of Hmox activity, has been implicated as a neuromodulator and as a retrograde messenger involved in presynaptic contributions to potentiated synaptic transmission following the induction of LTP. In this study, we generated mice homozygous for a null mutation in the *Hmox2* gene, which encodes the major isoform of Hmox present in the central nervous system. As expected, Hmox catalytic activity was undetectable in *Hmox2*$^{-/-}$ brains. *Hmox2*$^{-/-}$ mice exhibited no obvious abnormalities in appearance, and a systematic histological scan of mutant tissues revealed no anomalies. Moreover, based on maximal field EPSP amplitudes and paired-pulse facilitation, basal hippocampal synaptic transmission appeared normal in the *Hmox2*$^{-/-}$ mice. Most importantly, we were unable to find any differences between wild-type and *Hmox2*$^{-/-}$ mice in CA1 LTP produced by several different induction protocols. Even the weakest protocol yielding small LTP produced similar potentiation in wild-type and *Hmox2*$^{-/-}$ slices. Our results clearly demonstrate that Hmox2 is not required for LTP.

There are two likely reasons for the discrepancy between our observations of normal LTP in *Hmox2*$^{-/-}$ hippocampal slices and previous observations of disrupted LTP in metalloporphyrin-treated slices. First, as immunohistochemical staining has detected the Hmox1 isoform in scarce, randomly distributed cells of the hippocampus (13), it is

possible that residual CO contribution from Hmox1 is adequate for LTP. Secondly, as mentioned above and addressed by Meffert et al. (24), the ability of metalloporphyrins to inhibit LTP in hippocampal slices might not be solely due to their effects on Hmox. Our observation that 15 μM ZnPP inhibits LTP in mutant slices addresses this issue. Importantly, previous experiments have demonstrated that Hmox1 and Hmox2 activities are equally inhibited by a wide range of ZnPP concentrations (32). Therefore, if only a minority of Hmox activity (< 5% of wild-type levels) functions to accommodate LTP in the *Hmox2*$^{-/-}$ hippocampi, then a nonsaturating concentration of ZnPP should in theory have more pronounced effects on LTP in *Hmox2*$^{-/-}$ slices, compared with its effects on LTP in wild-type slices which have normal levels of Hmox expression and activity. However, we observed that 15 μM ZnPP produces a nearly identical, partial inhibition of LTP in both *Hmox2*$^{-/-}$ and wild type slices, suggesting that it is unlikely that the sustained normal LTP in *Hmox2*$^{-/-}$ mice is due to Hmox1 activity. Accordingly, our results are most consistent with the notion that metalloporphyrins inhibit LTP via Hmox-independent mechanisms. Since the concentration of ZnPP used in our experiments does not significantly obstruct NOS activity in hippocampal slices (24), the ability of ZnPP to inhibit LTP is probably not due to nonselective effects on Nos. However, because ZnPP also inhibits sGC activity (23, 33), nonselective effects on other components of the putative NO signaling pathway may account for the capacity of ZnPP to block LTP.

In this light, the LTP-like enhancement of synaptic responses due to CO application observed in a previous study could best be explained by the idea that this type of potentiation is either not an LTP-related occurrence, or it is not representative of in vivo mechanisms. For instance, exogenous CO may stimulate GC or other enzymes in slices and lead to potentiation, but no significant amount is generated endogenously by Hmox for this purpose. It might be possible to similarly explain other pharmacological results suggesting Hmox and CO-related function in the olfactory system and cerebellum (12, 17). However, because ZnPP does potently inhibit Hmox, we cannot assume that systems such as olfaction and smooth muscle relaxation are similar to hippocampal LTP with respect to participation of Hmox2 and CO. Hmox2-deficient mice should be appropriate models for testing these systems as well.

Although we best interpret our data as being inconsistent with the notion that CO is a retrograde messenger in LTP, it is unreasonable to exclude CO based solely on analysis of *Hmox2*$^{-/-}$ mice. The examination of LTP in a strain of mice deficient in Hmox1, or ideally, in both *Hmox* genes, would help resolve this issue. It remains imaginable that compensatory mechanisms such as increased production of other retrograde factors manifest themselves in the mutant background and sustain normal capacity for LTP in the

absence of CO production. NO could be involved, as well as other previously suggested retrograde signals, arachidonic acid and platelet-activating factor (34, 35). An extensive pharmacological, biochemical and/or genetic analysis would be necessary in order to discount this possibility.

References

1. Bliss, T. V. P. & Lomo, T. (1973). *J. Physiol.* **232**, 331-356.
2. Kelso, S. R., Ganong, A. H. & Brown, T. H. (1986). *Proc. Natl. Acad. Sci. USA* **83**, 5326-5330.
3. Collingridge, G. L., Kehl, S. J. & McLennan, H. (1983). *J. Physiol.* **334**, 33-46.
4. Bliss, T. V. P. & Collinridge, G. L. (1993). *Nature* **361**, 31-39.
5. Manabe, T. & Nicoll, R. A. (1994). *Science* **265**, 1888-1892.
6. Stevens, C. F. & Wang, Y. (1994). *Nature* **371**, 704-707.
7. Schuman, E. M. & Madison, D. V. (1991). *Science* **254**, 1503-1506.
8. O'Dell, T. J., Hawkins, R. D., Kandel, E. R. & Arancio, O. (1991). *Proc. Natl. Acad. Sci. USA* **88**, 11285-11289.
9. Williams, J. H., Li, Y.-G., Nayak, A., Errington, M.L., Murphy, K. P. S. J. & Bliss, T. V. P. (1993). *Neuron* **11**, 877-884.
10. O'Dell, T. J., Huang, P. L., Dawson, T. M., Dinerman, J. L., Snyder, S. H., Kandel, E. R. & Fishman, M. C. (1994). *Science* **265**, 542-546.
11. Maines, M. D. (1988). *FASEB J.* **2**, 2557-2568.
12. Verma, A., Hirsch, D. J., Glatt, C. E., Ronnett, G. V. & Snyder, S. H. (1993). *Science* **259**, 381-384.
13. Ewing, J. F., Haber, S. N. & Maines, M. D. (1992). *J. Neurochem.* **58**, 1140-1149.
14. Ewing, J. F. & Maines, M. D. (1993). *J. Neurochem.* **60**, 1512-1519.
15. Utz, J. & Ullrich, V. (1991). *Biochem. Pharmacol.* **41**, 1195-1201.
16. Farrugia, G., Irons, W. A., Rae, J. L., Sarr, M. G. & Szurszewski, J. H. (1993). *Am. J. Physiol.* **264**, G1184-G1189.
17. Nathanson, J. A., Scavone, C., Scanlon, C. & McKee, M. (1995). *Neuron* **14**, 781-794.
18. Stevens, C. F. & Wang, Y. (1993). *Nature* **364**, 147-149.
19. Zhuo, M., Small, S. A., Kandel, E. R. & Hawkins, R. D. (1993). *Science* **260**, 1946-1950.
20. Zhuo, M., Hu, Y., Schultz, C., Kandel, E. R. & Hawkins, R. D. (1994). *Nature* **368**, 635-639.
21. Ignarro, L. J. (1989). *Sem. Hematol.* **26**, 63-76.
22. Brune, B., Schmidt, K. U. & Ullrich, V. (1990). *Eur. J. Biochem.* **192**, 683-688.
23. Ignarro, L. J., Ballot, B. & Wood, K. S. (1984). *J. Biol. Chem.* **259**, 6201-6207.
24. Meffert, M. K., Haley, J. E., Schuman, E. M., Schulman, H. & Madison, D. V. (1994). *Neuron* **13**, 1225-1233.
25. Rotenberg, M. O. & Maines, M. D. (1990). *J. Biol. Chem.* **265**, 7501-7506.
26. Bradley, A. (1987) in *Teratocarcinomas and Embryonic Stem Cells: A Practical Approach*, ed. Robertson, E. (IRL Press, Oxford), pp. 113-151.
27. Sunderman, F. W., Downs, J. R., Reid, M. R. & Bibeau, L. M. (1982). *Clin. Chem.* **28**, 2026-2032.
28. McCoubrey, W. K. & Maines, M. D. (1994). *Gene* **130**, 155-161.
29. Trakshel, G. M., Kutty, R. K. & Maines, M. D. (1988). *Arch. Biochem. Biophys.* **260**, 732-739.
30. Yoshida, T. & Kikuchi, G. (1978). *J. Biol. Chem.* **253**, 4224-4229.
31. Trakshel, G. M., Kutty, R. K. & Maines, M. D. (1986). *J. Biol. Chem.* **261**, 411-419.
32. Maines, M. D. & Trakshel, G. M. (1992). *Biochim. Biophys. Acta* **1131**, 166-174.
33. Luo, D. & Vincent, S. (1994). *Eur. J. Pharmacol.* **267**, 263-267.

34. Williams, J. H., Errington, M. L., Lynch, M. A. & Bliss, T. V. P. (1989). *Nature* **341**, 739-742.
35. Kato, K., Clark, G. D., Bazan, N. G. & Zorumski, C. F. (1994). *Nature* **367**, 175-179.

Fig. 1. Targeted disruption of the *Hmox2* gene. A, *Hmox2* genomic locus and targeting vector. A 3.4 kb region including exons corresponding to rat exons 4 and 5 was replaced with a *pgk-neo* cassette. The murine *Hmox2* exon-intron structure has not yet been conclusively determined. 5' and 3' probes used for screening ES cell clones and genotyping mice are shown. The 3' probe hybridizes to a 20 kb EcoRV fragment containing the native *Hmox2* gene and a 6 kb EcoRV fragment from the disrupted gene. Abbreviations: E = EcoRI site; R = EcoRV; S = SpeI; X = XbaI. B, Southern blot analysis of EcoRV-digested tail DNA from ES cell-derived mice. The blot was hybridized with the 3' *Hmox2* probe. Genotypes of one *Hmox2* homozygous mutant mouse (-/-), one wild-type mouse (+/+), and four heterozygotes (+/-) are indicated. C, Northern blot analysis of total RNA from the brain of a wild type (+/+) and a homozygous mutant (-/-) mouse. The blot was probed with a region of murine *Hmox2* sequence contained in putative exon 4, which recognizes an mRNA in wild type samples of approximately 1.8 kb, corresponding to the *Hmox2* message. This band is absent in RNA samples from mutant mice. Similar results were obtained after probing with a full length rat *Hmox2* cDNA probe (data not shown). Afterwards, blots were probed with a human *B-actin* cDNA fragment to control for amounts loaded. D, Hmox activity, as measured by bilirubin production with hemin substrate, in wild-type (WT) and *Hmox2*$^{-/-}$ mice. Data are shown as mean ± SEM. Each value represents 8-10 assays done in two or three experimental trials. A star indicates that no Hmox activity was detected in *Hmox2*$^{-/-}$ brains.

A

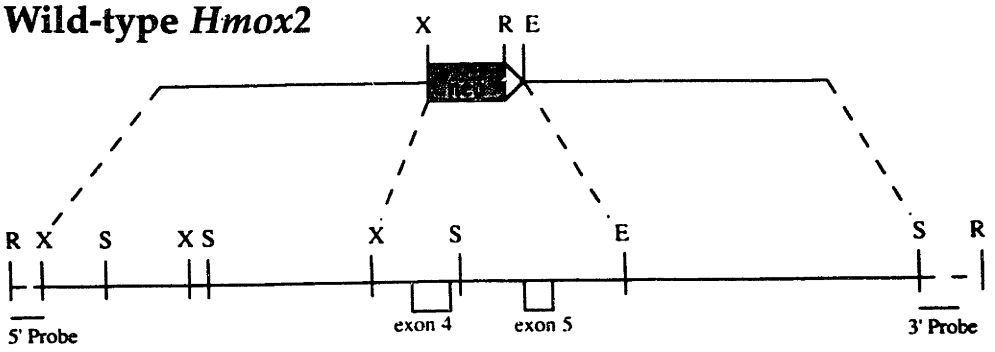
Wild-type Hmox2
X
R E
R X S X S X S E S R
5' Probe
exon 4
exon 5
3' Probe
Mutant Hmox2
R X S X S X R E S R
5' Probe
3' Probe

B

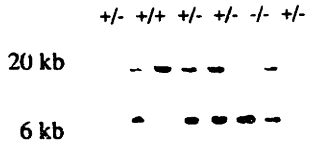
+/- +/+ +/- +/- -/- +/-
20 kb
6 kb

C

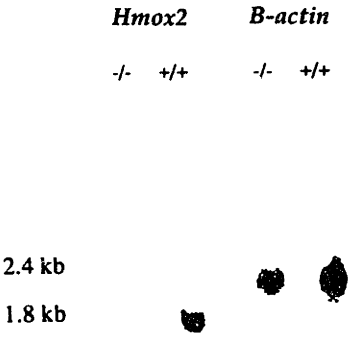
Hmox2
B-actin
-/- +/+
-/- +/+
2.4 kb
1.8 kb

D

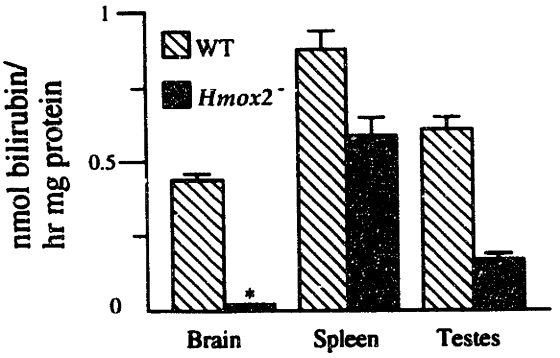
nmol bilirubin/
hr mg protein
1
0.5
0
WT
Hmox2
*
Brain
Spleen
Testes

Fig. 2. LTP induced by both high- and low-frequency stimulation protocols is normal in *Hmox2*$^{-/-}$ mice. A, LTP was induced by two trains of high-frequency stimulation (100 Hz, 1 s duration, 10 s inter-train interval) delivered at time zero. The amount of potentiation seen 60 min after high frequency stimulation in slices from *Hmox2*$^{-/-}$ mice (*Hmox2*$^{-/-}$; filled circles, n = 6 mice, 13 slices) is not different from that observed in slices from wild-type slices (WT; open circles, n = 6 mice, 13 slices). Each point is the mean response (normalized to pre-tetanus baseline levels), and error bars (SEM) are shown every 5 min. The traces at the top show field EPSPs recorded just before (smaller response) and 60 min after (larger response) high-frequency stimulation. Calibration bars are 2.0 mV and 5.0 ms. B-D, 900 pulses of 20 Hz (B), 10 Hz (C), or 5 Hz (D) stimulation were delivered beginning at time zero. Following an initial depression, field EPSPs potentiated to different levels depending on the frequency of synaptic stimulation. At each frequency, the amount of LTP observed 60 min later was not significantly different in slices from *Hmox2*$^{-/-}$ mice (*Hmox2*$^{-/-}$;filled circles) and wild-type controls (WT; open circles). Average data were obtained from the following: (B) wild-type: n =4 mice, 10 slices; *Hmox2*$^{-/-}$: n = 4 mice, 9 slices, (C) wild-type: n = 4 mice, 9 slices; *Hmox2*$^{-/-}$: n = 5 mice, 12 slices, (D) wild-type: n = 6 mice, 15 slices; *Hmox2*$^{-/-}$: n = 5 mice, 14 slices.

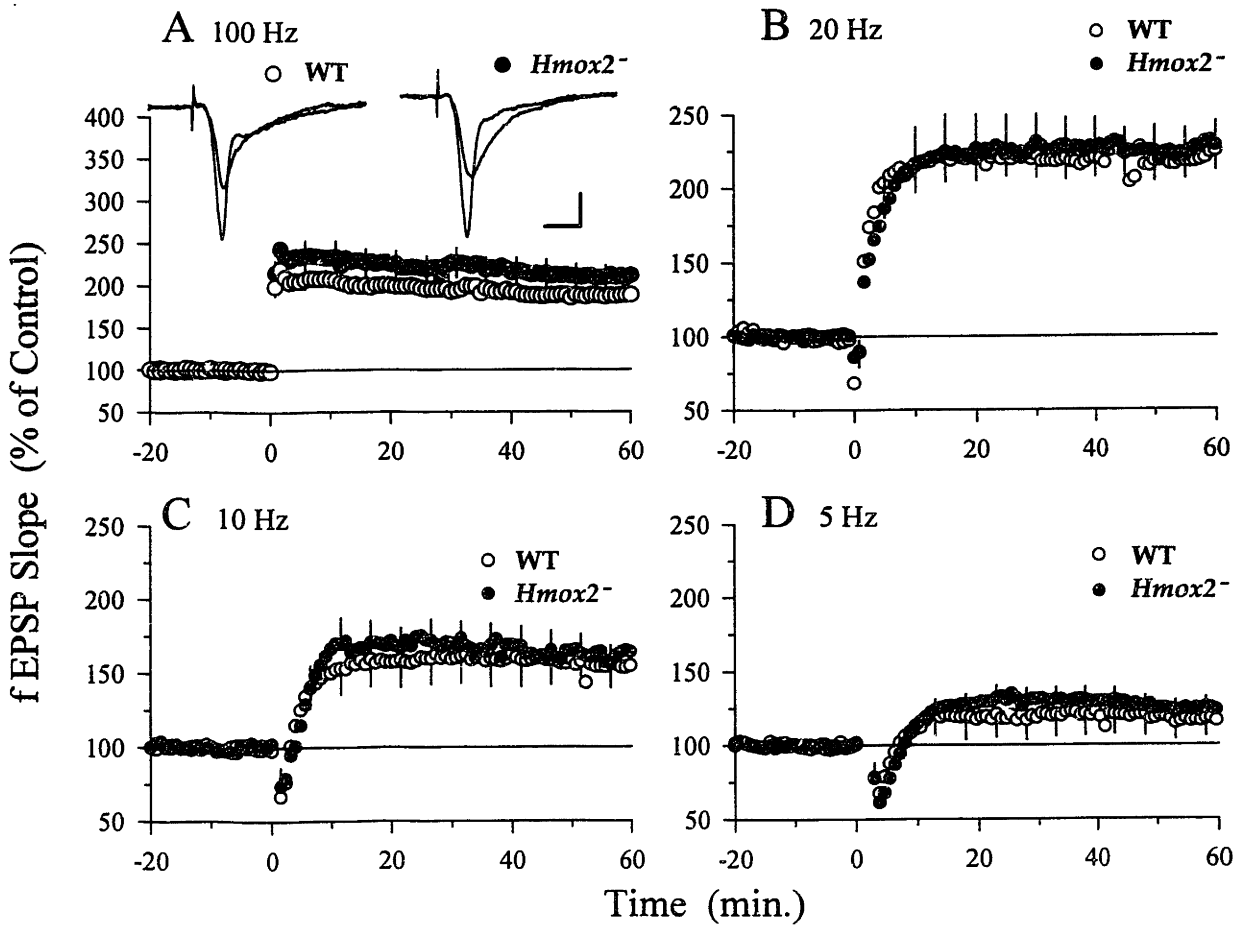
A 100 Hz
WT
Hmox2-
B 20 Hz
WT
Hmox2-
C 10 Hz
WT
Hmox2-
D 5 Hz
WT
Hmox2-
f EPSP Slope (% of Control)
Time (min.)
400
350
300
250
200
150
100
50
-20
0
20
40
60

Fig. 3. Intracellular LTP induced by pairing protocol is normal in *Hmox2*$^{-/-}$ mice. Pairing postsynaptic depolarization with 40 presynaptic stimulation pulses (at time zero) produces similar amounts of LTP in CA1 pyramidal cells from *Hmox2*$^{-/-}$ (*Hmox2*$^{-/-}$; filled circles, n = 5 mice, 9 cells) and wild-type mice (WT; open circles, n = 4 mice, 8 cells). Traces show intracellular EPSPs recorded from CA1 pyramidal cells in slices from wild-type (left) and *Hmox2*$^{-/-}$ mice (right) just before (smaller responses) and 60 min after inducing LTP (larger responses). Calibration bars are 5.0 mV and 10.0 ms.

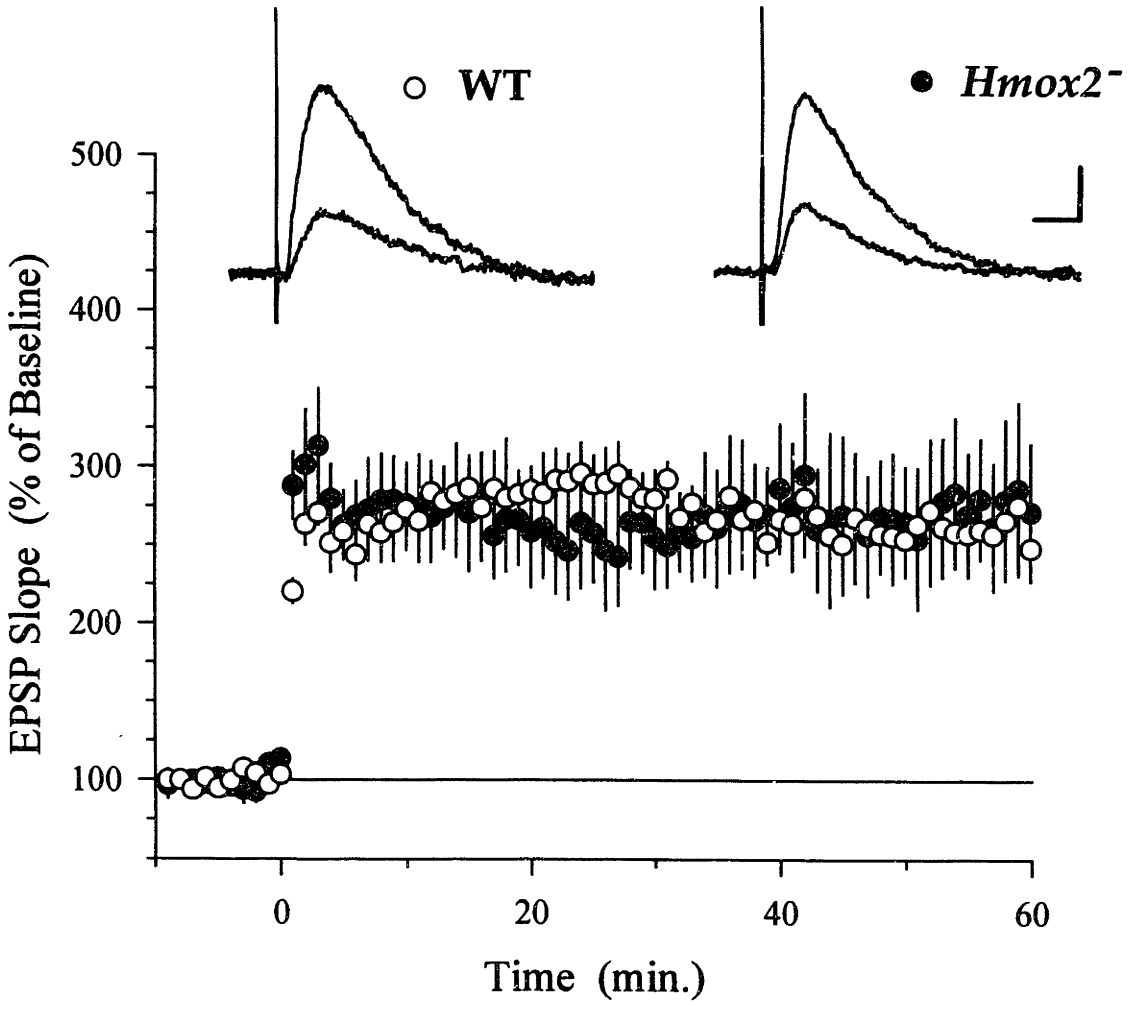
WT
Hmox2-
500
400
300
200
100
EPSP Slope (% of Baseline)
0
20
40
60
Time (min.)

Fig. 4 ZnPP inhibits CA1 LTP in slices from wild-type and *Hmox2*$^{-/-}$ mice. Slices were continuously bathed in ZnPP (beginning at least 30 min prior to high-frequency stimulation) and LTP was induced with a single train of 100 Hz stimulation (1 s duration). In control experiments (open circles), this protocol produced similar amounts of LTP in slices from (A) wild-type (WT; n = 5 mice, 11 slices) and (B) *Hmox2*$^{-/-}$ mice (*Hmox2*$^{-/-}$; n = 5 mice, 11 slices). ZnPP (filled circles) produced a comparable, although incomplete block of LTP in slices from (A) wild-type (n = 5 mice, 11 slices) and (B) *Hmox2*$^{-/-}$ mice (n = 4 mice, 8 slices).

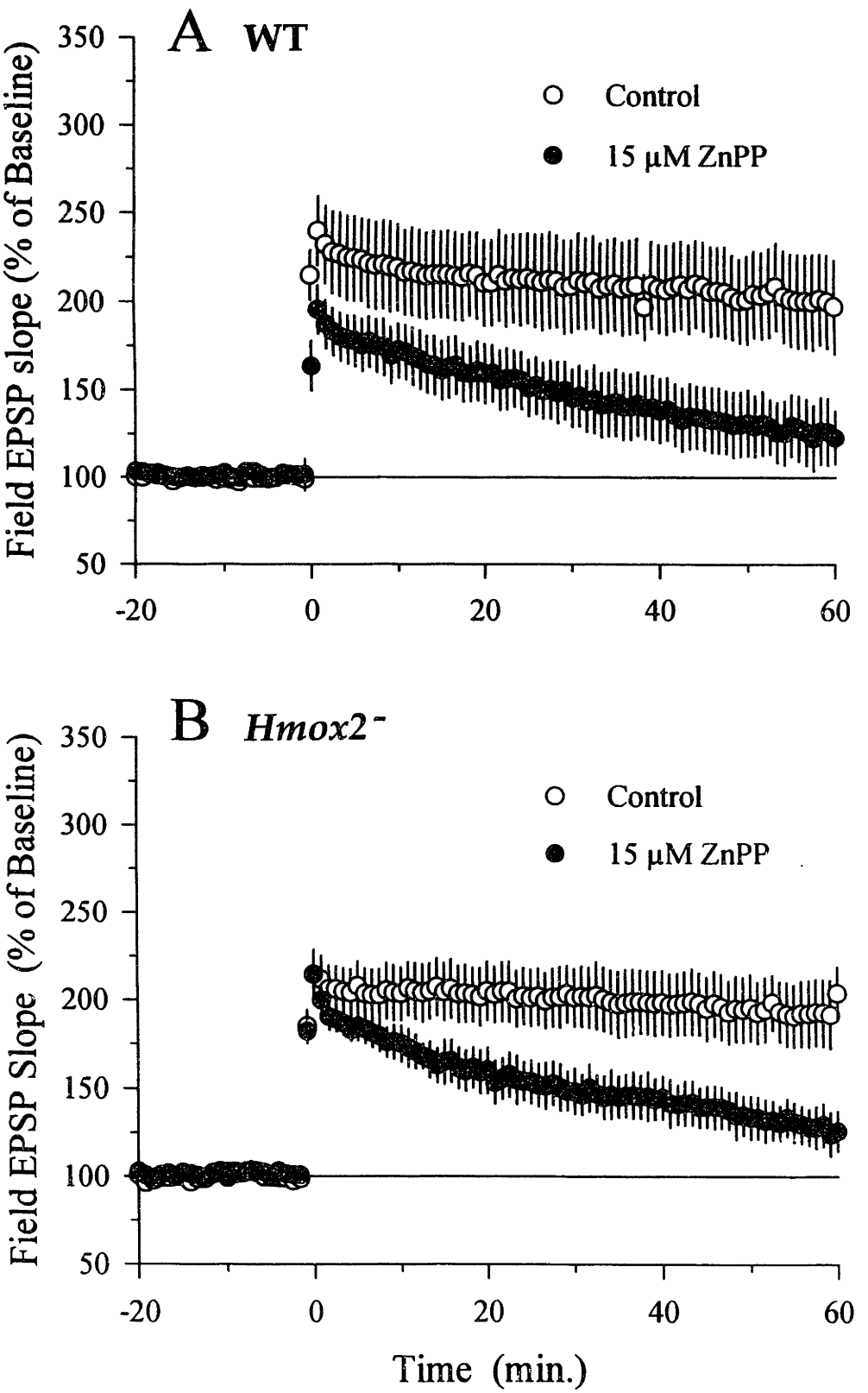
A WT
Control
15 μM ZnPP
Field EPSP slope (% of Baseline)
350
300
250
200
150
100
50
-20
0
20
40
60
B Hmox2-
Control
15 μM ZnPP
Field EPSP Slope (% of Baseline)
350
300
250
200
150
100
50
-20
0
20
40
60
Time (min.)

Chapter 3

Heme Oxygenase-1 Is Required For Mammalian Iron Reutilization

Note: This work is adapted from that published in *Proc. Natl. Acad. Sci. USA* **94**, pp. 10919-10924, by Kenneth D. Poss and Susumu Tonegawa.

Summary

The majority of iron essential for mammalian biological activities such as erythropoiesis is thought to be recycled from cellular hemoproteins. Here, we generated mice lacking functional heme oxygenase-1 (Hmox1), which catabolizes heme to biliverdin, carbon monoxide, and free iron, to assess its participation in iron homeostasis. Many *Hmox1*$^{-/-}$ fetuses died during midgestation, displaying anemia, growth retardation, and placental dysmorphogenesis. Surviving *Hmox1*$^{-/-}$ adult mice developed an anemia associated with abnormally low serum iron levels, yet accumulated hepatic and renal iron that contributed to macromolecular oxidative damage, tissue injury, and chronic inflammation. Our results indicate important roles for Hmox1 in midgestational development and in adult iron reutilization.

Introduction

Iron is a crucial ligand in virtually all cell types for a vast number of cellular processes, including ATP generation, oxygen transport, and detoxification. It has catalytic function within heme or iron-sulfur clusters, or directly bound to proteins. Iron metabolism disorders are quite common in the human population. For instance, dietary iron deficiency results in millions of cases of anemia yearly, while functional hypoferremia contributes to the anemia that is frequently observed in chronic inflammatory diseases (1). While these conditions result from iron insufficiency, other human disorders are caused by excessive iron storage. Notably, free iron is a potent oxidant that damages cellular macromolecules, presumably through reaction with hydrogen peroxide to form the deleterious hydroxyl radical (2). Frequent blood transfusions often result in iron overloading and related symptoms, requiring iron chelation therapy. In addition, hereditary hemochromatosis, a disorder of increased iron absorption and storage yielding multiorgan pathology, affects approximately 1 in 200 individuals within the Caucasian population (3). Therefore, it is important to understand iron metabolism not only at the molecular and cellular levels, but at the level of the whole organism.

Normally in humans, about 1 mg of iron is absorbed by the intestine daily, and at the same time an approximately equal amount is eliminated from the body. Remarkably, this dietary iron accounts for only 1-3% of the iron that is supplied daily to the blood. Most of the iron requirement is provided through reutilization from existing total body stores of 3-4 g, of which about 70% is maintained within hemoglobin (4). From these facts, it is clear that dissociation of iron from heme moieties and subsequent cellular release constitute a major component of iron homeostasis. Nevertheless, the mechanisms and regulation of heme iron reutilization are poorly understood.

Mammalian heme oxygenase (Hmox; also known as HO), which catabolizes cellular heme to biliverdin, carbon monoxide, and free iron, is represented by two isoforms, Hmox1 and Hmox2, encoded by separate genes. Evidence has recently accumulated suggesting that carbon monoxide generated by Hmox2 may be a physiological signaling molecule (5-8). On the other hand, the Hmox1 isoform is thought to provide an antioxidant defense mechanism, based on its marked upregulation in stressed cells (9-12). Both Hmox isoforms might be largely responsible for the recycling of iron via its liberation from heme and hemoproteins, although their contribution to total iron homeostasis has not been carefully examined.

Here, to study the extent to which Hmox1 participates in iron homeostasis, we generated mice with targeted *Hmox1* null mutations and analyzed parameters of iron metabolism. We initially found that Hmox1 is required in utero for normal placental and

embryonic development. Furthermore, we discovered that adult Hmox1-deficient animals develop both serum iron deficiency and pathological iron-loading, suggesting that Hmox1 is crucial for the expulsion of iron from tissue stores.

Materials and Methods

Hmox1 Targeting Vector

The published murine *Hmox1* cDNA sequence was utilized for synthesis of primers toward generating a DNA probe by PCR amplication of genomic DNA (13). This probe had sequence contained in exon 5 of the murine *Hmox1* gene, and was used to screen a λEMBL3 library containing 129/Sv strain genomic fragments, from which the *Hmox1* gene was obtained. A 4.4 kb HindIII-XhoI fragment and a 4.0 kb HindIII fragment were used as 5' and 3' arms of the contruct, surrounding a 1.8 kb *pgk-neo* fragment in pBluescript KS(+). The construct was designed to remove a 3.7 kb XhoI-HindIII fragment of murine DNA with intron sequence and coding sequence containing the final 226 amino acids.

Targeting Experiments and Generation of *Hmox1*$^{-/-}$ Mice

D3 ES cells were utilized for transfection as previously described (14). Genomic DNA for KpnI restriction digests was isolated from 240 colonies grown in 24-well plates. Southern blotting and hybridization with the 5' 160 bp external probe or the 3' 250 bp internal probe revealed that approximately 25% of the colonies were homologous recombinants. Three of these positive clones were used for injection into C57BL/6 blastocysts. Chimeric mice were generated as described (15). *Hmox1*$^{+/-}$ mice were obtained by mating male chimeras with C57BL/6 females; these *Hmox1*$^{+/-}$ animals were intercrossed to produce *Hmox1*$^{-/-}$ mice. Genotypes of mice were determined by Southern analysis of progeny tail DNA as described above. In vitro fertilization with sperm from *Hmox1*$^{-/-}$ mice and eggs from *Hmox1*$^{+/-}$ animals was performed as described (16). Pseudopregnant (C57BL/6 x DBA/2)F1 or Swiss Webster females were used as two-cell embryo recipients.

Serum Iron Parameters

Mice were bled retroorbitally, and 200μl serum from each animal was used for analysis of iron and total iron-binding capacity using a kit (Sigma), and ferritin using an immunoassay kit (Microgenics). All assays were performed by Genox Corporation using a Cobas Fara II chemical analyzer.

Blood Cell Counts and Histology

Blood was obtained by retro-orbital sampling, and blood cell counts were determined using a Coulter automatic cell counter (performed by MIT Division of Comparative

Medicine Laboratories). For histology, tissues were dissected and fixed in 4% paraformaldehyde or 10% formalin for 24 hours, and embedded in paraffin. Four μm mictrotome sections were mounted onto slides and stained with hematoxylin and eosin, Prussian blue-staining methods to detect ferric iron, periodic acid-schiff reagent, or Masson's tri-chrome staining methods using standard procedures.

Analysis of Oxidative Damage

Protein carbonyl content was measured using a protocol slightly modified from previous reports (17, 18). Tissue was dissected, washed in phosphate-buffered saline and disrupted with a tissuemizer. From the soluble protein fraction, 300 μl aliquots containing 1.4-2.5 mg protein were treated with either 300 μl of 2 N HCl (control) or 300 μl of 10 mM 2,4-dinitrophenylhydrazine dissolved in 2 N HCl. Samples were incubated at room temperature for one hour with occasional mixing, precipitated with an equal volume of 20% trichloroacetic acid, and pelleted. The pellet was washed three times with 1 ml of a 1:1 mixture of ethanol/ethyl acetate, and dissolved in 1 ml of 6 M guanidine hydrochloride at 42 ^{o}C. The difference in absorbance between the control and treated samples was determined at 364 nm, and an extinction coefficient of 22 $mM^{-1}cm^{-1}$ for aliphatic hydrazones was used. Results were expressed as nmol carbonyl groups per mg protein. Lipid peroxidation was measured using a kit (Oxis International).

Immunological Analyses

Thymus, spleen, and lymph node single cell suspensions were prepared by disrupting the organs between glass slides. Approximately 1 x 10^6 cells were incubated with labeled antibodies at 4 ^{o}C for 30 minutes. Cells were washed and analyzed with a FACScan (Becton Dickinson) for fluorescein isothiocyanate (FITC) and phycoerythrin (PE) stainings. Cells were initially gated by size and scatter to restrict consideration to live, lymphoid cells. Data from 10,000 cells were collected.

Results

Generation of Mice Containing Targeted *Hmox1* Mutations

A construct was designed to replace 3.7 kb within the murine *Hmox1* locus, including approximately 85% of the coding sequence, with a neomycin resistance cassette containing a *pgk* promoter (Fig. 1*a*). Following standard procedures for the production of recombinant embryonic stem cells and chimeras (see Methods), we generated heterozygous mice in the (129/Sv x C57BL/6) hybrid strain background.

Requirement for Hmox1 in Prenatal Development

Matings between heterozygous mice did not yield the expected Mendelian ratio. As genotyped at weening age, the first several litters included 69 wild-type, 143

heterozygous, and 11 homozygous *Hmox1* mutant animals (hereafter referred to as *Hmox1*$^{+/+}$, *Hmox1*$^{+/-}$, and *Hmox1*$^{-/-}$ mice, respectively; Fig. 1*b*). This *Hmox1*$^{-/-}$ survival percentage was maintained in matings between *Hmox1*$^{-/-}$ and *Hmox1*$^{+/-}$ mice (Table 1); *Hmox1*$^{-/-}$ mating pairs did not yield viable litters. Fig. 1*c* indicates the extreme effects of the targeted mutation on *Hmox1* mRNA expression in *Hmox1*$^{-/-}$ animals.

The majority of *Hmox1*$^{-/-}$ embryos died on embryonic day 10 (E10) or E11, while few mortalities occurred after E16.5 (Table 1). Examination of viable or recently expired *Hmox1*$^{-/-}$ embryos indicated varying degrees of embryonic growth retardation, pallor in the embryo and amniotic sac suggestive of anemia, and most prominently, a reduction in placental size (Fig. 2). Histological analysis revealed no anomalies in *Hmox1*$^{-/-}$ embryonic tissues (data not shown). However, we noticed subtle histological differences between *Hmox1*$^{-/-}$ and *Hmox1*$^{+/-}$ midgestational placentas. For instance, the labyrinth vascular space appeared reduced in many *Hmox1*$^{-/-}$ placentas (Fig. 3). Abnormal placental formation probably contributed to embryonic growth retardation and the high prevalence of midgestational deaths. In support of this reasoning, we could successfully reduce the rate of mortality by altering the maternal placental contribution to *Hmox1*$^{-/-}$ prenatal development. When we transplanted in vitro-fertilized (129/Sv x C57BL/6) *Hmox1*$^{+/-}$ and *Hmox1*$^{-/-}$ embryos into pseudopregnant Swiss Webster mice, the survival rate of *Hmox1*$^{-/-}$ embryos was nearly tripled as compared to natural matings (Table 1).

Because we repeatedly utilized this method to obtain *Hmox1*$^{-/-}$ animals for use in subsequent experiments, *Hmox1*$^{+/-}$ littermates rather than *Hmox1*$^{+/+}$ mice were often used as experimental controls. *Hmox1*$^{-/-}$ neonates, though usually slightly smaller than *Hmox1*$^{+/-}$ or *Hmox1*$^{+/+}$ littermates, survived normally to early adulthood, during which they maintained grossly normal eating, breeding, and grooming behavior.

Hypoferremia and Anemia in Hmox1-Deficient Mice

While mice lacking Hmox1 were indistinguishable from littermates during early adulthood, we noticed that, as early as 25 weeks of age, most *Hmox1*$^{-/-}$ animals became thin and poorly groomed, bred poorly, and appeared less active than *Hmox1*$^{+/+}$ or *Hmox1*$^{+/-}$ mice. Although one *Hmox1*$^{-/-}$ mouse has lived up to 22 months, premature mortalities in *Hmox1*$^{-/-}$ mice after 25 weeks of age were not uncommon. Fig. 4*a* indicates the extent to which the disease reduced average weights of *Hmox1*$^{-/-}$ mice compared to apparently healthy *Hmox1*$^{+/-}$ littermates.

Associated with the disease was an anemia, involving reductions in both erythrocyte number and size, that was present by 20 weeks of age in *Hmox1*$^{-/-}$ animals (Fig. 4*b*). Analyses of blood smears (Fig. 5) and erythrocyte volume (Fig. 4*b*) indicated that this

anemia was microcytic. Although erythocytic hemoglobin concentration was normal in *Hmox1*$^{-/-}$ samples by measurement, blood smears suggested that the anemia was also hypochromic (Fig. 5). Since this description is characteristic of iron deficiency anemia in humans, we analyzed serum iron levels in *Hmox1*$^{-/-}$ mice. As predicted, *Hmox1*$^{-/-}$ serum iron values were severely reduced by 20 weeks of age (Fig. 4*c*). Similarly to hypoferremia caused by iron deficiency, the total iron binding capacity (largely represented by serum levels of transferrin, the major extracellular iron-carrying protein) was high in *Hmox1*$^{-/-}$ mice, resulting in a reduced iron saturation percentage (Fig. 4*c*). These results indicate that heme catabolism by Hmox1 contributes to maintaining the blood iron levels that are necessary for optimal erythropoeisis.

Mice Lacking Functional Hmox1 Accumulate Tissue Iron

Serum levels of ferritin, the main intracellular chelator of iron, typically reflect body iron stores in humans (4). Although *Hmox1*$^{-/-}$ mice displayed serum iron deficiency, we found that they also had significantly increased levels of serum ferritin (Fig. 4*d*). Examination of *Hmox1*$^{-/-}$ organs for iron showed that while no 6-9 week-old *Hmox1*$^{-/-}$ tissues had evidence of iron deposition (as assessed by Prussian blue staining, which recognizes loosely-bound non-heme iron; data not shown), renal proximal cortical tubules of virtually all *Hmox1*$^{-/-}$ mice over 20 weeks contained non-heme iron deposits, likely in the form of hemosiderin and ferritin (Fig. 6*b*). In addition, some 20-24 week and all 40-55 week-old *Hmox1*$^{-/-}$ mice had considerable hepatic iron-staining in both Kupffer cells and hepatocytes (Fig. 6*d, f*). *Hmox1*$^{+/+}$ or *Hmox1*$^{+/-}$ animals had very little or no positive iron-staining in kidneys or liver (Fig. 6*a, c, e*). The amount of stainable iron detected in other *Hmox1*$^{-/-}$ organs appeared normal (data not shown), including that in spleen, which is normally the organ with highest Hmox1 activity (19).

Iron-loading had a range of pathological consequences in *Hmox1*$^{-/-}$ mice, mildly evident by 20-24 weeks of age, when the anemia and iron deposition were first noticed, and more severe by 40-55 weeks of age. To assess oxidative stress that may have resulted from iron deposition, we analyzed levels of oxidized proteins and lipids in tissues of 20-24 week-old *Hmox1*$^{-/-}$ and *Hmox1*$^{+/-}$ mice. *Hmox1*$^{-/-}$ livers showed increases in oxidized proteins and lipid peroxidation values of 51% and 95% over *Hmox1*$^{+/-}$ values, respectively, while kidneys had increases of 69% and 74% (Fig. 7*a*). Furthermore, *Hmox1*$^{-/-}$ mice contracted a progressive chronic inflammatory disease, demonstrated by enlarged spleens (due to both extra-medullary hematopoeisis and follicular hyperplasia) and lymph nodes, high peripheral white blood cell counts, high splenic and lymph node CD4^{+}:CD8^{+} T-cell ratios (Fig. 7*b*) with numerous activated CD4^{+} T cells (data not shown), and consistently observed hepatic inflammatory cell

infiltrates, composed of lymphocytes, plasma cells, neutrophils, and macrophages (Fig. 8*a*, *b*). Fibrosis was evident within infiltrates (Fig. 7*c*), and regenerative nodules indicative of hepatic injury were occasionally noted (see Fig. 6*b*). While many of the infiltrates were periportal (as in Fig. 8*c*), others had a predilection for the portal venous tissue itself, which often contained iron deposits. Notably, we observed many instances where monocytes had adhered to vessel walls, a hallmark of vascular injury (Fig. 8*d*, *e*). Occasionally observed were vascular and perivascular infiltrates in *Hmox1*$^{-/-}$ lungs (data not shown), and glomerulonephritis, which may have been caused either by iron toxicity or by deposition of immune complexes (Fig. 8*f*, *g*).

The appearance of pathological iron-loading in *Hmox1*$^{-/-}$ tissues temporally correlated with the diminishing of serum iron levels. The simplest explanation for these results is that *Hmox1*$^{-/-}$ mice have a defect in iron reutilization, that is, delivery from tissue stores to blood. An unusually large amount of non-heme iron accumulates in *Hmox1*$^{-/-}$ tissues. We suggest that this iron originates from heme being catabolized through an Hmox1-independent pathway. Therefore, our interpretation is that Hmox1 activity predominantly contributes to extracellular release of iron, while an alternative heme-metabolizing pathway(s) mainly leads to its intracellular storage.

Discussion

The extent to which Hmox1 is required for mammalian iron metabolism had been unknown. In this paper, we addressed this issue by generating and analyzing mice homozygous for a null mutation within the *Hmox1* gene. We found that although many *Hmox1*$^{-/-}$ mice die prenatally because of placental deformities, surviving adult *Hmox1*$^{-/-}$ mice develop serum iron deficiency and excessive tissue iron deposition, indicative of defects in the release of cellular iron to blood.

Role of Hmox1 in Iron Reutilization

The bulk of total body iron is contained within cellular heme moieties. The two symptoms associated with a Hmox1 deficiency, hypoferremia and iron-loading, illustrate the requirement of Hmox1-mediated heme catabolism as a part of physiological iron homeostasis. Our study also defines at least two distinct cellular mechanisms for the employment of catabolized heme iron. One is the Hmox1-dependent pathway, where free iron liberated from heme is released relatively efficiently to the extracellular space. It is unknown how Hmox1 accomplishes this, but we speculate that Hmox1-dependent cellular iron discharge may depend on the microsomal location of Hmox, which could allow interaction of the free iron product with recycling endosomal transferrin and transferrin receptors or with yet-unidentified iron transporters. The second pathway of

heme catabolism, independent of Hmox1, seems to generate free iron that is predominantly shuttled to intracellular stores such as ferritin. In fact, that heme might be catabolized by an alternative mechanism was implied in a previous study, which indicated that less than 50% of endogenous hepatic heme degradation in rats was accounted for by measurement of the exhaled Hmox product, carbon monoxide (20). Possible minor mediators of heme degradation include microsomal NADPH-dependent cytochrome P-450 reductase, a cytosolic xanthine oxidase, and a mitochondrial heme-degrading activity not fully characterized (21).

The Hmox isoform Hmox2 is an obvious candidate for carrying out an Hmox1-independent heme catabolic pathway. Hmox2 is chiefly distinguished from Hmox1 by its regulation, as it is constitutively expressed at relatively high levels in most major organs. However, our previous work indicated that mice lacking functional Hmox2 have no anemia or iron deposition (14; K. D. P., unpublished data). Therefore, it is unclear whether Hmox2 is linked to either of the two catabolic mechanisms mentioned above.

Conspicuous *Hmox1*$^{-/-}$ iron-loading is only observed in renal cortical tubules, Kupffer cells, hepatocytes, and hepatic vascular tissue. Interestingly, preliminary work has indicated that irradiated *Hmox1*$^{+/+}$ mice reconstituted with Hmox1-deficient bone marrow do not show anemia or hepatic and renal iron deposition at 20 weeks after transplantation (K. D. P. and S. Marusic-Galesic, unpublished data). These results suggest that, although hemolysis usually occurs in phagocytic cells (22), the parenchymal cells of the liver and kidney, which are known to incorporate the vast majority of plasma heme (20, 23), are important mediators of Hmox1-dependent heme iron reutilization.

Developmental Role of Hmox1

In addition to elucidating the role of Hmox1 in adult mice, we found that Hmox1 is required prenatally for normal murine embryonic and placental development. Most deaths in *Hmox1*$^{-/-}$ pups occur between E10 and E11, when the function of the placenta is first required in mice (24). In addition, the clearest anatomical defect in Hmox1-deficient pups was a reduction in placental size. Interestingly, we were able to circumvent a significant proportion of midgestational deaths by transplantation of *Hmox1*$^{-/-}$ embryos into mice of different strain backgrounds. This maternal enhancement of survival must be due to a change in either the backgound strain or the *Hmox1* genotype. We were unable to directly test this, since the (C57BL/6 x 129/Sv) hybrid strain females used for natural mating appear to be very poor embryo recipients (K. D. P., unpublished observations). However, we have observed that in *Hmox1*$^{+/-}$ x *Hmox1*$^{-/-}$ matings, the *Hmox1* genotype of the mother does not affect *Hmox1*$^{-/-}$ pup survival. Therefore, we

suspect that the maternal strain background mainly affects survival of *Hmox1*$^{-/-}$ pups, presumably by alterations in placental anatomy/physiology.

How Hmox1 contributes to prenatal development at a molecular level is unclear. One possibility is that Hmox1 participates in the derivation of iron, which is thought to stem from hemolysis of maternal erythrocytes by placental trophoblastic giant cells and endothelial cells (25, 26). If this is true, an excess of heme iron might damage placental vasculature in the absence of Hmox1, or fetal iron deficiency might affect placental formation. Experiments examining the maternal provision of iron to *Hmox1*$^{-/-}$ pups may be informative in better determining the nature of the placental Hmox requirement. Interestingly, while mice lacking the Hmox2 isoform complete gestation (14), embryos containing homozygous null mutations in both *Hmox1* and *Hmox2* genes die prenatally with complete penetrance. From 140 progeny derived from matings of *Hmox1*$^{+/-}$ *Hmox2*$^{-/-}$ mice, 96 were heterozygous at the *Hmox1* locus while 44 were wild-type. This indicates a strict early developmental requirement for some form of Hmox activity.

Mouse Model of Iron Retention

The *Hmox1*$^{-/-}$ mouse described here represents an animal model of human iron overload disorders. Parenchymal iron-loading displayed by *Hmox1*$^{-/-}$ animals constitutes the most obvious similarity with hereditary hemochromatosis, which is caused by a mutation in a non-classical MHC class I-type gene (27). Several other symptoms of of *Hmox1*$^{-/-}$ mice are similar to those shown by hemochromatosis patients. These include the progression of symptoms, splenomegaly, high $CD4^+$:$CD8^+$ T-cell ratios, increased lipid peroxidation, fibrosis and hepatic injury, late-onset weight loss, decreased mobility, and premature mortality (3, 28). Furthermore, mature *Hmox1*$^{-/-}$ males have a nearly 25% reduction in the size of testes as compared with similarly-sized *Hmox1*$^{+/-}$ littermates (mean ± SEM; *Hmox1*$^{+/-}$: 258 ± 15 mg, *Hmox1*$^{-/-}$: 197 ± 8 mg; Student's *t* test: $n = 12$, $p < 0.002$). Hypogonadism and lack of libido are common in males affected with hereditary hemochromatosis.

Interestingly, symptoms of *Hmox1*$^{-/-}$ mice are also similar to those of patients with anemia of chronic inflammation, who also show hypoferremia with increased serum ferritin and tissue iron stores (1, 29). Hmox1 activity is normally strongly upregulated by inflammatory cytokines (30-32), and the enzyme appears to be important in preserving serum iron levels and reducing inflammation in mice. Therefore, it is conceivable that an iron release pathway involving Hmox1 is downregulated in the course of chronic inflammatory illnesses. In this light, modulation of Hmox1 activity might be a novel therapeutic approach to improve serum iron levels and perhaps even reduce the extent of

inflammation in chronically ill patients. The *Hmox1*$^{-/-}$ mouse appears to provide an especially useful model of this prevalent iron metabolic disorder.

References

1. Means, R. T. & Krantz, S. B. (1992). *Blood* **80**, 1639-1647.
2. Halliwell, B. & Gutteridge, J. M. C. (1990). *Meth. Enzymol.* **186,** 1-85.
3. Bacon, B. R. & Tavill, A. S. (1996) in *Hepatology. A Textbook of Liver Disease*, eds. Zakim, D. & Boyer, T. D. (Saunders, Philadelphia), pp. 1439-1472.
4. Bothwell, T. H., Charlton, R. W. & Motulsky, A. G. (1995) in *The Metabolic and Molecular Bases of Inherited Disease*, eds. Scriver, C. R., Beaudet, A. L., Sly, W. S. & Valle, D. (McGraw-Hill, New York), pp. 2237-2269.
5. Verma, A., Hirsch, D. J., Glatt, C. E., Ronnett, G. V. & Snyder, S. H. (1993). *Science* **259**, 381-384 .
6. Nathanson, J. A., Scavone, C., Scanlon, C. & McKee, M. (1995). *Neuron* **14**, 781-794 .
7. Zakhary, R., Gaine, S. P., Dinerman, J. L., Ruat, M., Flavahan, N. A., & Snyder, S. H. (1996). *Proc. Natl. Acad. Sci. USA* **93**, 795-798.
8. Zakhary, R., Poss, K. D., Jaffrey, S. R., Ferris, C. D., Tonegawa, S., & Snyder, S. H. (submitted)
9. Keyse, S. M. &Tyrrell, R. M. (1989). *Proc. Natl. Acad. Sci. USA* **86,** 99-103.
10. Eisenstein, R. S., Garcia-Mayol, D., Pettingell, W. & Munro, H. N. (1991). *Proc. Natl. Acad. Sci. USA* **88**, 688-692 .
11. Ewing, J. F. & Maines, M. D. (1991). *Proc. Natl. Acad. Sci. USA* **88**, 5364-5368.
12. Kutty, R. K., Kutty, G., Wiggert, B., Chader, G. J., Darrow, R. M., & Organisciak, D. T. (1995). *Proc. Natl. Acad. Sci. USA* **92**, 1177-1181.
13. Shibahara, S., Muller, R., Taguchi, H. & Yoshida, T. (1985). *Proc. Natl. Acad. Sci. USA* **82**, 7865-7869.
14. Poss, K. D., Thomas, M. J., Ebralidze, A. K., O'Dell, ... J. & Tonegawa, S. (1995). *Neuron* **15,** 867-873.
15. Bradley, A. (1987) in *Teratocarcinomas and Embryonic Stem Cells: A Practical Approach*, ed. Robertson, E. (IRL Press, Oxford), pp. 113-151.
16. Hogan, B., Constantini, F. & Lacy, E. (1986) *Manipulating the Mouse Embryo.* (Cold Spring Laboratory Press, Cold Spring Harbor).
17. Oliver, C. N., Ahn, B., Moerman, E. J., Goldstein, S. & Stadtman, E. R. (1987). *J. Biol. Chem.* **262,** 5488-5491.
18. Sohal, R. S., Agarwal, S., Dubey, A. & Orr, W. C. (1993). *Proc. Natl. Acad. Sci. USA* **90**, 7255-7259.
19. Braggins, P. E., Trakshel, G. M., Kutty, R. K. & Maines, M. D. (1986). *Biochem. Biophys. Res. Commun.* **141,** 528-533.
20. Bissell, D. M. & Guzelian, P. S. (1980). *J. Clin. Invest.* **65,** 1135-1140.
21. Maines, M. D. (1997). *Annu. Rev. Pharmacol. Toxicol.* **37**, 517-554.
22. Noyes, W. D., Bothwell, T. H. & Finch, C. A. (1960). *Br. J. Haematol.* **6**, 43-55.
23. Hershko, C., Cook, J. D. & Finch, C. A. (1972). *J. Lab. Clin. Med.* **80,** 624-634.
24. Copp, A. J. (1995). *Trends Genet.* **11,** 87-93.
25. Dumartin, B. & Canivenc, R. (1992). *Anat. Embryol.* **185**, 175-179.
26. Kaufman, M. H. (1992) in *The Atlas of Mouse Development*, (Academic Press Limited, Cambridge), pp. 469-477.
27. Feder, J. N. et al. (1996). *Nature Genet.* **13**, 399-408.
28. Arosa, F. A., da Silva, A. J., Godinho, I. M., ter Steege, J. C., Porto, G., Rudd, C. E., & de Sousa, M. (1994). *Scand. J. Immunol.* **39,** 426-432.
29. Lee, G. R. (1983). *Semin. Hematol.* **20**, 61-80.
30. Cantoni, L., Rossi, C., Rizzardini, M. & Ghezzi, P. (1991). *Biochem. J.* **279**, 891-894 .
31. Kutty, R. K., Naginemi, G. N., Kutty, G., Hooks, J. J., Chader, G. J., & Wiggert, B. (1994). *J. Cell. Physiol.* **159**, 371-378.

32. Rizzardini, M., Terao, M., Falciani, F. & Cantoni, L. (1993). *Biochem. J.* **290**, 343-347.

Table 1. Viability of Embryos from *Hmox1*$^{-/-}$ x *Hmox1*$^{+/-}$ Matings

Age	Genotype of live animals		Survival percentage
	Hmox1$^{+/-}$	*Hmox1* $^{-/-}$	
E9.5	17	16	97%
E10.5	23	22	98%
E11.5	41	14	51%
E12.5	65	18	43%
E13.5	40	9	37%
E16.5	27	4	26%
E19	28	3	19%
W3	216	26	21%
W3*	236	57	39%
W3**	133	61	63%

E9.5 to E19, and W3 represent days 9.5 to 19 of gestation, and 3 weeks after birth, respectively. Survival percentage is calculated as 100[2(#living *Hmox1*$^{-/-}$)]/total living progeny. *These mice were produced from gametes of (129/Sv x C57BL/6) *Hmox1*$^{-/-}$ and *Hmox1*$^{+/-}$ mice, but had been transplanted as 2-cell embryos into (C57BL/6 x DBA/2)F1* or Swiss Webster** pseudopregnant recipients.

Fig. 1. Targeted disruption of the *Hmox1* gene. *a*, *Hmox1* genomic locus and targeting vector. A 3.7 kb region including exons 3, 4, and a portion of 5 (e3-e5) was replaced with a pgk-neo cassette. The 5' and 3' probes used for screening ES cell clones and genotyping mice are shown. The 5' probe hybridizes to an 11 kb KpnI fragment of the native *Hmox1* gene and a 6.5 kb fragment from the disrupted gene. D, HindIII site; K, KpnI; X, XhoI; Xb, XbaI. *b*, Southern blot analysis of KpnI-digested tail DNA from ES cell-derived mice. The blot was hybridized with the 5' *Hmox1* probe. Genotypes of one *Hmox1* homozygous mutant mouse (-/-), 2 wild-type mice (+/+), and 2 heterozygous mice (+/-) are indicated. *c*, Northern blot analysis of total splenic RNA from a wild-type mouse (+/+), a heterozygous mouse (+/-), and a homozygous mutant mouse (-/-). The blot was hybridized with an *Hmox1* cDNA probe, which recognizes a major mRNA band of approximately 1.5 kb. The *Hmox1* probe recognized an aberrantly-sized mRNA from *Hmox1*$^{-/-}$ mice that was barely detectable even in an overloaded lane.

a

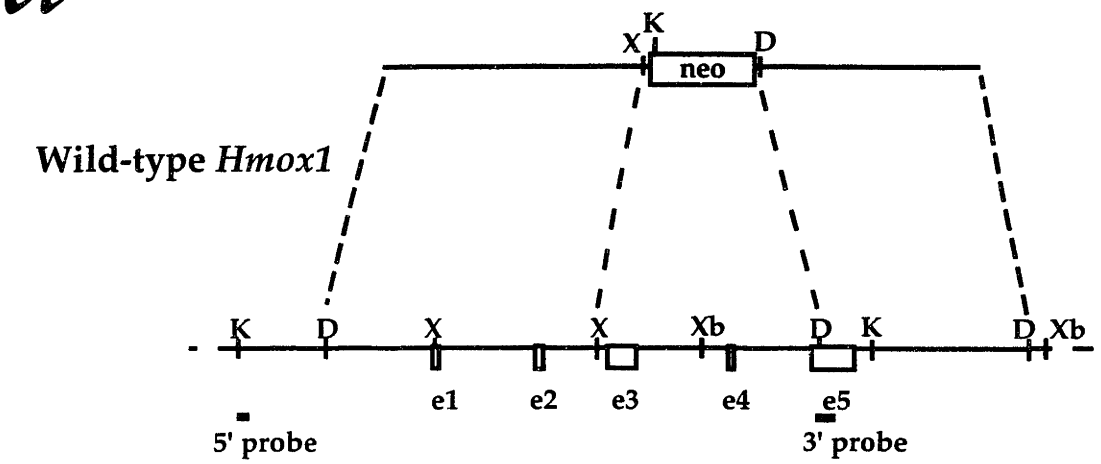
Wild-type *Hmox1*
K
X
D
neo
K
D
X
X
Xb
D
K
D
Xb
e1
e2
e3
e4
e5
5' probe
3' probe
Mutant *Hmox1*
K
K
D
X
X
D
K
D
Xb
neo
e1
e2
e5*
5' probe
3' probe

b

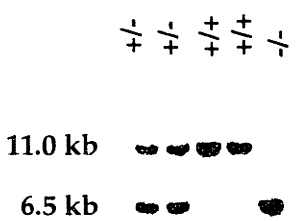
+/-
+/-
+/+
+/+
-/-
11.0 kb
6.5 kb

c

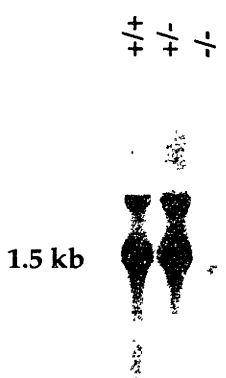
+/+
+/-
-/-
1.5 kb

Fig. 2. Morphology of *Hmox1*$^{-/-}$ embryos and placentas. *a*, Appearance of *Hmox1*$^{+/-}$ and *Hmox1*$^{-/-}$ pups at E10.5. Note the slight reduction in the *Hmox1*$^{-/-}$ embryonic size (right), and the considerable decrease in placental size. *Hmox1*$^{-/-}$ pups were usually viable at this stage, but placentas were consistently small and often very difficult to locate and dissect. *b*, Appearance of *Hmox1*$^{+/-}$ and *Hmox1*$^{-/-}$ pups at E12.5. Note pallor in the *Hmox1*$^{-/-}$ embryo (right), accompanying growth retardation and placental hypoplasia. Most embryonic deaths of *Hmox1*$^{-/-}$ pups had occurred by this stage. View is at a lower magnification of that in (*a*).

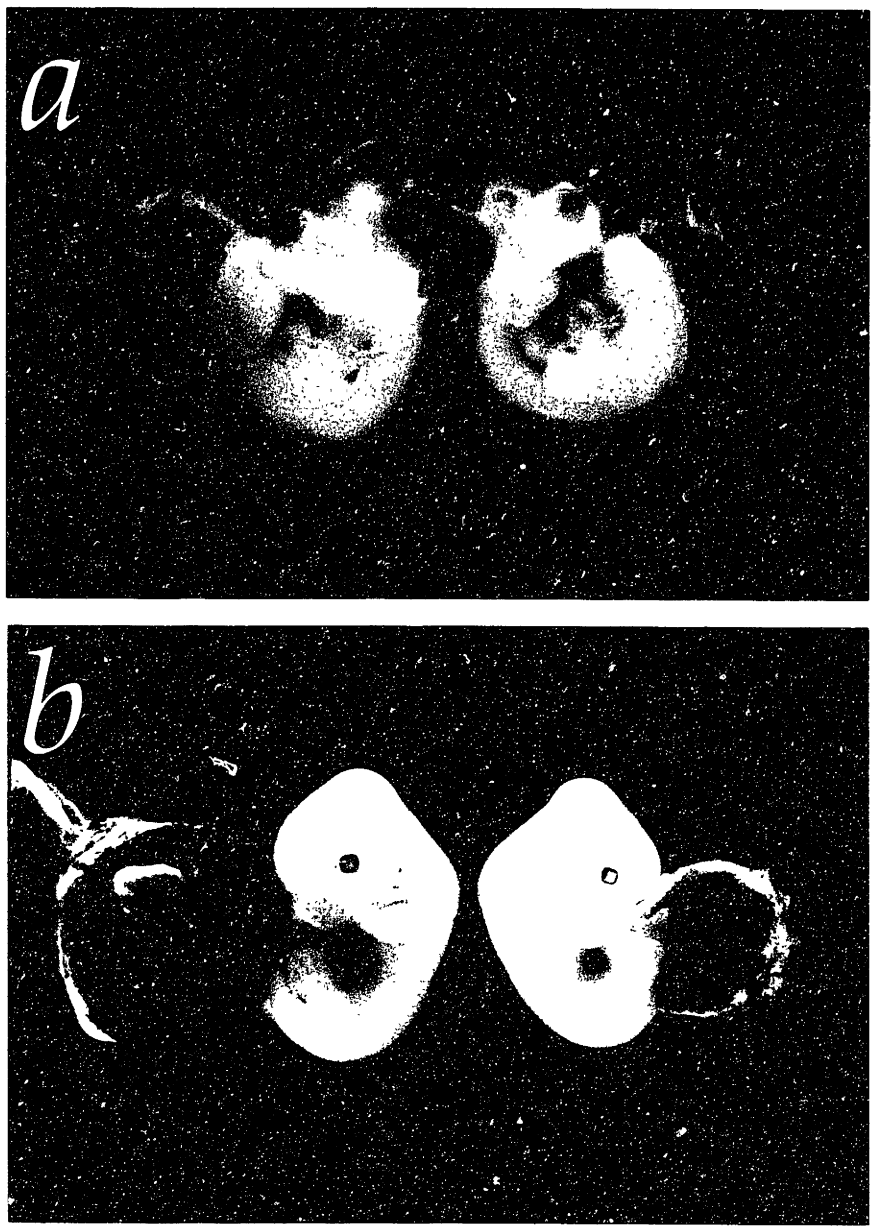
a
b

Fig. 3. Histology of *Hmox1*$^{-/-}$ placental labyrinth region. Parafin-embedded tissue sections of placentas from E12.5 (*a*) *Hmox1*$^{+/-}$ and (*b*) *Hmox1*$^{-/-}$ mice were stained with periodic acid-schiff reagent and hematoxylin. This treatment stains basement membranes reddish purple and nuclei dark purple. Placental labyrinth architecture largely consists of maternal sinuses containing adult erythocytes (arrows), and fetal vessels with fetal erythrocytes (arrowheads). Note that placental histology appears more congested in the section from *Hmox1*$^{-/-}$ mice, with less vascular space contributed by both maternal and fetal vessels. This might be the result of what appears to be greater cellularity and/or thickened vascular walls, possibly contributing to placental hypoplasia and frequent midgestional lethalities.

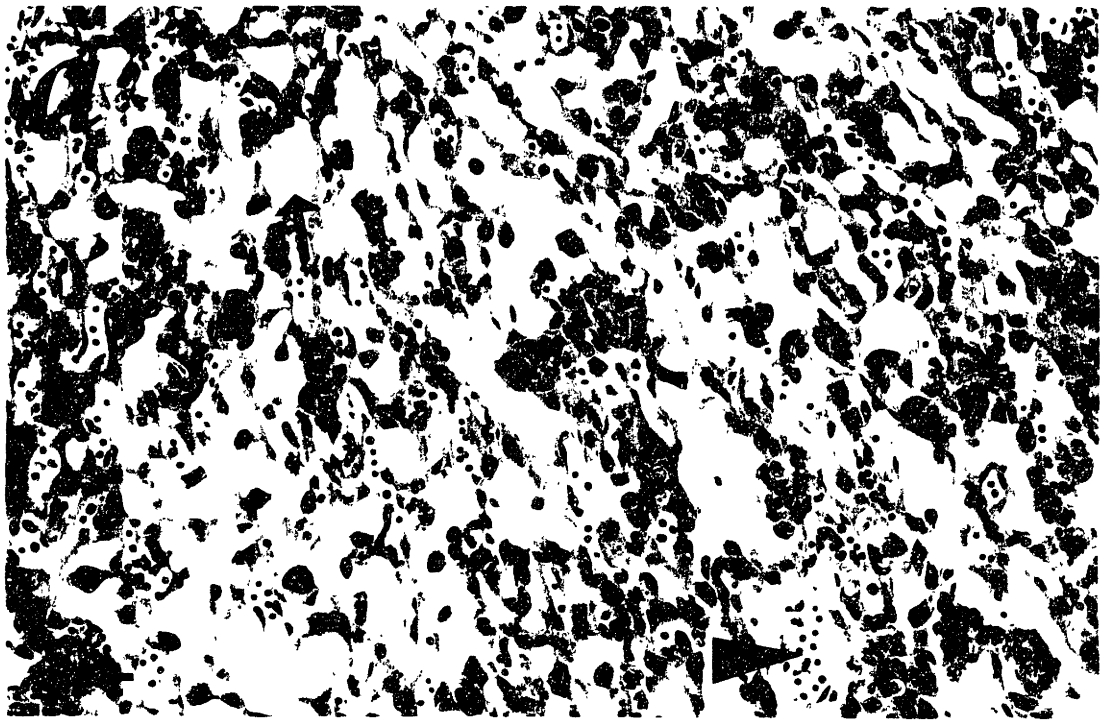

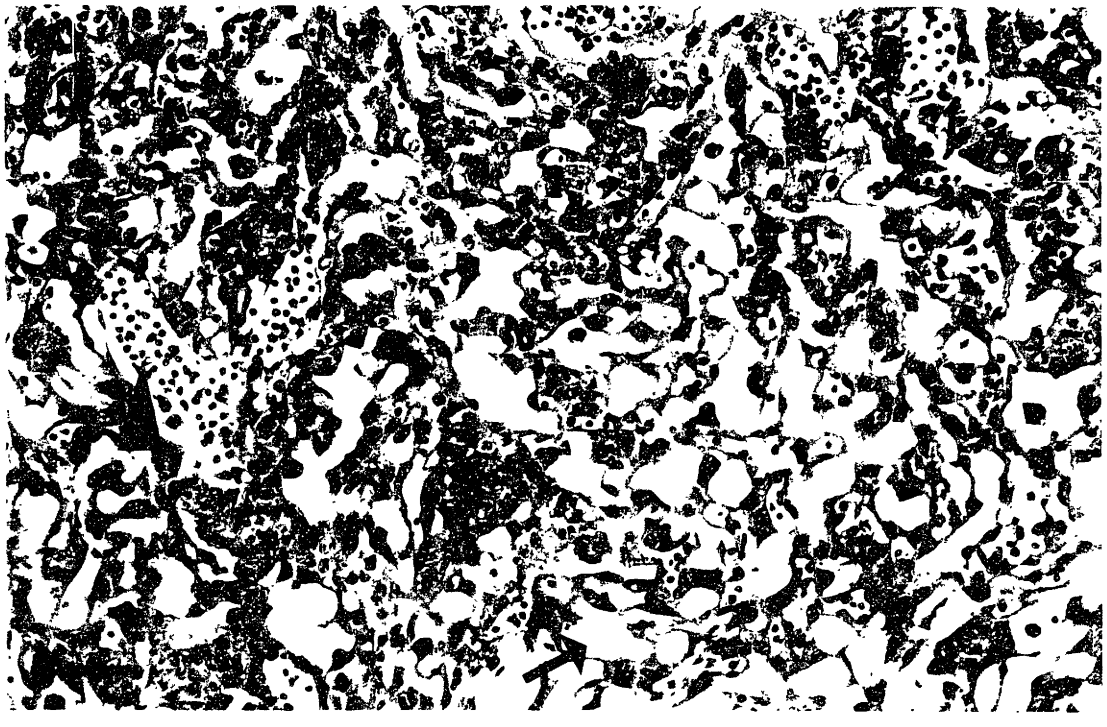

Fig. 4. Wasting, anemia, and serum iron deficiency in *Hmox1*$^{-/-}$ mice. *a*, *Hmox1*$^{-/-}$ mice were consistently slightly smaller than *Hmox1*$^{+/-}$ littermates, but weight loss between 20 and 40 weeks of age was clearly indicative of wasting. Data are shown mean ± SEM. One and three weeks: 9-19 males and females analyzed, 6 weeks: 12-24 males, 20 weeks: 9-11 males, 40 weeks: 13-15 males. Significant differences ($p < 0.05$) were observed between *Hmox1*$^{-/-}$ and *Hmox1*$^{+/-}$ masses at all ages. In (*a-d*), open squares represent *Hmox1*$^{+/-}$ mean values and closed squares represent *Hmox1*$^{-/-}$ mean values. *b*, Red blood cell counts (RBC), packed cell volume (Hct), blood hemoglobin concentration (Hb), and mean cell volume (MCV) analyzed in 7-11 male and female *Hmox1*$^{-/-}$ and *Hmox1*$^{+/-}$ littermates at 6, approximately 20, and approximately 50 weeks of age. Significant differences ($p < 0.05$) were observed for each parameter at all ages except for 6 week RBC and Hb values. *c*, Serum iron (Fe), total iron-binding capacity (TIBC), and iron saturation analyzed in 5 *Hmox1*$^{+/-}$ and 5 *Hmox1*$^{-/-}$ male mice of each age group. Significant differences ($p < 0.05$) were observed in each parameter except for 6 week serum iron values. Iron saturation percentage is equal to 100(serum iron/TIBC). *d*, Serum ferritin values analyzed in mice from (*c*). Significant differences ($p < 0.05$) were observed at each age examined.

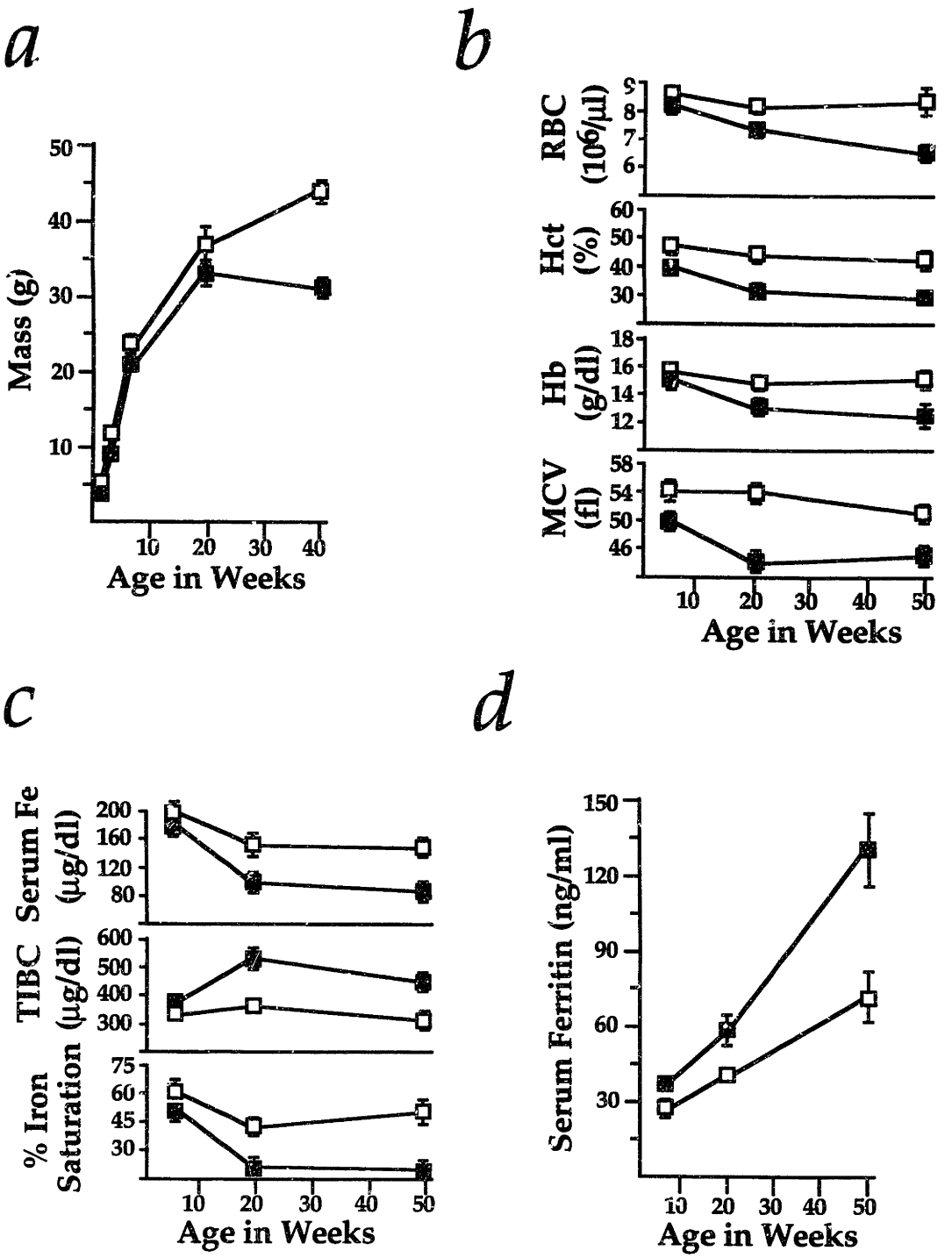
a
Mass (g)
50
40
30
20
10
10 20 30 40
Age in Weeks
b
RBC (10⁶/µl)
9
8
7
6
Hct (%)
60
50
40
30
Hb (g/dl)
18
16
14
12
MCV (fl)
58
54
50
46
10 20 30 40 50
Age in Weeks
c
Serum Fe (µg/dl)
200
160
120
80
TIBC (µg/dl)
600
500
400
300
% Iron Saturation
75
60
45
30
10 20 30 40 50
Age in Weeks
d
Serum Ferritin (ng/ml)
150
120
90
60
30
10 20 30 40 50
Age in Weeks

Fig. 5. Anatomy of erythrocytes from *Hmox1*$^{-/-}$ and *Hmox1*$^{+/-}$ mice. *a*, Wright-Giemsa-stained blood smear from 50 week-old *Hmox1*$^{+/-}$ mouse indicating normal erythrocyte morphology. *b*, Stained blood smear from 50 week-old *Hmox1*$^{-/-}$ mouse indicating many red blood cells of small size (microcytic), low density (hypochromic), or abnormal shapes (poikilocytotic). *Hmox1*$^{-/-}$ erythrocytes consistently showed varying degrees of these characteristics.


a
b

Fig. 6. Iron-loading in *Hmox1*$^{-/-}$ tissues. *a*, Kidney section from 50 week-old *Hmox1*$^{+/-}$ mouse stained with Prussian blue for detection of loosely bound ferric iron, shown at low magnification. Stainable renal iron was rarely detectable in *Hmox1*$^{+/-}$ or *Hmox1*$^{+/+}$ mice. *b*, Kidney section from 50 week-old *Hmox1*$^{-/-}$ mouse stained with Prussian blue. Note the intense blue positive staining in the proximal cortical tubules, which was consistently observed in *Hmox1*$^{-/-}$ renal tissue. *c*, Liver section from 50 week-old *Hmox1*$^{+/-}$ mouse stained with Prussian blue and at low magnification. Mice containing functional Hmox1 displayed no hepatic iron deposits. *d*, Liver section from 50 week-old *Hmox1*$^{-/-}$ mouse stained with Prussian blue, demonstrating iron-loaded Kupffer cells (arrows), as well as diffusely-staining hepatocytes. Note the faint-staining regenerative nodule indicative of injury (asterisk). All *Hmox1*$^{-/-}$ mice displayed hepatic iron-loading by 50 weeks of age, varying in severity. *e*, High magnification view of liver section from 50 week-old *Hmox1*$^{+/-}$ mouse stained with Prussian blue, displaying no detectable iron in hepatocytes. *f*, High magnification view of liver section from 50 week *Hmox1*$^{-/-}$ mouse stained with Prussian blue, indicating iron-positive granules in hepatocytes (arrowheads), and intensely-staining Kupffer cells (arrows). All magnification bars = 100 μm.

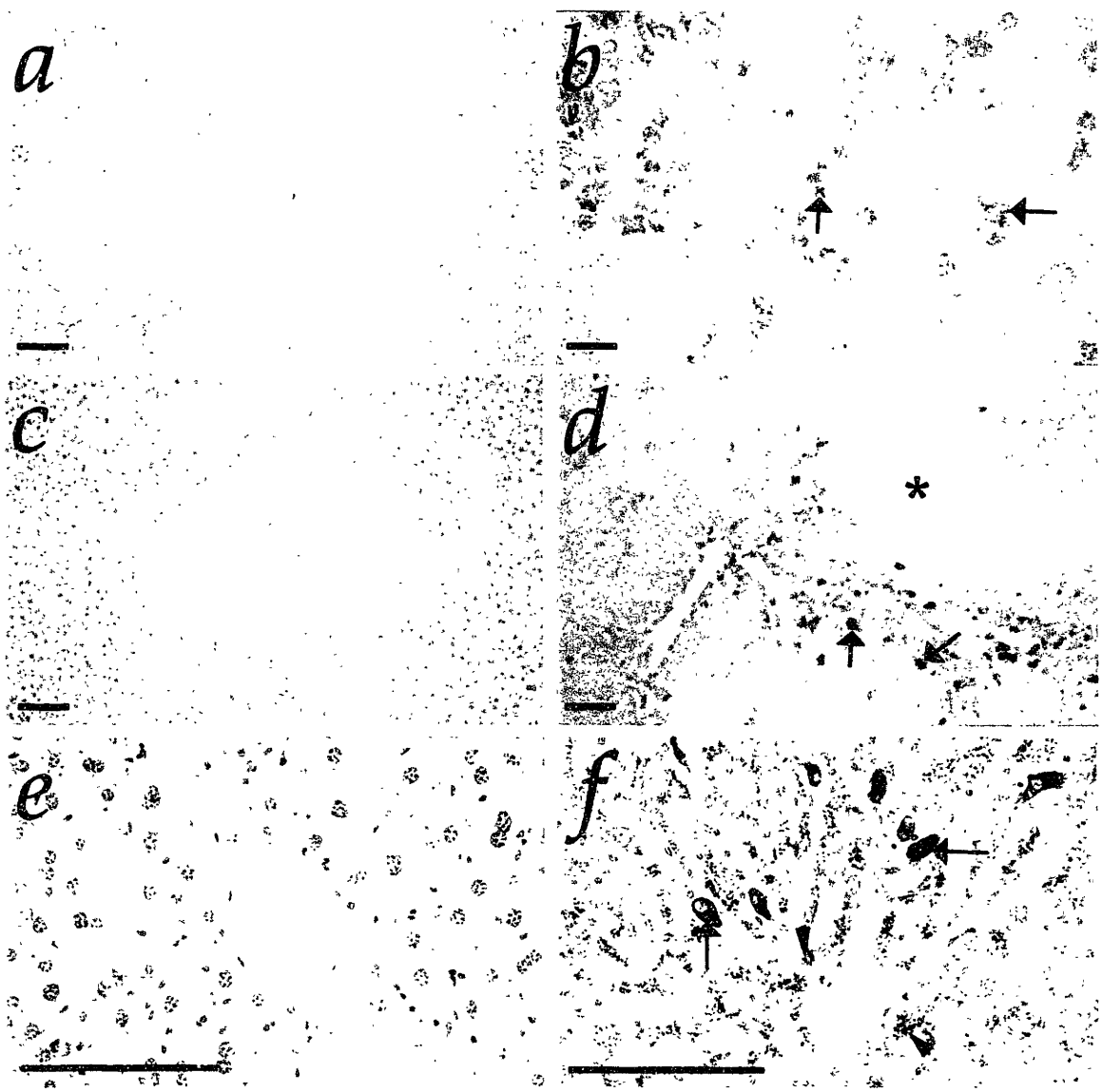
a
b
c
d
e
f

Fig. 7. Markers of stress and inflammation in *Hmox1*$^{-/-}$ mice. *a*, Protein carbonyls were measured by the method utilizing 2,4-dinitrophenylhydrazine in supernatant harvested from *Hmox1*$^{+/-}$ and *Hmox1*$^{-/-}$ brain, liver, or kidneys. Estimates of lipid peroxidation were obtained by malondialdehyde (MDA) measurements of tissue homogenates. Data represent mean ± SEM from duplicate or triplicate determinations from each of 4 mice of each genotype for brain samples, and each of 6-8 mice of each genotype for liver and kidney samples. Open bars represent *Hmox1*$^{+/-}$ values, while closed bars represent *Hmox1*$^{-/-}$ values. **Hmox1*$^{-/-}$ liver and kidneys, which consistently showed iron loading, had significantly greater oxidative damage that those from *Hmox1*$^{+/-}$ animals ($p < 0.05$). Note that *Hmox1*$^{-/-}$ brains, which had no iron deposition, showed no evidence of enhanced oxidative damage. *b*, Average white blood cell counts (WBC), splenic mass, and splenic $CD4^+$:$CD8^+$ T-cell ratios analyzed from 7-11 mice of each age group for WBC, and 4-7 mice of each age group for splenic mass and T-cell ratios, at 6, approximately 20, and approximately 50 weeks of age. Significant differences ($p < 0.05$) were observed for each parameter at each age examined. Open squares represent *Hmox1*$^{+/-}$ values, while closed squares represent *Hmox1*$^{-/-}$ values.

a

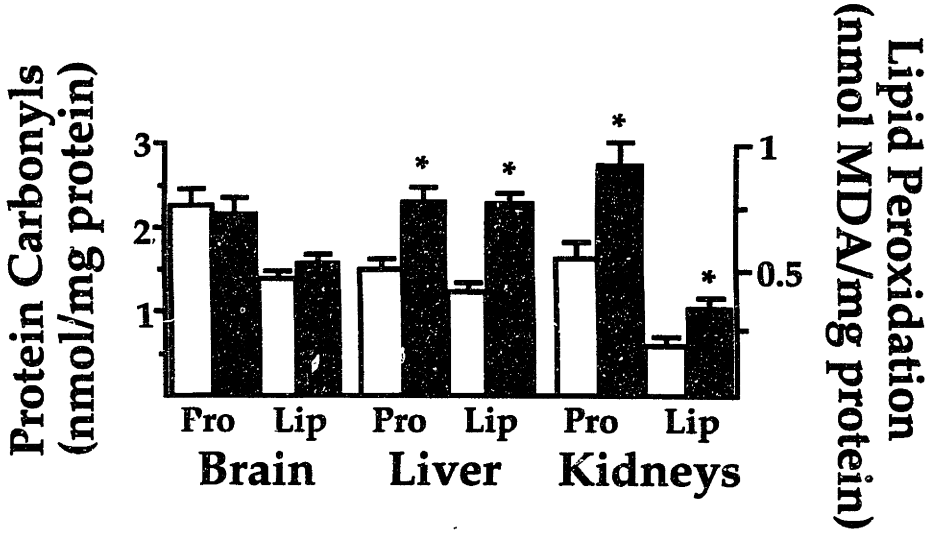
Protein Carbonyls (nmol/mg protein)
Lipid Peroxidation (nmol MDA/mg protein)
3
2
1
1
0.5
*
Fro
Lip
Pro
Lip
Pro
Lip
Brain
Liver
Kidneys

b

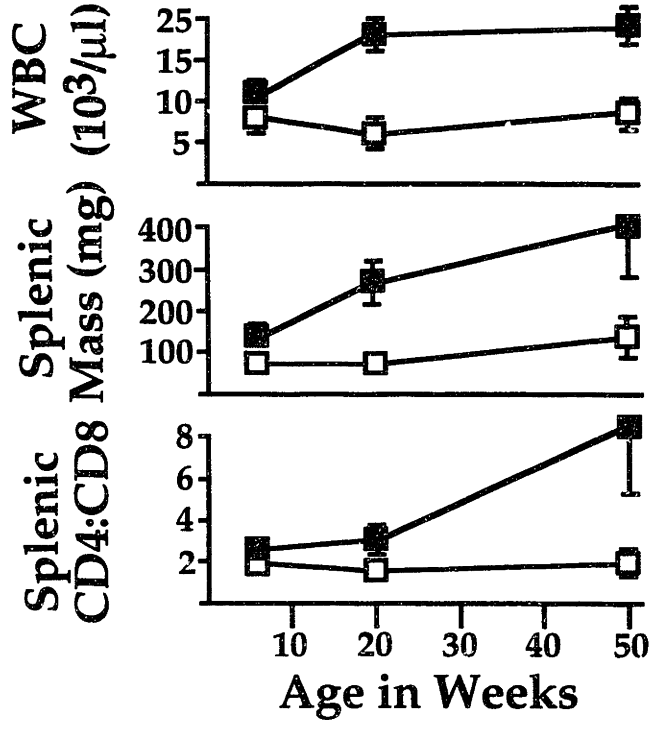
WBC (10³/μl)
25
15
10
5
Splenic Mass (mg)
400
300
200
100
Splenic CD4:CD8
8
6
4
2
10
20
30
40
50
Age in Weeks

Fig. 8. Hepatic and renal pathology of *Hmox1*$^{-/-}$ animals. *a*, Liver section from 50 week-old *Hmox1*$^{+/-}$ mouse, stained with hematoxylin and eosin and shown at low magnification. *b*, Liver section from 50 week-old *Hmox1*$^{-/-}$ mouse, with typical pattern of lesions. Vascular lesions are indicated by arrows. *c*, High magnification view of typical periportal fibrosis and inflammation from a 50 week-old *Hmox1*$^{-/-}$ mouse. This section was stained with Masson's trichrome reagent, which reacts with collagen, an indicator of fibrosis, as bright blue. *d*, High magnification view of hepatic vascular lesion shown in (*b*) stained with hematoxylin and eosin. Note the proliferation of smooth muscle, the infiltration of neutrophils and lymphocytes into the vessel wall, and the monocytes adhered to the inner vessel wall (arrows). *e*, High magnification view of hepatic vascular lesion from a 50 week-old *Hmox1*$^{-/-}$ mouse. This section was stained for ferric iron (blue). Note the iron-laden monocytes adhered to the vessel wall (arrows), as well as the iron laden vascular and connective tissue (arrowheads). *f*, High magification view of kidney section of 75 week-old *Hmox1*$^{+/-}$ mouse, stained with hematoxylin and eosin, displaying normal glomerular morphology (arrows). *g*, Kidney section of 75 week-old *Hmox1*$^{-/-}$ mouse displaying severely damaged glomeruli with membranous proliferation, lobularity, crescent formation, and sclerosis (arrows). All magnification bars = 100 μm.

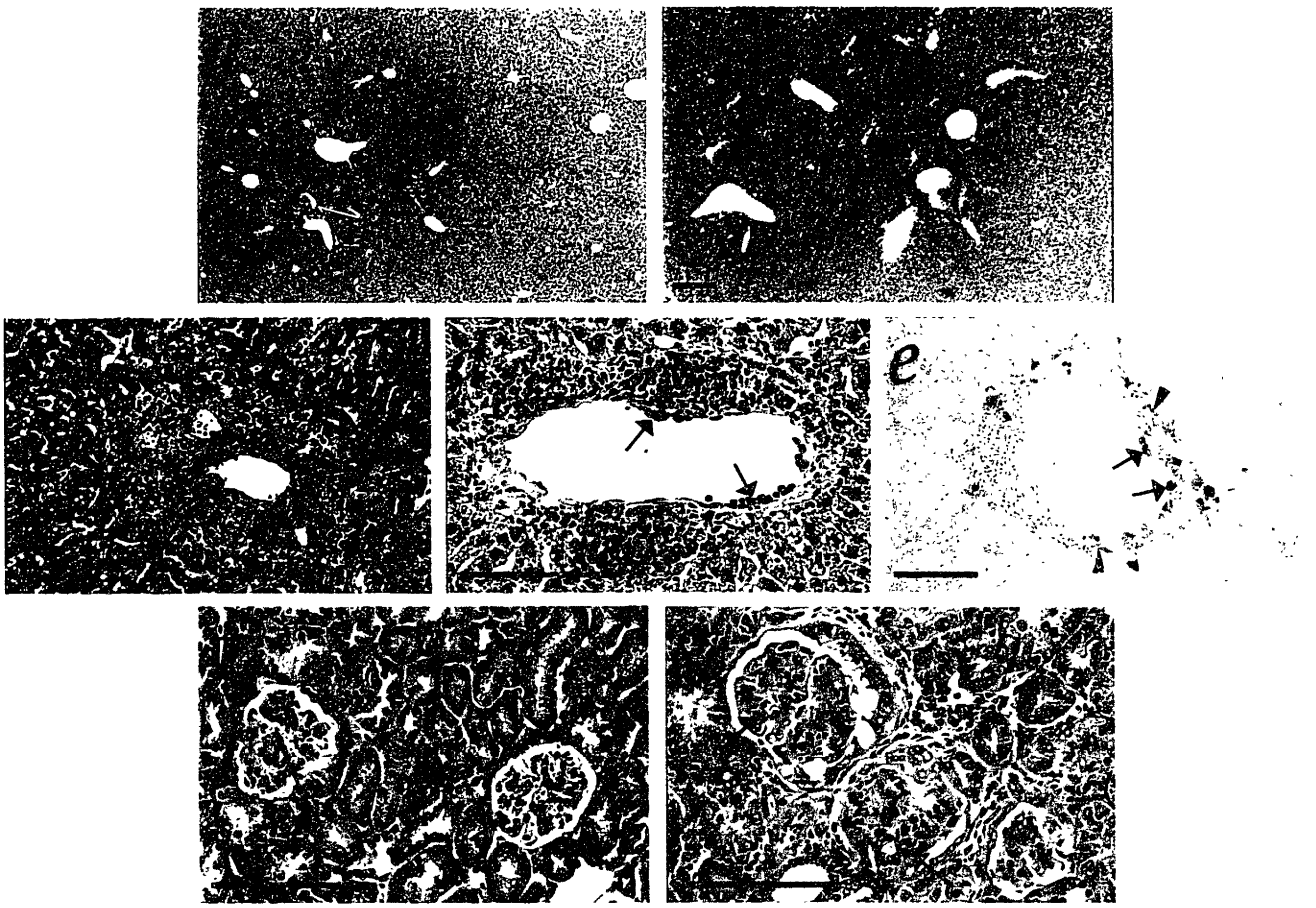
e

Chapter 4

Reduced Stress Defense In Heme Oxygenase-1-Deficient Cells

Note: This work is adapted from that published in *Proc. Natl. Acad. Sci. USA* **94**, pp. 10925-10930, by Kenneth D. Poss and Susumu Tonegawa.

Summary

Stressed mammalian cells upregulate heme oxygenase-1 (Hmox1), which catabolizes heme to biliverdin, carbon monoxide, and free iron. In order to assess the potential role of Hmox1 in cellular antioxidant defense, we analysed the responses of cells from mice lacking functional Hmox1 to oxidative challenges. Cultured *Hmox1*$^{-/-}$ embryonic fibroblasts demonstrated high free radical production when exposed to hemin, hydrogen peroxide, paraquat, and cadmium chloride, and were hypersensitive to cytotoxicity caused by hemin and hydrogen peroxide. Furthermore, young adult *Hmox1*$^{-/-}$ mice were vulnerable to mortality and hepatic necrosis when given oxidative challenges with endotoxin. Our in vitro and in vivo results provide genetic evidence that upregulation of Hmox1 serves as an adaptive mechanism to protect cells from oxidative damage during stress.

Introduction

Oxidative stress is believed to underly the etiology of numerous human conditions, including atherosclerosis, cerebral ischemia, and several neurodegenerative and neuromuscular disorders (1). Cellular antioxidants appear to be crucial for the reduction of oxidative stress and the prevention of associated pathology. Of the known enzymatic antioxidant systems, perhaps the best-characterized are superoxide dismutases, catalases, and glutathione peroxidase, which directly metabolize free radical precursors (2). In addition, certain proteins of the heat shock family are strongly induced during hyperthermia and stress, and ostensibly act to maintain the structural and functional integrity of damaged proteins (3).

Mammalian heme oxygenase-1 (Hmox1), one of two isoforms of heme oxygenase (Hmox) that catabolize cellular heme to biliverdin, carbon monoxide, and free iron, is also upregulated strongly during stress, and is considered one of the most sensitive and reliable indicators of cellular oxidative stress. Hmox1 expression is normally difficult to detect in cells other than macrophages, but is markedly activated in virtually all cell types by initiators of stress such as hyperthermia (4), heme and metals (5, 6), oxidized lipoproteins (7), UV and visible light (8, 9), inflammatory cytokines (10, 11), and hypoxia (12), and is found to be upregulated in disease models such as endotoxemia and ischemia in rodents (13, 14), and in human Alzheimer Disease (15). This response is explained by the multitude of stress-activated recognition sites contained within the *Hmox1* promoter, including activator protein-1 sites, CCAAT/enhancer binding proteins sites, phorbol ester response elements, heme response elements, and antioxidant response elements (16).

By analogy to heat shock regulation, several researchers have proposed that upregulation of Hmox1 during stress is an adaptive mechanism that may protect cells from oxidative damage. Experimental evidence for this hypothesis stems from observations that cellular resistance to oxidative stress correlates positively with levels of Hmox1 expression. In fact, researchers using various in vitro or in vivo stress paradigms have found that experimental upregulation of Hmox1 by treatment with heme or hemoglobin affords protection against subsequent oxidative challenges (17-19).

In our accompanying paper, we describe the important role of Hmox1 in adult iron homeostasis, based on the analysis of mice with targeted *Hmox1* mutations (20). Here, to examine the extent to which Hmox1 participates in the stress response, we analysed the effects of in vitro oxidative challenges to cells isolated from Hmox1-deficient mice. In addition, we examined how mice lacking Hmox1 respond to oxidative stress caused by administration of endotoxin. Our results indicate that murine cells lacking Hmox1 are

susceptible to the accumulation of free radicals and to oxidative injury in vitro and in vivo, and establish that Hmox1 is an important enzymatic antioxidant system.

Materials and Methods

Isolation of Embryonic Fibroblasts

Litters of *Hmox1*$^{-/-}$ and *Hmox1*$^{+/-}$ pups were obtained at E12.5 after timed matings between *Hmox1*$^{-/-}$ males and *Hmox1*$^{+/-}$ females. Or, E12.5 litters of *Hmox1*$^{+/-}$ and *Hmox1*$^{+/+}$ pups were obtained after timed matings between *Hmox1*$^{+/-}$ males and *Hmox1*$^{+/+}$ females. Each pup was decapitated, viscera were removed, and the remaining portion was trypsinized and plated in 2 wells of a 6-well plate. After overnight growth, the murine embryonic fibroblasts (MEFs) were expanded to either 6-well plates for RNA analysis, 12-well plates for oxygen radical analysis, or 24-well plates for cytotoxicity analysis, and grown to confluency overnight prior to drug treatments. Concurrently, DNA was isolated from head tissue of each pup and genotyped as previously reported (20). Each experiment compared responses of 1-3 pups of each genotype.

Analysis of Free Radical Generation in MEFs

Hmox1$^{-/-}$ and *Hmox1*$^{+/-}$ MEFs plated in 12-well plates were exposed to various oxidants for 24 hours. Cells were washed, trypsinized, and incubated with 10 μM 2', 7' -dichlorodihydrofluorescein diacetate (Molecular Probes), which releases the fluorescent dye 2', 7' dichlorofluorescein when oxidized, at 37 ^{o}C for 20 minutes. 10,000 cells/sample were analyzed for flourescein fluorescence using flow cytometry (Becton Dickinson). Only data from live cells were collected.

Cytotoxicity

MEFs plated in 24-well plates were exposed to oxidants for 24 hours. For cells treated with hemin and H_2O_2, cells were collected, stained with trypan blue, and 250-500 cells were analyzed for viability using a hemocytometer. Because toxicity with $CdCl_2$ and paraquat tended to lyse cells rapidly, cytotoxicity was assessed in cells treated with these chemicals by measurements of lactate dehydrogenase, an indicator of lysis, in culture medium using a kit (Boerringer Mannheim).

LPS Administration

Hmox1$^{+/+}$, *Hmox1*$^{+/-}$ and *Hmox1*$^{-/-}$ littermates 6-9 weeks old were injected with LPS from E. coli serotype O26:B6 (Sigma) dissolved in saline. Doses ranged from 0.5 mg/kg to 25 mg/kg. Mice were monitored for signs of endotoxemia and lethality twice daily for 4 days. To examine *Hmox1* mRNA induction, *Hmox1*$^{+/+}$ mice were sacrificed 6-24 hours post-injection, and peritoneal macrophages and livers were dissected for RNA isolation. For liver enzyme analyses (performed by Tufts Veterinary Diagnostic Labs),

animals were bled retro-orbitally 60 hours post-injection and serum was isolated. When histopathology was required, 3 mice of each genotype representing each dose were sacrificed 60 hours post-injection for organ dissection and fixation. Histology was performed as described (20).

Nitrite generation was analyzed from in vitro-stimulated macrophages as described (21). Free radical generation was measured by incubating untreated or phorbol 12-myristate 13-acetate-treated resident or in vivo-stimulated peritoneal macrophages with 10 μM of the free radical-activated dye 2', 7' -dichlorodihydrofluorescein diacetate (Molecular Probes) for 20 minutes, followed by analyis of mean cellular fluorescein fluorescence by flow cytometry (Becton Dickinson). Gating was adjusted so that 10,000 live macrophages/sample were assayed.

Results

Decreased Stress Defense in *Hmox1*$^{-/-}$ Embryonic Fibroblasts

MEFs were utilized as an in vitro system for testing the requirement of Hmox1 in stress defense. We first examined whether MEFs isolated from wild-type embryonic day 12.5 (E12.5) embryos demonstrate induction of *Hmox1* mRNA. When exposed for 6 hours to the oxidants hemin (a substrate of Hmox), hydrogen peroxide (H_2O_2), the superoxide generator paraquat, or cadmium chloride ($CdCl_2$), a dose-dependent upregulation of *Hmox1* mRNA transcription was observed (Figure 1). The strongest induction was observed in cells exposed to 50 μM hemin or 10 μM $CdCl_2$ (Fig. 1, lanes 3 and 12).

To determine whether the presence or absence of this particular stress response affects the magnitude of oxidative stress, we measured free radical generation in MEFs that had been isolated from either heterozygous (*Hmox1*$^{+/-}$) or homozygous (*Hmox1*$^{-/-}$) mutant E12.5 mice and exposed for 24 hours to the oxidants mentioned above. 50 μM hemin applied to *Hmox1*$^{+/-}$ cells caused a significant but minor 11% increase in free radical generation over untreated cells, based on quantification of a oxidation-activated fluorescent dye. In contrast, hemin applied at 50 μM to *Hmox1*$^{-/-}$ MEFs resulted in an increase in free radical generation of 232% over untreated cells. Similar exposure of *Hmox1*$^{+/-}$ cells to 0.8 mM H_2O_2, 0.8 mM paraquat, and 20 μM $CdCl_2$ revealed insignificant changes in free radical production of +5%, +20%, an[illegible]-5%, respectively, while *Hmox1*$^{-/-}$ MEFs treated with these oxidants incurred significant increases of 31%, 53%, and 48% over untreated cells (Fig. 2).

We next studied the survival of *Hmox1*$^{+/-}$ and *Hmox1*$^{-/-}$ MEFs exposed to several doses of each oxidant. Both hemin and H_2O_2 had significantly more severe effects on the viability of *Hmox1*$^{-/-}$ MEFs. For instance, hemin concentrations of 100 μM and 200

μM resulted in 84% and 38% survival of *Hmox1*$^{+/-}$ cells, but only 32% and 4% survival of *Hmox1*$^{-/-}$ cells, respectively (Fig. 3*a*). Similarly, H_2O_2 concentrations of 1 mM and 1.2 mM resulted in 88% and 56% survival of *Hmox1*$^{+/-}$ cells, compared to only 46% and 19% survival of *Hmox1*$^{-/-}$ cells (Fig. 3*b*). *Hmox1*$^{+/-}$ cell viability was comparable to *Hmox1*$^{+/+}$ cell viability when exposed to hemin or H_2O_2 (Fig. 3*a, b*). When treated with different concentrations of paraquat or $CdCl_2$, *Hmox1*$^{-/-}$ cells showed similar vulnerability as *Hmox1*$^{+/-}$ cells (Fig. 3*c, d*). From our in vitro experiments, we deduced that MEFs which cannot induce functional Hmox1 are hypersusceptible to free radical formation and cytotoxicity during direct exposure to certain oxidants.

Abnormal Responses of *Hmox1*$^{-/-}$ Mice to Endotoxin

To address whether *Hmox1*$^{-/-}$ cells also show hypersensitivity to in vivo oxidative challenges, we chose endotoxemia, a mouse model of sepsis in humans. Previous studies have shown that pathology resulting from high doses of endotoxin is attributable to oxidative mechanisms, such as phagocytic cell oxidative respiratory bursts that may damage vascular endothelial cells (23, 24), major organ hypoxia due to vasorelaxation (25), and the direct oxidative effects of endotoxin on hepatocytes (26, 27).

Adult *Hmox1*$^{-/-}$ mice show a variety of disease symptoms including anemia, iron-loading, and chronic inflammation that are first evident by around 20 weeks of age, but are not yet detectable at 6-9 weeks of age (20). Therefore, we examined the responses of 6-9 week-old *Hmox1*$^{+/+}$, *Hmox1*$^{+/-}$, and *Hmox1*$^{-/-}$ mice to inflammatory stress caused by endotoxin administration, which induced *Hmox1* mRNA in both peritoneal macrophages and livers of *Hmox1*$^{+/+}$ mice (Fig. 4*a*). In tests of survival, *Hmox1*$^{-/-}$ mice were clearly more vulnerable than *Hmox1*$^{+/-}$ and *Hmox1*$^{+/+}$ mice to a high dose (25 mg/kg) of lipopolysaccharides (LPS) administered intraperitoneally (Fig. 4*b*).

To determine if any organ(s) was especially susceptible to LPS treatment in *Hmox1*$^{-/-}$ animals, we examined the pathological effects of this high dose and of two lower doses of LPS. *Hmox1*$^{+/-}$ mice given 1, 5, or 25 mg/kg LPS had no significant histopathological abnormalities (Fig. 4*c*). However, LPS had conspicuous effects on *Hmox1*$^{-/-}$ hepatic tissue. A low dose of 1 mg/kg did not result in histopathological anomalies (Fig. 4*c*), but caused increases in serum liver enzyme levels significantly greater than in *Hmox1*$^{+/-}$ animals (Table 1). Furthermore, livers from *Hmox1*$^{-/-}$ animals given an intermediate dose of 5 mg/kg LPS showed hepatocellular vacuoles indicative of toxicity (Fig. 4*d*). Livers harvested from moribund *Hmox1*$^{-/-}$ mice that had received the high dose of 25 mg/kg LPS had massive necrotic infarcts, evident in the lower left portion of Fig. 4*e* by a large, faint-staining region.

Consistent with the notion that this pathology was due to hepatic rather than macrophage defects, both nitric oxide and total free radical production in LPS-stimulated *Hmox1*$^{-/-}$ macrophages were normal (Fig. 5*a*, *b*). Also, there appeared to be specific defects of hepatic iron metabolism in endotoxemic *Hmox1*$^{-/-}$ mice. No evidence of iron-loading was observed in livers isolated from *Hmox1*$^{+/-}$ mice three days following administration of 1, 5, or 25 mg/kg LPS, nor in *Hmox1*$^{-/-}$ animals given an LPS dose of 1 mg/kg (Fig. 5*c*). However, *Hmox1*$^{-/-}$ mice that were given 5 mg/kg LPS displayed diffuse but widespread iron-loading in hepatocytes (Fig. 5*d*). Moreover, *Hmox1*$^{-/-}$ mice administered 25 mg/kg LPS developed what appeared to be even more severe iron-loading, with hepatocellular necrotic foci in close proximity to areas of heavy iron deposition (Fig. 5*e*). Thus, LPS had dose-dependent effects on both hepatic iron-loading and injury, exclusively in *Hmox1*$^{-/-}$ mice. Therefore, we suspect that iron deposition contributed to hepatic injury in LPS-treated *Hmox1*$^{-/-}$ animals.

As an important supplement to our in vitro data, these results demonstrate that *Hmox1*$^{-/-}$ tissues are exquisitely sensitive to endotoxemic stress. We conclude from our findings in total that expression of functional Hmox1 is essential for resistance to oxidative damage.

Discussion

In the accompanying paper, we show that oxidation of macromolecules and tissue injury arise spontaneously in *Hmox1*$^{-/-}$ mice, substantiating the idea that Hmox-1 may normally perform an antioxidant role (20). Here, in further addressing this idea, we examined the responses of *Hmox1*$^{-/-}$ cells to in vitro and in vivo oxidative challenges. First, we demonstrated increased free radical production and reduced survival in cultured *Hmox1*$^{-/-}$ MEFs exposed to several oxidants. Subsequently, we showed that *Hmox1*$^{-/-}$ mice are markedly sensitive to hepatic injury and mortality caused by oxidative challenges with endotoxin.

Hmox1 is an Antioxidant Defense Enzyme

A wide variety of stress inducers cause robust upregulation of Hmox1 activity in mammalian cells. Many researchers have suggested that this response may afford protection from oxidative damage, and have proposed several mechanisms whereby Hmox1 activity could provide this protection, including production of the antioxidants biliverdin and bilirubin (28), depletion of the oxidant heme (29), elevation of intracellular free iron levels to facilitate ferritin upregulation (30, 31), and regulation of vascular tension through carbon monoxide generation (32, 33). On the other hand, other groups have suggested that Hmox1 upregulation is purely correlative without functions related to

modulation of oxidative damage (34). Still others have postulated that positive effects of Hmox1 activity on intracellular free iron levels may even enhance the consequences of oxidative stress (35).

By revealing the increased vulnerability of Hmox1-deficient cells to oxidative stress, our results confirm the notion that Hmox1 activity supplies protective effects. Since both free radical generation and cytotoxicity are markedly enhanced in *Hmox1*$^{-/-}$ MEFs after incubation with the Hmox substrate and oxidant hemin, we infer that Hmox1 performs an important in vivo antioxidant function purely by depletion of heme. This may be most pertinent in vascular cells, or in hemorrhaged tissues, where deleterious heme is abundant. Notably, we also observed an increased sensitivity of *Hmox1*$^{-/-}$ cells to H_2O_2, paraquat, and $CdCl_2$. We do not know the mechanism(s) by which Hmox1 normally protects against these oxidative insults. However, from our data, it is apparent that MEFs have adequate antioxidant systems to compensate and protect viability when exposed to paraquat and $CdCl_2$ in the absence of functional Hmox1, even though abnormally high free radical generation occurs.

We found it especially interesting that endotoxin administration resulted in a rapid hepatic iron-loading in *Hmox1*$^{-/-}$ mice, the extent of which correlated with the severity of hepatic injury and incidence of mortality. To our knowledge, hepatic iron-loading after LPS administration has not been previously reported in animal models of endotoxemia. It might be relevant that other researchers have found reductions in hepatocellular heme levels concurrent with increases in ferritin iron levels immediately after induction of systemic inflammation in rats (36). Therefore, upregulation of Hmox1 during inflammatory stress might be a homeostatic device that redirects heme iron to the extracellular space and thereby attenuates the accumulation of intracellular iron. In agreement with this idea, data in our accompanying paper indicate that heme catabolism by Hmox1 seems to be important for reducing intracellular storage iron levels and maintaining blood iron levels (20).

Functions of Hmox1 during Disease

Previously, it was shown that the pretreatment of rats with hemoglobin both upregulated *Hmox1* mRNA and protected from inflammatory injury during endotoxemia (18). Also, in a rodent model of renal failure following experimental rhabdomyolysis, similar upregulation of Hmox1 before experimental insults reduced subsequent injury (19). Our results confirm these findings and suggest that Hmox1 may in fact be a key mediator of this protection. Therefore, induction of Hmox1 expression might constitute an effective clinical defense against trauma associated with sepsis and renal failure. Hmox1-deficient

mice should also be useful in testing the participation of Hmox1 in stress defense for other models of human conditions.

Numerous Roles of Hmox

In summary, we have demonstrated by analysis of Hmox1-deficient mice in this and elsewhere that Hmox1 is important for prenatal development, adult mammalian iron homeostasis (20), and for rapid protection of cells from potential oxidative damage during stress. Furthermore, recent studies utilizing pharmacological Hmox inhibitors and analyses of mice lacking the other Hmox isoform, Hmox2, have provided evidence suggesting that the carbon monoxide product of the Hmox reaction participates in a variety of second messenger signaling systems (32, 37-39). That Hmox has roles in these anatomically and functionally diverse processes illustrates the physiological versatility of this one enzymatic reaction.

References

1. Halliwell, B. & Gutteridge, J. M. C. (1990). *Meth. Enzymol.* **186**, 1-85.
2. Coyle, J. T. & Puttfarcken, P. (1993). *Science* **262**, 689-695.
3. Parsell, D. A. & Lindquist, S. (1993). *Annu. Rev. Genet.* **27**, 437-496.
4. Ewing, J. F. & Maines, M. D. (1991). *Proc. Natl. Acad. Sci. USA* **88**, 5364-5368.
5. Shibahara, S., Yoshida, T. & Kikuchi, G. (1978). *Arch. Biochem. Biophys.* **188**, 243-250.
6. Taketani, S., Kohno, H., Yoshinaga, T. & Tokunaga, R. (1988). *Biochem. Int.* **17**, 665-672.
7. Siow, R. C., Ishii, T., Taketani, S., Leske, D. S., Sweiry, J. H., Pearson, J. D., Bannai, S., & Mann, G. E. (1995). *FEBS Lett.* **368**, 239-242.
8. Keyse, S. M. & Tyrrell, R. M. (1989). *Proc. Natl. Acad. Sci. USA* **86**, 99-103.
9. Kutty, R. K., Kutty, G., Wiggert, B., Chader, G. J., Darrow, R. M., & Organisciak, D. T. (1995). *Proc. Natl. Acad. Sci. USA* **92**, 1177-1181.
10. Rizzardini, M., Terao, M., Falciani, F. & Cantoni, L. (1993), *Biochem. J.* **290**, 343-347.
11. Kutty, R. K., Naginemi, G. N., Kutty, G., Hooks, J. J., Chader, G. J., & Wiggert, B. (1994). *J. Cell. Physiol.* **159**, 371-378.
12. Murphy, B. J., Laderoute, K. R., Short, S. M. & Sutherland, R. M. (1991). *Br. J. Cancer* **64**, 69-73.
13. Rizzardini, M., Carelli, M., Cabello Porras, M. R. & Cantoni, L. (1994). *Biochem. J.* **304**, 477-483.
14. Takeda, A., Onododera, H., Sugimoto, A., Itoyama, Y., Kogure, K. & Shibahara, S. (1994). *Brain Res.* **666**, 120-124.
15. Yan, S. D., Chen, X., Fu, J., Chen, M., Zhu, H., Roher, A., Slattery, T., Zhao, L., Nagashima, M., Morser, J., Migheli, A., Nawroth, P., Stern, D., & Schmidt, A. M. (1996). *Nature* **382**, 685-691.
16. Inamdar, N. M., Ahn, Y. I. & Alam, J. (1996). *Biochem. Biophys. Res. Commun.* **221**, 570-576.
17. Balla, J., Jacob, H. S., Balla, G., Nath, K., Eaton, J. W., Vercellotti, G. M. (1993). *Proc. Natl. Acad. Sci. USA* **90**, 9285-9289.
18. Otterbein, L., Sylvester, S. L. & Choi, A. M. (1995). *Am. J. Respir. Cell. Mol. Biol.* **13**, 595-601.
19. Nath, K. A., Balla, G., Vercellotti, G. M., Balla, J., Jacob, H. S., Levitt, M. D., & Rosenberg, M. E. (1992). *J. Clin. Invest.* **90**, 267-270.
20. Poss, K. D. & Tonegawa, S. (1997). *Proc. Natl. Acad. Sci. USA* (in press)
21. Green, S. J., Aniagolu, J. & Raney, J. J. (1995) in *Current Protocols in Immunology* , eds. Coligan, J. E., Kruisbeek, A. M., Margulies, D. H., Shevach, E. M. & Strober, W. (Wiley, New York), pp. 14.5.1-14.5.11.
22. Shibahara, S., Muller, R., Taguchi, H. & Yoshida, T. (1985). *Proc. Natl. Acad. Sci. USA* **82**, 7865-7869.
23. Warner, S. J. C. & Libby, P. (1989). *J. Immunol.* **142**, 100-109.
24. Schletter, J., Heine, H., Ulmer, A. J. & Rietschel, E. T. (1995). *Arch. Microbiol.* **164**, 383-389.
25. Cain, S. M. (1992). *Adv. Exp. Med. Biol.* **317**, 35-45.
26. Nolan, J. P. (1981). *Hepatology* **1**, 458-465.
27. Bautista, A. P., Meszaros, K., Bojta, J. & Spitzer, J. J. (1990). *J. Leukocyte Biol.* **48**, 123-128.
28. Stocker, R., Yamamoto, Y., McDonagh, A. F., Glazer, A. N. & Ames, B. N. (1987). *Science* **235**, 1043-1046.
29. Hunt, R. C., Handy, I. & Smith, A. (1996). *J. Cell. Physiol.* **168**, 81-86.
30. Eisenstein, R. S., Garcia-Mayol, D., Pettingell, W. & Munro, H. N. (1991). *Proc. Natl. Acad. Sci. USA* **88**, 688-692.

31. Vile, G. F., Basu-Modak, S., Waltner, C. & Tyrrell, R. M. (1994). *Proc. Natl. Acad. Sci. USA* **91**, 2607-2610.
32. Zakhary, R., Gaine, S. P., Dinerman, J. L., Ruat, M., Flavahan, N. A., & Snyder, S. H. (1996). *Proc. Natl. Acad. Sci. USA* **93**, 795-798.
33. Agarwal, A., Kim, Y., Matas, A., Alam, J. & Nath, K. A. (1996). *Transplantation* **61**, 93-98.
34. Nutter, L. M., Sierra, E. E. & Ngo, E. O. (1994). *J. Lab. Clin. Med.* **123**, 506-514.
35. Van Lenten, B. J., Prieve, J., Navab, M., Hama, S., Lusis, A. J., & Fogelman, A. M. (1995). *J. Clin. Invest.* **95**, 2104-2110.
36. Hershko, C., Cook, J. D. & Finch, C. A. (1974). *Br. J. Haematol.* **28**, 67-75.
37. Verma, A., Hirsch, D. J., Glatt, C. E., Ronnett, G. V. & Snyder, S. H. (1993). *Science* **259**, 381-384.
38. Nathanson, J. A., Scavone, C., Scanlon, C. & McKee, M. (1995). *Neuron* **14**, 781-794.
39. Zakhary, R., Poss, K. D., Jaffrey, S. R., Ferris, C. D., Tonegawa, S., & Snyder, S. H. (submitted)

Table 1. Effects of LPS on Serum ALT and AST Levels in *Hmox1*$^{-/-}$ and *Hmox1*$^{+/-}$ Mice

	Genotype of mice	
Liver enzyme	***Hmox1*$^{+/-}$**	***Hmox1*$^{-/-}$**
ALT (units/L)	**87 ± 15**	**80 ± 14**
ALT (1 mg/kg LPS)	**115 ± 20**	**298 ± 124**
AST (units/L)	**330 ± 74**	**252 ± 26**
AST (1 mg/kg LPS)	**418 ± 70**	***1320 ± 476**

Data are shown as mean ± SEM. Serum was obtained from 4 untreated mice of each genotype, and from 8 LPS-treatedmice of each genotype at 6 weeks of age for analysis of ALT and AST. *Significant difference between *Hmox1*$^{-/-}$ and *Hmox1*$^{+/-}$ mice (Student's *t*-test: p = 0.05).

Fig. 1. Induction of *Hmox1* mRNA in oxidant-exposed embryonic fibroblasts. Fibroblasts isolated from E12.5 *Hmox1*$^{+/+}$ embryos and plated in 6-well plates were untreated or exposed to the indicated concentrations of hemin, H_2O_2, paraquat (PQ), or $CdCl_2$. After 6 hours, total RNA was extracted, Northern-blotted, and hybridized with a rat *Hmox1* cDNA probe, which recognizes a major mRNA band of approximately 1.5 kb (22).

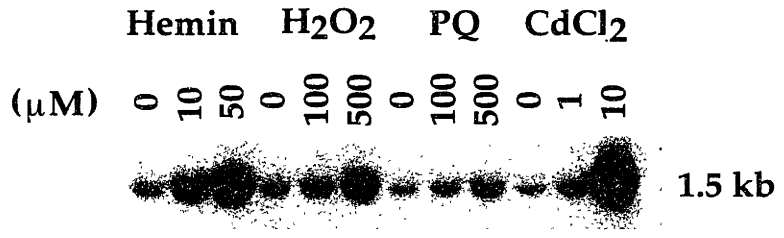
Hemin
H_2O_2
PQ
$CdCl_2$
(μM)
0
10
50
0
100
500
0
100
500
0
1
10
1.5 kb

Fig. 2. Enhanced free radical production in *Hmox1*$^{-/-}$ embryonic fibroblasts. Percentage mean cellular fluorescence of oxidant-treated cells compared to that of untreated cells, as detected by flow cytometry. Fibroblasts plated in 12-well plates were untreated or exposed with the indicated oxidants for 24 hours and incubated for 20 minutes with an oxidation-activated dye. Open bars represent *Hmox1*$^{+/-}$ percentages, while closed bars represent *Hmox1*$^{-/-}$ percentages. Data are shown mean ± SEM. Each bar represents combined data from 4-5 experiments sampled in duplicate. *Significant differences were observed between treated and untreated fibroblasts of that genotype ($p < 0.05$).

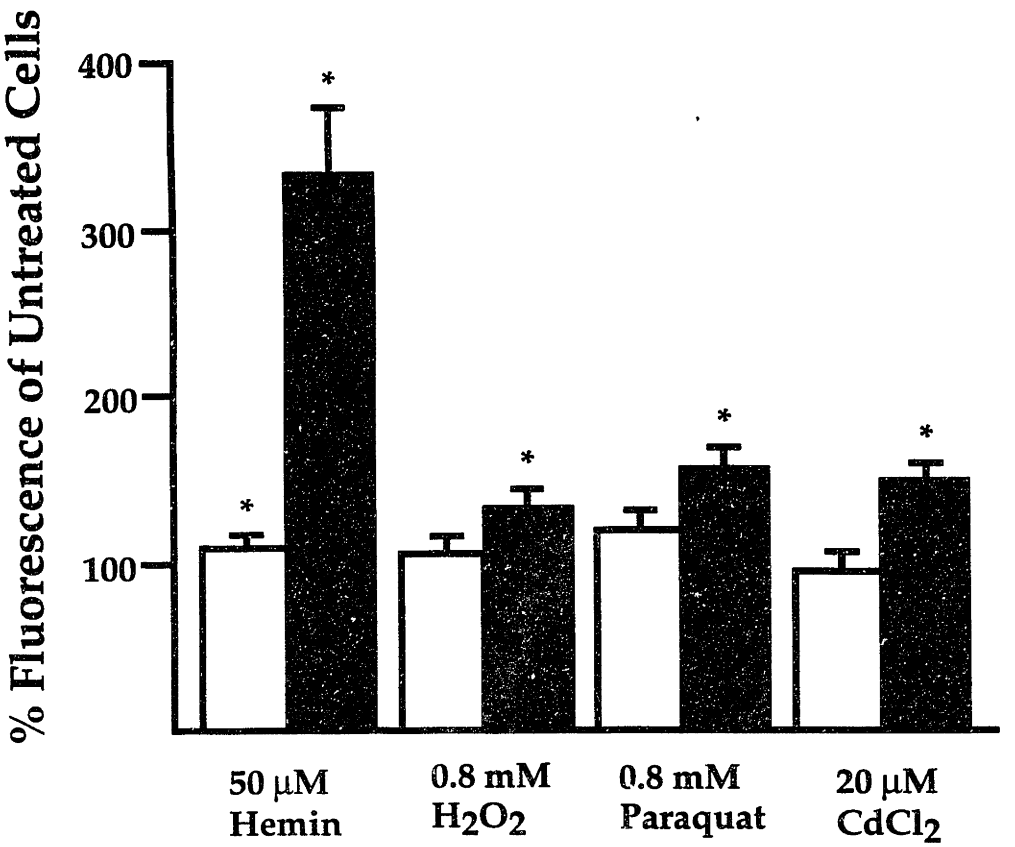
% Fluorescence of Untreated Cells
400
300
200
100
*
*
*
*
*
*
50 μM Hemin
0.8 mM H_2O_2
0.8 mM Paraquat
20 μM $CdCl_2$

Fig. 3. Survival of *Hmox1*$^{-/-}$ embryonic fibroblasts exposed to oxidants. (*a-d*) Fibroblasts plated in 24-well plates were exposed for 24 hours to several doses each of hemin (*a*), H_2O_2 (*b*), paraquat (*c*), or $CdCl_2$ (*d*). Cell survival was assayed by tryphan blue exclusion or lactate dehydrogenase release, as described in Materials and Methods. Open circles represent *Hmox1*$^{+/+}$ values, open squares represent *Hmox1*$^{+/-}$ values, and closed squares represent *Hmox1*$^{-/-}$ values. Data are shown mean ± SEM. For each genotype and each drug tested, survival data are from 3-6 experiments sampled in duplicate or triplicate for each drug concentration. *Significant differences were observed between *Hmox1*$^{+/-}$ and *Hmox1*$^{-/-}$ cell survival ($p < 0.05$).

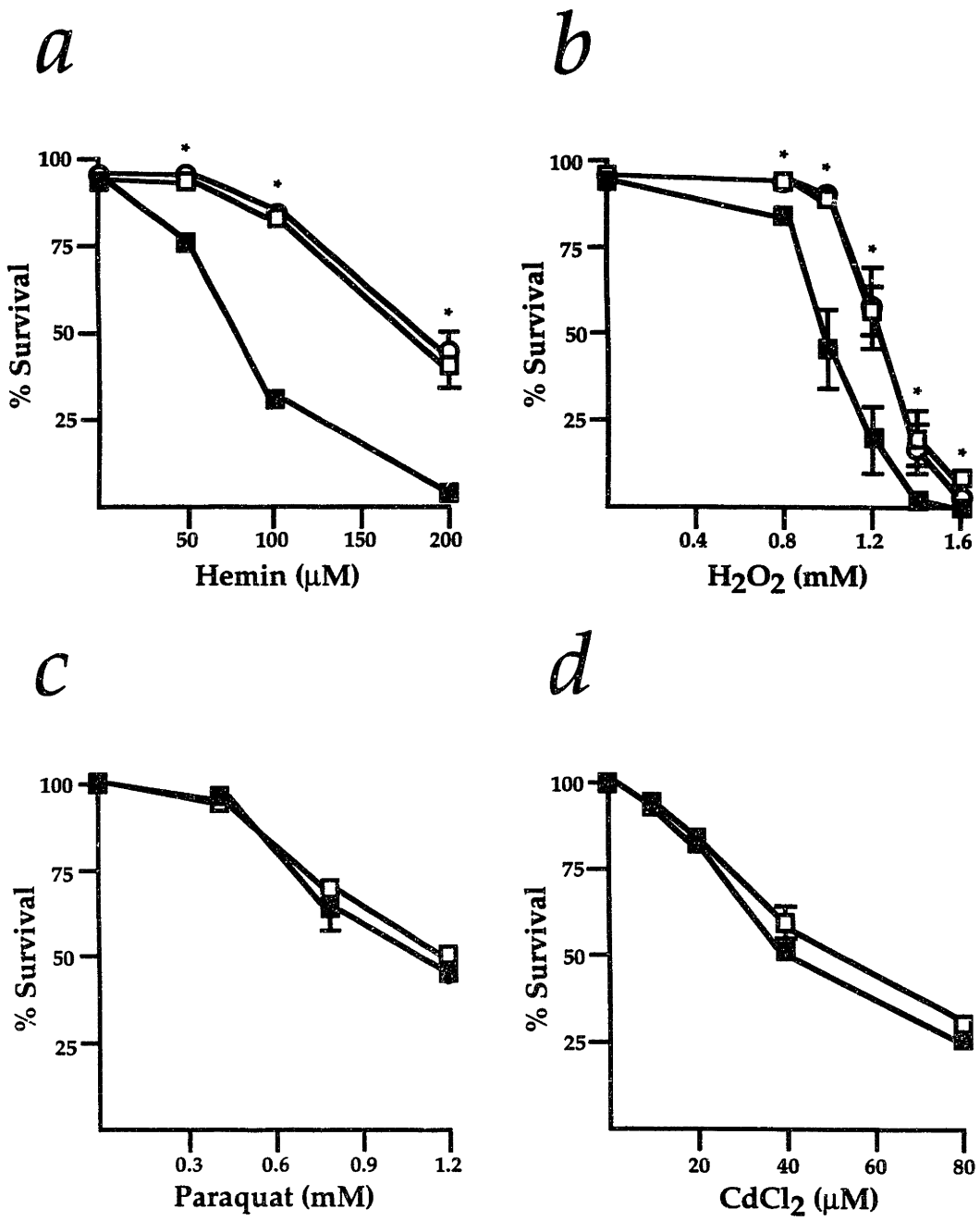
a
b
c
d
100
75
50
25
% Survival
50
100
150
200
Hemin (μM)
0.4
0.8
1.2
1.6
H_2O_2 (mM)
0.3
0.6
0.9
1.2
Paraquat (mM)
20
40
60
80
$CdCl_2$ (μM)

Fig. 4. Responses of *Hmox1*$^{-/-}$ mice to endotoxemia. *a*, Induction of *Hmox1* mRNA in *Hmox1*$^{+/+}$ mice injected with 2.5 mg/kg LPS. At 0, 6, 12, and 24 hours, total RNA was extracted from isolated peritoneal macrophages and liver, Northern-blotted, and hybridized with a rat *Hmox1* cDNA probe. *b*, Survival of 6-9 week-old *Hmox1*$^{+/-}$ (hatched bar) and *Hmox1*$^{-/-}$ (closed bar) littermates as well as similarly-aged *Hmox1*$^{+/+}$ mice (open bar) after intraperitoneal injection with 25 mg/kg LPS. The data are combined from 5 independent experiments using 44 female mice. Deaths occurred 2-3 days post-injection in all cases. *c*, High magnification view of hematoxylin and eosin-stained liver section from 6-9 week-old *Hmox1*$^{-/-}$ mice 60 hours after being given 1 mg/kg LPS. These histological results were indistinguishable from those of *Hmox1*$^{+/-}$ mice given 1, 5, or 25 mg/kg LPS, with no signs of toxicity. *d*, High magnification view of liver pathology 60 hours following administration of 5 mg/kg LPS to 6-9 week-old *Hmox1*$^{-/-}$ mice. Note hepatocellular fatty vacuoles indicative of toxicity. *e*, Low magnification view of liver pathology 60 hours following administration of 25 mg/kg LPS to 6-9 week-old *Hmox1*$^{-/-}$ mice. These mice were moribund and near death when tissues were harvested. Note the large, anuclear necrotic infarct in the lower left portion of the photo (arrows point from necrotic tissue toward region of viable tissue). All magnification bars = 100 μm.

a

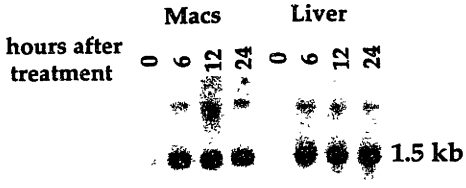
Macs
Liver
hours after treatment
0
6
12
24
0
6
12
24
1.5 kb

b

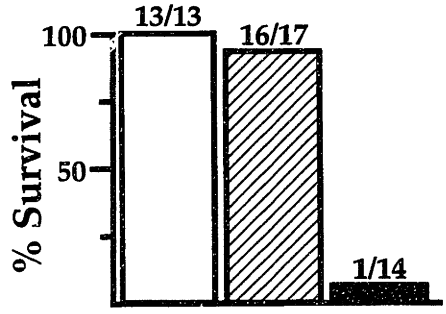
% Survival
100
50
13/13
16/17
1/14

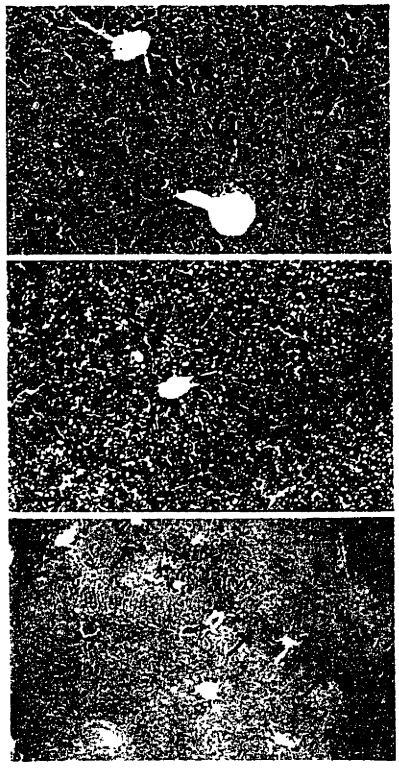

Fig. 5. Normal macrophage reponses but atypical hepatic iron-loading in endotoxemic *Hmox1*$^{-/-}$ mice. *a*, Nitrite measured in peritoneal macrophages cultured for 48 hours with 50 U/ml interferon-γ and the indicated concentrations of LPS or tumor necrosis factor-α (TNFα). Open circles represent *Hmox1*$^{+/+}$ values, open squares represent *Hmox1*$^{+/-}$ values, and closed squares represent *Hmox1*$^{-/-}$ values. Data are shown mean ± SEM from 3 experiments with each drug concentration sampled in triplicate. *b*, Fluorescein fluoresence in macrophages isolated from untreated mice or mice treated with 5 μg LPS and 1000 U interferon-γ, incubated with or without 100 ng/ml phorbol 12-myristate 13-acetate (PMA) and with a free radical-activated dye for 20 minutes, and analyzed by flow cytometry. Open bars represent *Hmox1*$^{+/+}$ values, hatched bars represent *Hmox1*$^{+/-}$ values, and closed bars represent *Hmox1*$^{-/-}$ values. Data are shown mean ± SEM from 3 experiments with each treatment sampled in duplicate. *c*, Representative liver section from *Hmox1*$^{-/-}$ mice given 1 mg/kg LPS stained with Prussian blue to detect iron. These histological results were indistinguishable from that of *Hmox1*$^{+/-}$ mice treated with 1, 5, or 25 mg/kg LPS, in that no significant iron staining was observed. *d*, Liver section of *Hmox1*$^{-/-}$ mice given 5 mg/kg LPS, stained with Prussian blue. Note the diffuse blue iron staining in many of the hepatocytes (arrows). *e*, Liver section of *Hmox1*$^{-/-}$ mice given 25 mg/kg LPS, stained with Prussian blue. Iron staining (arrows) is visible in viable hepatocytes adjacent to a necrotic focus (along the bottom edge of the photo). All magnification bars = 100 μm.

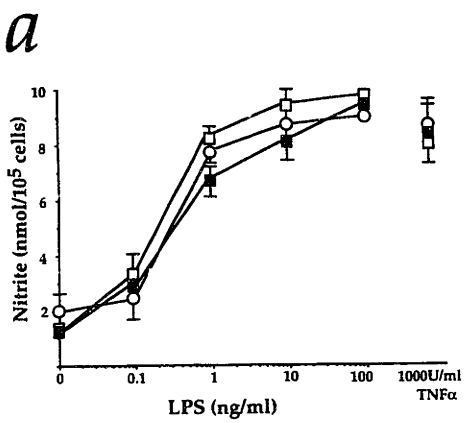
a
Nitrite (nmol/10^5 cells)
10
8
6
4
2
0
0.1
1
10
100
1000U/ml
TNFα
LPS (ng/ml)

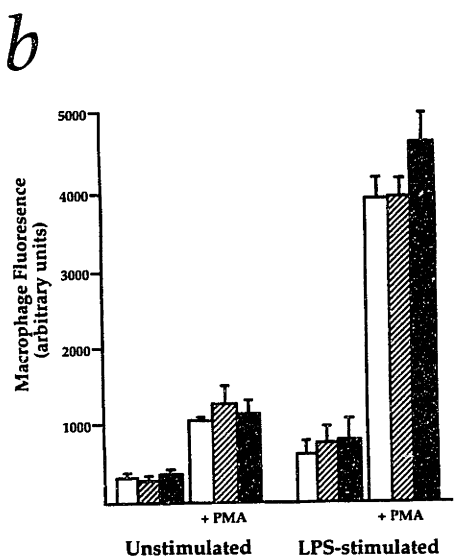
b
Macrophage Fluoresence (arbitrary units)
5000
4000
3000
2000
1000
+ PMA
+ PMA
Unstimulated
LPS-stimulated


c
d
e

Chapter 5

Genetic Evidence For A Neural Role Of Heme Oxygenase-2

Note: This work is adapted from a manuscript submitted 8/13/97 to *Nature*, by Randa Zakhary,* Kenneth D. Poss,† Samie R. Jaffrey,* Christopher D. Ferris,¶ Susumu Tonegawa,† and Solomon H. Snyder.*‡§

Departments of *Neuroscience, ‡Pharmacology and Molecular Sciences,
§Psychiatry and Behavioral Sciences, and
¶Division of Gastroenterology, Department of Medicine
Johns Hopkins University School of Medicine
Baltimore, Maryland 21205
†Howard Hughes Medical Institute and Center for Learning and Memory
Department of Biology
Massachusetts Institute of Technology
Cambridge, Massachusetts 02139

Summary

In neurons, nitric oxide (NO) is generated primarily by neuronal nitric oxide synthase (nNos), while carbon monoxide (CO) is synthesized by heme oxygenase-2 (Hmox2). Lines of evidence support neurotransmitter roles for both NO and CO through stimulation of soluble guanylyl cyclase; however, a role for CO has been controversial. Here, we showed that Hmox2 and nNos colocalize to myenteric ganglionic neurons. Then, we employed mice with targeted mutations of either *Hmox2* or *nNos* genes and examined neurally-evoked intestinal relaxation. Both *nNos*$^{-/-}$ and *Hmox2*$^{-/-}$ mice displayed dimished relaxation, reduced cGMP production, and delayed intestinal transit. Thus, in the myenteric plexus, both Hmox2 and nNos are important for neurotransmission.

Introduction

There is an abundance of evidence suggesting that nitric oxide (NO), generated by nitric oxide synthase (Nos), functions as a signaling molecule in both peripheral and central nervous systems. Its neural function has generally been established by detection of NO release following neuronal stimulation, and by the ability of NO donors and Nos inhibitors to affect synaptic transmission (1-5). Furthermore, mice lacking both neuronal Nos (nNos) and endothelial Nos isoforms show defects in hippocampal long-term potentiation, a form of synaptic plasticity (6). The signaling actions of NO are mediated, at least in part, by the stimulation of cGMP synthesis by soluble guanylyl cyclase (sGC) (7).

Analogously to NO, carbon monoxide (CO) is generated in neurons and may function as a messenger molecule via stimulation of sGC (8). The majority of physiological CO generation appears to stem from heme oxygenase (Hmox) activity, which is represented by two isoforms, Hmox1 and Hmox2. Like nNOS, Hmox2 is localized to neuronal populations in the brain and in the periphery (9). The idea that CO affects neural activity is based on the findings that Hmox inhibitors deplete cGMP levels in olfactory neurons, influence hippocampal long-term potentiation, and reduce relaxation of smooth muscle following neuronal depolarization (9-12).

In this study, we were specifically interested in a rigorous examination of the functions of NO and CO in a component of intestinal relaxation poorly understood at the molecular level; that mediated by nonadrenergic noncholinergic (NANC) neurotransmission. Regulated contraction and relaxation of enteric smooth muscle ensure that material moves through the gastrointestinal tract in a coordinated fashion, providing thorough and systematic digestion and absorption. In the enteric nervous system, multiple nerve-cell bodies are grouped into ganglia that are connected by nerve fibers; this organization of ganglia and fibers forms the submucosal plexus and the myenteric plexus. NANC nerves associated with the myenteric plexus are thought to mediate relaxation of enteric smooth muscle (13). Experimentally, NANC relaxation can be elicited from smooth muscle throughout the gastrointestinal tract by stimulation of enteric neurons with a ganglionic stimulant, 1,1-dimethyl-4 phenylpiperazinium (DMPP) or by electrical field stimulation (EFS) (13, 14). Here, to further study whether NO and also CO support NANC processes in the intestine, we employed both of these methods in mice lacking either nNos or Hmox2. Our results suggest that both NO and CO contribute as signaling molecules in ileal relaxation through cGMP-mediated pathways.

Materials and Methods

Immunohistochemistry and Double Labeling

Tissue specimans were dissceted and pinned flat on a styrofoam platform. Adherent fascia was carefully removed and tissue was fixed overnight in 4% paraformaldehyde. After cryoprotection in 30% sucrose, specimans were embedded in OCT, frozen on dry ice, and cut in a cryostat at a thickness of 15μM. The anti-Hmox2 antibody was prepared and used as described (15). Rhodamine-conjugated secondary antibodies (Vector) were used at 1:2000. Nuclear red was used for histochemical staining.

For double-label immunofluorescence, intestinal segments from male Sprague-Dawley rats were placed into an oxygenated organ chamber containing Krebs (see organ bath methods) and held at 37 ^{o}C. Colchicine was added directly into the organ chamber and tissue was fixed in 4% paraformaldehyde following 12 hr incubataion in 95% O_2/5% CO_2 at 37 ^{o}C. Tissue was fixed and sectioned as above. The anti-Hmox2 antibody was employed at a dilution of 1:1000. Preincubation of antisera with immunogenic peptide abolished immunoreactivity. In additional control experiments sections treated with Hmox2 preimmune sera showed no immunoreactivity. Anti-nNos antibodies (Transduction Labs) generated in either mouse or rat were used at 1:1000. Secondary antibodies conjugated either to rhodamine or FITC were employed at a dilution of 1:2000. When antibodies were from the same species (rabbit), sections were sequentially labeled. Sections were incubated in excess unlabeled anti-rabbit antibodies before application of the second primary antisera to prevent cross-reactivity of secondary antibodies with the inappropriate antigen. To assess validity of staining, the order of incubation of the primary antibody was reversed with similar results. Omission of either primary antibodies resulted in singly-labeled cells. For confirmation of neuronal staining and for quantitative determinations of neurons expressing nNos or Hmox2, sections were incubated in either nNos or Hmox2 antisera and neurofilament antibodies (Sigma) and peroxidase-linked secondary antibodies (data not shown). After development with peroxidase substrates, sections were counterstained with cresyl violet before viewing. Rat primary cortical cultures were prepared as described and labeled as above (16).

Organ Bath Experiments

Ileal segments were prepared from male mice after cervical dislocation. The entire gastrointestinal tract was removed as one block. The ileum was resected from this block and rinsed briefly in Ca^{2+}-free Krebs buffer, (119 mM NaCl, 4.6 mM KCl, 15 mM $NaHCO_3$, 1.2 mM $MgCl_2$, 1.2 mM NaH_2PO_4, 0.1 mM EGTA, and 11 mM glucose) pre-equilibrated with 95% O2/5% CO2 at 37 ^{o}C. Adherent tissue was removed and ileal segments of circular smooth muscle 2 cm in length were dissected in Ca^{2+}-free Krebs buffer as previously described (17). Strips were mounted between two L-shaped hooks in

temperature-controlled (37 ^{o}C) 25-ml tissue baths containing Krebs buffer (including 1.5 mM $CaCl_2$) continuously bubbled with 95% O_2/5% CO_2. Tension was measured with a force transducer which was attached to one of the l-shaped hooks. After equilibration for 1 hr, only strips that developed spontaneous tone were used. Strips were pretreated with 1 μM atropine, 1 μM propranolol, and 10 μM indomethacin for 20 min to eliminate cholinergic, adrenergic, and prostaglandin-mediated responses, respectively, before addition of DMPP or EFS.

Transit Analysis

Briefly, animals were fasted 24 hr before experiments, with ad libitum access to water. Polystyrene rings were removed from Sizmark capsules and cut into 1 mm pieces. Animals were administered 10-15 markers and radiographed 30 min after ingestion, and then at multiple intervals over the next thirty hr.

Measurements of cGMP

Tissue was prepared as described in organ bath methods. To rule out confounding effects of cyclic nucleotide phophodiesterases, experiments were performed in the presence of 0.5 mM isobutylmethylxanthine. Ileal strips were instantaneously frozen in liquid nitrogen 30 s after stimulation with 30 μM DMPP, and cGMP content was determined by radioimmunoassay (Amersham) in duplicate and standardized for protein content (Pierce).

Results

Ileal Localization of nNos and Hmox2

Previous experiments have indicated that nNos is expressed strongly in the myenteric plexus (18, 19). We have localized Hmox2 by immunohistochemistry in structures of the gastrointestinal tract (Fig. 1). In wild-type mice, immunoreactivity was observed in both the submucosal and myenteric plexuses, with most immunoreactive neurons associated with myenteric ganglia. Both cell bodies and nerve fibers coursing in parallel with inner circular muscle stained intensely in wild-type mice (Fig. 1b, c). No immunoreactivity was observed in *Hmox2*$^{-/-}$ mice (Fig. 1d). Gross histochemical analysis revealed no obvious differences between wild-type and *Hmox2*$^{-/-}$ mice (Fig. 1e, f).

We compared the expression of Hmox2 and nNos, and found that, in doubly-labeled sections from colchicine-treated murine ilea, both enzymes were expressed within the same subpopulations of myenteric neurons, representing about 60-70% of ganglionic neurons (Fig. 1g-i). In contrast, Hmox2 and nNos did not colocalize in primary cultures of rat cortical neurons (Fig. j-l).

Defective NANC Relaxation in *nNos*$^{-/-}$ *and Hmox2*$^{-/-}$ Mice

Stimulation of enteric neurons in intestinal segments from both strains of mutant mice as well as wild-type mice resulted in NANC relaxation that was dose-dependent and frequency-dependent (Figs. 2 and 3). However, segments from wild-type mice relaxed significantly more than segments from either *nNos*$^{-/-}$ *and Hmox2*$^{-/-}$ mice (Fig. 3a, b). Upon stimulation with 30 μM DMPP or EFS (16Hz, 2 ms), relaxation in tissues from *nNos*$^{-/-}$ *and Hmox2*$^{-/-}$ mice approached half that of wild-type animals. All relaxations were abolished by tetrodotoxin, which blocks nerve conductance, establishing that these methods of neuronal stimulation reflected neuronal depolarization rather than activation of smooth muscle or non-neuronal cells.

We next examined whether the deficits in mutant animals could be occluded by provision of NO or CO. Hemoglobin, which scavenges both CO and NO, completely eliminated NANC responses (Fig. 3a, b). Furthermore, concentration-response curves of intestinal smooth muscle responses to CO and sodium nitroprusside (SNP), an NO donor, in the absence of stimulation were similar between wild-type and mutant mice (Fig 3c, d). These results suggested that the lack of CO and NO production in mutants may be responsible for the reduced intestinal relaxation.

Then, we tested the influence of Nos and Hmox inhibitors on NANC relaxation in wild-type and mutant mice (Fig. 3e). Tin protoporphyrin-IX (SnPP), an inhibitor of Hmox which is thought to be specific for Hmox at concentrations less than 50 μM (15, 20), reduced relaxations in wild-type intestine from 75% to 32% (expressed as a percentage of maximal stimulation by SNP), and reduced relaxation in *nNos*$^{-/-}$ mice from 46% to 18%, when applied at 10 μM. No effect of SnPP was observed in preparations from *Hmox2*$^{-/-}$ mice. In wild-type mice, the Nos inhibitor N^G-nitro-L-arginine (L-NNA) reduced relaxation from 75% to 27%, while reducing relaxation in *Hmox2*$^{-/-}$ mice from 40% to 11%, when applied at 100 μM. L-NNA had no effect on intestinal relaxation in preparations from *nNos*$^{-/-}$ mice. The provision of NO or CO during stimulation of relaxation resulted in normal responses in the mutant animals (Fig. 3*f*) These results suggest that gaseous products of nNos and Hmox2 both provide major components of NANC relaxation.

Effects of *nNos* and *Hmox2* Mutations on Intestinal cGMP Levels

CO and NO are believed to function by stimulation of sGC. Also, previous experiments as well as those shown in Fig. 3*c* and *d* indicated that inhibitors of guanylyl cyclase such as 1H-(1,2,4) oxadiazol (4,3-a) quinolalin-1-one (ODQ) also block intestinal relaxation (21). We examined cGMP levels before and after depolarizing enteric neurons with 50 μM DMPP (Table 1). Basal cGMP levels in *Hmox2*$^{-/-}$ mice were only 55% that of wild-type controls. Moreover, the magnitude of activation of cGMP levels upon DMPP

stimulation in *Hmox2*$^{-/-}$segments was only 29% of that obtained in wild-type segments. In *nNos*$^{-/-}$intestines, basal cGMP levels were 74% of wild-type levels, while activation with DMPP yielded 46% of the magnitude of increase in cGMP levels seen in wild-type mice. These findings are consistent with the notion that the lack of sGC stimulation by NO and CO is responsible for the reduced intestinal relaxation in *nNos*$^{-/-}$ and *Hmox2*$^{-/-}$ mice, respectively.

CO, SNP, SnPP, and L-NNA had analogous effects on cGMP production in mutant animals as they had on intestinal relaxation (Table 1). CO and SNP application along with DMPP stimulation restored cGMP levels to that observed in wild-type mice. SnPP had no effects in *Hmox2*$^{-/-}$ mice, but reduced cGMP levels to 71% of untreated, DMPP-stimulated levels in wild-type mice, and 35% of untreated, DMPP-stimluated levels in *nNos*$^{-/-}$ mice. Similarly, while L-NNA had no effects in *nNos*$^{-/-}$ mice, it reduced cGMP levels to 56% of untreated, DMPP-stimulated levels in wild-type mice, and 33% of untreated, DMPP-stimulated levels in *Hmox2*$^{-/-}$ mice. These results support the findings from intestinal relaxation studies, in that Hmox2 and nNos both appear to provide components of relaxation, and suggest that this is done through stimulation of cGMP levels.

Delayed Gastrointestinal Transit in *nNos*$^{-/-}$ and *Hmox2*$^{-/-}$ Mice

In order to determine whether the in vitro physiological defects observed in *nNos*$^{-/-}$ and *Hmox2*$^{-/-}$mice had in vivo manifestations, we examined gastrointestinal transit. *Hmox2*$^{-/-}$ mice showed significantly slower overal transit than wild-type mice, while *nNos*$^{-/-}$ mice exhibitted delayed gastric emptying with nearly normal transit through the intestine and colon (Fig. 4). Although total transit was delayed in *Hmox2*$^{-/-}$ and *nNos*$^{-/-}$ mice, all markers used to track transit were excreted by 30 hr after ingestion. These results indicate that the mutant mice have gastrointestinal dysmotility without mechanical bowel obstruction.

Discussion

We chose the myenteric plexus as a system for examining roles of CO and NO as gaseous messenger molecules. Our results demonstrate impaired enteric neurotransmission, as well as reduced cGMP levels before and after enteric stimulation in both *Hmox2*$^{-/-}$ and *nNos*$^{-/-}$ mice. Treatment with CO or an NO donor could occlude these deficits in mutant animals. Furthermore, a Hmox2 inhibitor only blocked components of wild-type and *nNos*$^{-/-}$ relaxation and cGMP production, while a Nos inhibitor specifically blocked components of wild-type and *Hmox2*$^{-/-}$relaxation and cGMP production. Finally, we showed that intestinal function was impaired in both strains of mutant mice.

Our finding that nNos is required for maximal cGMP generation and intestinal relaxation agrees with a large body of evidence supporting NO as a physiological signaling molecule, including that from intestinal pharmacological studies (22). However, the idea that CO may function in a similar manner has been heavily disputed. Some inhibitors used to affect Hmox activity have demonstrated nonspecificity, and may even inhibit potentially consequential enzymes such as Nos and sGC (20, 23). In addition, despite the findings that Hmox inhibitors disrupt hippocampal long-term potentiation (10, 11), a study examining synaptic plasticity in *Hmox2*$^{-/-}$ hippocampi revealed that Hmox2-generated CO is unlikely to be a messenger involved in that mechanism (24). In fact, intestinal defects in *Hmox2*$^{-/-}$mice define the initial phenotype linked to the *Hmox2* mutations. Because CO is a direct stimulator of sGC, and because deficits in *Hmox2*$^{-/-}$mice can be resolved by addition of CO, we believe that peripheral myenteric plexus-mediated relaxation does normally utilize Hmox2-generated CO.

It is interesting to discover that both NO and CO could function in the same neurons. nNos and Hmox2 colocalize to distinct neuronal subsets, and deficits in either enzyme partially reduce NANC relaxation, cGMP production, and intestinal transit. Furthermore, our evidence suggests that these systems collaborate in mediating NANC relaxation. Hmox inhibitors blocked the already reduced *nNos*$^{-/-}$ relaxation, while nNos inhibitors affected *Hmox2*$^{-/-}$ relaxation. It has been previously suggested that CO may actually inhibit the activation of guanylyl cyclase by competitively inhibiting stimulation by NO (25). Our data here suggest that instead, the two molecules perform similar functions. That myenteric plexus ganglia ostensibly utilize both of these gases for cGMP generation and smooth muscle relaxation suggests that there may be other physiological systems which also depend on participation by both CO and NO.

Proper ileal relaxation and contraction is necessary for efficient absoption and waste disposal. The delay in gastrointestinal transit times in *nNos*$^{-/-}$ mice seemed due in part to the fact that they develop enlarged stomachs with hypertrophied circular muscle layers. On the other hand, *Hmox2*$^{-/-}$ mice had normal gastrointestinal anatomy. In each case, ileal tissue morphology and baseline responses to CO and SNP were similar to wild-type mice, suggesting that the mutations did not affect intrinsic function of intestinal smooth muscle. The decrements in intestinal relaxation in *Hmox2*$^{-/-}$and *nNos*$^{-/-}$ mice can account for most of NANC transmission. We speculate that the action of other proposed NANC neurotransmitters such as VIP, ATP, or substance P in the myenteric plexus and in other systems may require the presence of CO or NO.

References

1. Bredt, D. S. & Snyder, S. H. (1989). *Proc. Natl. Acad. Sci. USA* **86**, 9030-9033.
2. Burnett, A. L., Lowenstein, C. J., Bredt, D. S., Chang, T. S. K. & Snyder, S. H. (1992). *Science* **257**, 401-403.
3. Hall, S., Milne, B. & Jhamandas, K. (1996). *Brain Res.* **739**, 182-191.
4. Arancio, O., Kiebler, M., Lee, C. J., Lev-Ram, V., Tsien, R. Y., Kandel, E. R. & Hawkins, R. D. (1996). *Cell* 87, 1025-1035.
5. Lev-Ram, V., Jiang, T., Wood, J., Lawrence, D. S. & Tsien, R. Y. (1997). *Neuron* **18**, 1025-1038.
6. Son, H., Hawkins, R. D., Martin, K., Kiebler, M., Huang, P. L., Fishman, M. C. & Kandel, E. R. (1996). *Cell* **87**, 1015-1023,
7. Ignarro, L. J., Byrns, R. E., Buga, G. M. & Wood, K. S. (1987). *Circ. Res.* **61**, 866-879.
8. Ignarro, L. J. (1989). *Sem. Hematol.* **26**, 63-76.
9. Verma, A., Hirsch, D. J., Glatt, C. E., Ronnett, G. V. & Snyder, S. H. (1993). *Science* **259**, 381-384.
10. Stevens, C. F. & Wang, Y. (1993). *Nature* **364**, 147-149.
11. Zhuo, M., Small, S. A., Kandel, E. R. & Hawkins, R. D. (1993). *Science* **260**, 1946-1950.
12. Rattan, S. & Chakder, S. (1993). *Am. J. Physiol.* **265**, G799-G804.
13. Bennet, M. R., Burnstock, G. & Holman, M. (1966). *J. Physiol.* **183**, 541-558.
14. Chen, G., Portman, G. & Wickel, A. (1951). *J. Pharmacol. Exp. Therap.* **103**, 330-336.
15. Zakhary, R., Gaine, S. P., Dinerman, J. L., Ruat, M., Flavahan, N. A., & Snyder, S. H. (1996). *Proc. Natl. Acad. Sci. USA* **93**, 795-798.
16. Dawson, V. L., Kizushi, V., Huang, P. L., Snyder, S. H. & Dawson, T. D. (1996). *J. Neuroscience* **16**, 2479-2487.
17. Pelckmans, P. A., Boeckstaens, G. E., Van Maercke, Y. M., Herman, A. G. & Verbeurenm, T. J. (1990). *Eur. J. Pharmacol.* **190**, 239-246.
18. Bredt, D. S., Huang, P. M. & Snyder, S. H. (1990). *Nature* **347**, 768-770.
19. Ward et al, (1992). *Am. J. Physiol.* **263**, G277-G284.
20. Meffert, M. K., Haley, J. E., Schuman, E. M., Schulman, H. & Madison, D. V. (1994). *Neuron* **13**, 1225-1233.
21. Kanada, A. et al (1992). *Eur. J. Pharmacol.* **216**, 287-292.
22. Stark, M. E., Bauer, A. J. & Szurszewski, J. H. (1991). *J. Physiol.* **444**, 743-761.
23. Ignarro, L. J., Ballot, B. & Wood, K. S. (1984). *J. Biol. Chem.* **259**, 6201-6207.
24. Poss, K. D., Thomas, M. J., Ebralidze, A. K., O'Dell, T. J. & Tonegawa, S. (1995). *Neuron* **15**, 867-873.
25. Ingi, T., Cheng, J. & Ronnett, G. V. (1996). *Neuron* **16**, 835-842.

Table 1. Modulation of cGMP Levels in NANC Relaxation

Treatment	cGMP (fmol/mg protein)		
	Wild-type	*Hmox2*$^{-/-}$	*nNos*$^{-/-}$
Unstimulated			
Control	817 ± 90	450 ± 49*	603 ± 52*
SnPP (10 μM)	787 ± 56	472 ± 24	589 ± 48
L-NNA (100 μM)	840 ± 70	415 ± 33	615 ± 42
ODQ (10 μM)	553 ± 48	302 ± 22	438 ± 32
DMPP-Stimulated			
Control	1785 ± 165	602 ± 63*	931 ± 74*
SnPP (10 μM)	1271 ± 89¶	588 ± 44	326 ± 39¶
L-NNA (100 μM)	1006 ± 70#	198 ± 22#	822 ± 67
ODQ (10 μM)	603 ± 58	389 ± 27	467 ± 32
CO (1 mM)	1960 ± 143	2100 ± 187	2050 ± 225
SNP (100 μM)	2197 ± 178	2267 ± 209	2003 ± 126

Ileal muscle strips were treated with 1,1-dimethyl-4-phenylpiperazinium (DMPP) for 30 s and instantaneously frozen. cGMP content was determined by radioimmunoassay. Data are shown as mean ± SEM. *$P < 0.01$ between mutant and wild-type values (Student's t test). ¶$P < 0.01$ between control and SnPP-treated samples. #$P < 0.01$ between control and L-NNA-treated samples. Abbreviations: SnPP, tin protoporphyrin-IX; L-NNA, N^G-nitroarginine; ODQ, 1H- (1,2,4) oxadiazol (4,3-a) quinolalin-1-one; CO, carbon monoxide; SNP, sodium nitroprusside.

Fig. 1. Hmox2 and nNos expression in the enteric nervous system. *a*, Nomarski view of ileum from wild-type mouse. S: submucosa, CM: circular muscle, LM: longitudinal muscle. *b*, *c*, Hmox2 expression in myenteric ganglia (arrowheads) in wild-type mice at low (*b*) and high (*c*) power magnification. *d*, No Hmox2 immunoreactivity is observed in *Hmox2*$^{-/-}$ mice. *e*, *f*, Cross sections of ilea from wild-type (*e*) and *Hmox2*$^{-/-}$ (*f*) mice stained with nuclear red for histochemical analysis. *g-i*, Myenteric ganglia (arrows denote example) from colchicine-treated ilea of wild-type mice doubly-labeled with anti-Hmox2 (*g*) and anti-nNos (*h*), double exposure (*i*). *j-l*, Rat primary cortical neurons doubly labeled with anti-Hmox2 (*j*) and anti-nNos (*k*), double exposure (*l*).

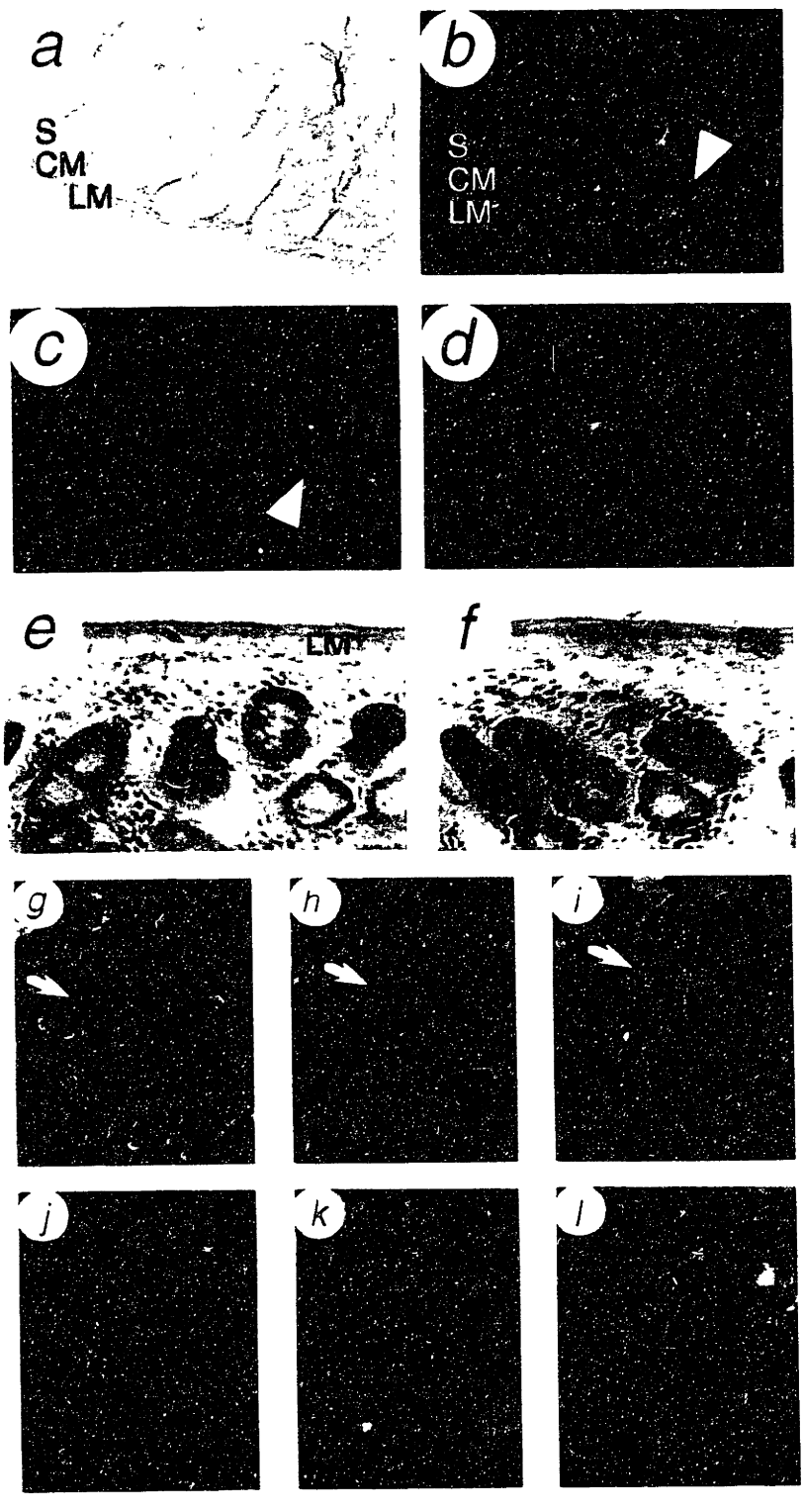
a
S
CM
LM
b
S
CM
LM
c
d
e
LM
f
g
h
i
j
k
l

Fig. 2. Sample tracings from a typical experiment in which NANC relaxation of mouse ileum was induced by 16 Hz EFS. Muscle strips were stimulated by EFS only once so that each tracing represents an independent experiment. Tetrodotoxin (TTX, 1 mM) abolished all NANC relaxations induced by EFS. Tin protoporphyrin-IX (SnPP, 10 mM) partially reduced relaxations in wild-type and *nNos*$^{-/-}$ preparations, but had no effect on *Hmox2*$^{-/-}$ relaxation. NG-nitro-L-arginine (L-NNA, 100 mM) partially reduced relaxation in wild-type and *Hmox2*$^{-/-}$ strips while exerting no significant effect on relaxation in *nNos*$^{-/-}$ tissue. Neither SnPP nor L-NNA affected baseline tensions (data not shown).

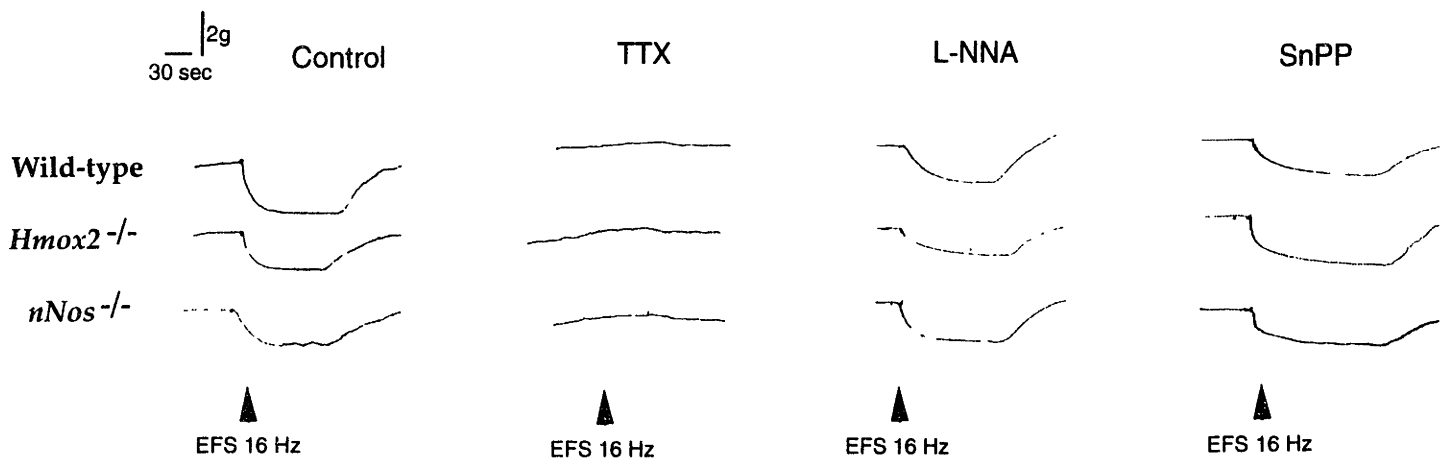
2g
30 sec
Control
TTX
L-NNA
SnPP
Wild-type
Hmox2 -/-
nNos -/-
EFS 16 Hz
EFS 16 Hz
EFS 16 Hz
EFS 16 Hz

Fig. 3. Intestinal relaxation in mice lacking either Hmox2 or nNos. *a*, *b*, NANC relaxation in ileal segments following electrical field stimulation or addition of DMPP. Results are expressed as a mean percentage of the maximal relaxation achieved with 100 μM SNP. In all figures, wild-type responses are expressed as an average of values from separate wild-type control strains for *Hmox2*$^{-/-}$ and *nNos*$^{-/-}$ mice. Standard error was between 4% and 13% from 5-7 experiments. Asterisks denote significant differences between wild-type responses and those of both *Hmox2*$^{-/-}$ and *nNos*$^{-/-}$ mice (*$p < 0.05$, **$p < 0.01$, ANOVA). Hgb: 100 μM hemoglobin. Note: each strip was stimulated only once, and values represent the mean of 7-11 independent experiments. *c*,*d*, Concentration-response curves of enteric muscle from wild-type and mutant mice to SNP (*c*) and CO (*d*). Results are expressed as a percentage of the maximal response to SNP. Standard error ranged between 5% and 11% from 5-7 experiments. ODQ: 10 μM 1H-(1,2,4) oxadiazol (4,3-a) quinolalin-1-one. *e*, Effect of pharmacologic inhibition of Nos and Hmox on EFS-elicited NANC relaxations in wild-type and mutant mice. Concentrations used are 10 mM SnPP, 100 mM L-NNA, and 1 mM TTX (tetrodotoxin) (**$p < 0.01$, compaired to untreated preparations from same genotype, Student's *t* test, from 7-9 experiments. *f*, Effect of 100 mM CO and 100 mM SNP on EFS-induced NANC relaxation. For *e* and *f*, experiments using DMPP yielded similar results.

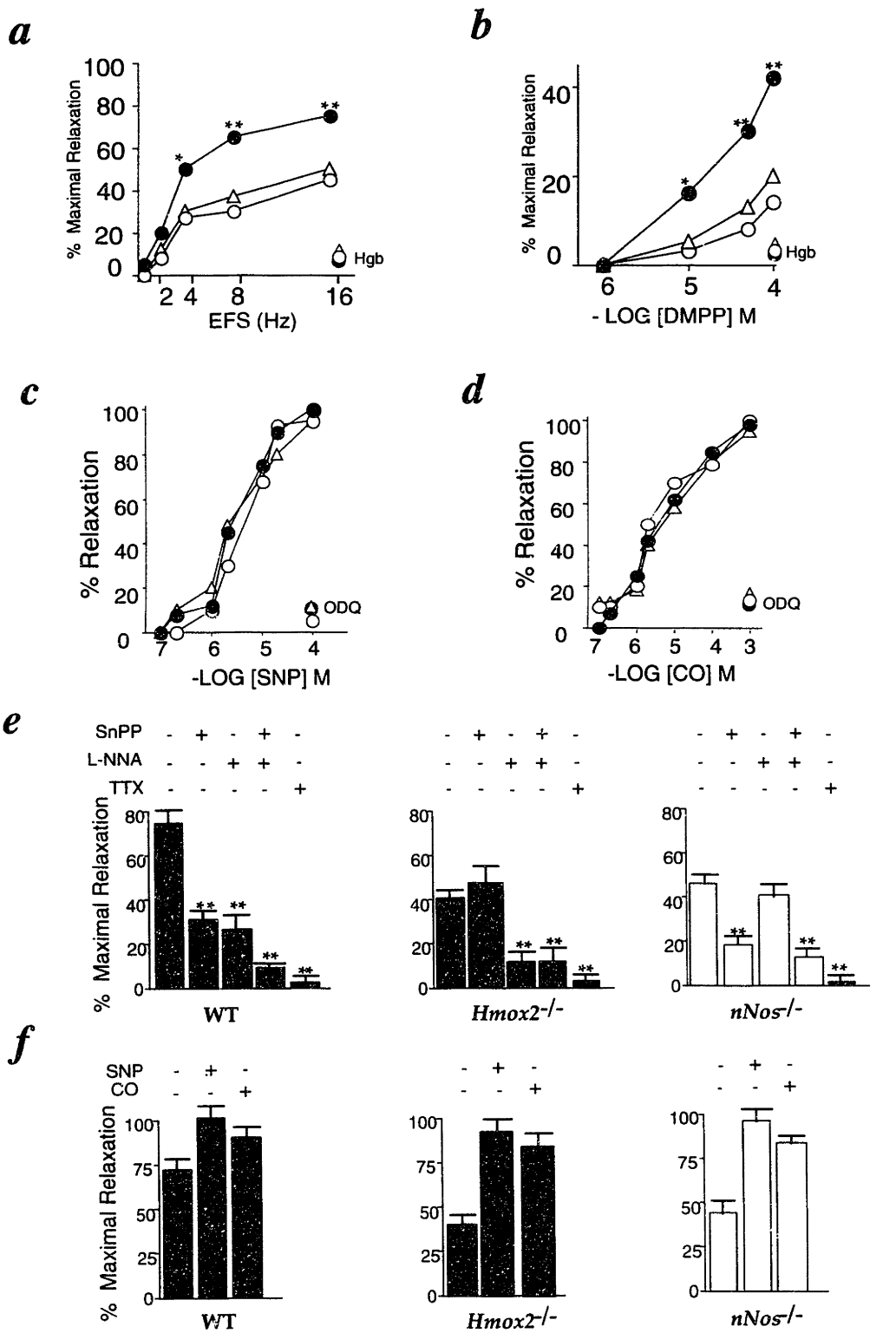
a
% Maximal Relaxation
EFS (Hz)
Hgb
b
% Maximal Relaxation
- LOG [DMPP] M
Hgb
c
% Relaxation
-LOG [SNP] M
ODQ
d
% Relaxation
-LOG [CO] M
ODQ
e
SnPP
L-NNA
TTX
% Maximal Relaxation
WT
Hmox2-/-
nNos-/-
f
SNP
CO
% Maximal Relaxation
WT
Hmox2-/-
nNos-/-

Fig. 4. Gastrointestinal transit in *Hmox2*$^{-/-}$ and *nNos*$^{-/-}$ mice. *a*, 10-14 radioopaque markers (arrow) were fed to mice and tracked by radiography at periodic intervals. Note the presence of markers in mutant intestines 2 hr after ingestion (T_{2h}). Excretion of markers was also monitored by x-ray (bottom panel). *b*, Average time to excrete all markers. Results are expressed as mean number of hours from marker consumption to excretion. (**$p < 0.01$, Students t test, from 7-11 experiments).

a

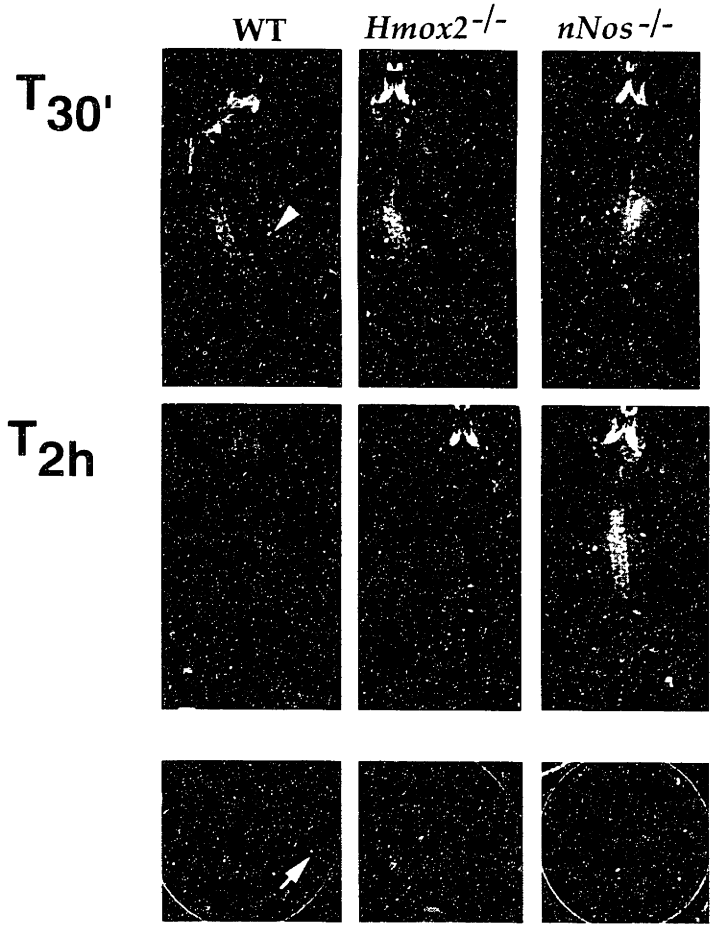
WT
Hmox2-/-
nNos-/-
T30'
T2h

b

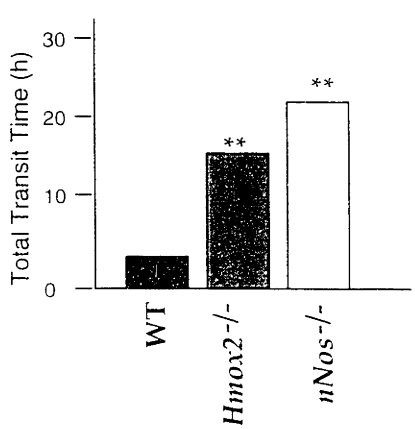
Total Transit Time (h)
30
20
10
0
**
**
WT
Hmox2-/-
nNos-/-

Chapter 6

Ejaculatory Abnormalities In Mice Deficient In Heme Oxygenase-2

Note: This work is adapted from a manuscript submitted 7/3/97 to *Nature Medicine*, by Arthur L. Burnett,* Devin G. Johns,† Lance J. Kriegsfeld,§ Sabra L. Klein,§ David C. Calvin,* Gregory E. Demas,§ Lawrence P. Schramm,† Susumu Tonegawa,# Randy J. Nelson,§ Solomon H. Snyder,¶‡¥ and Kenneth D. Poss.#

*Departments of Urology, †Biomedical Engineering, ¶Pharmacology and Molecular Science, ‡Neuroscience,¥Psychiatry, and §Psychology - College of Arts and Sciences, Johns Hopkins University School of Medicine
Baltimore, Maryland 21205
#Howard Hughes Medical Institute and Center for Learning and Memory
Department of Biology
Massachusetts Institute of Technology
Cambridge, Massachusetts 02139

Summary

Carbon monoxide (CO), generated by heme oxygenase-2 (Hmox2), has been suggested as a signaling molecule in several different neuronal systems. By immunohistochemistry, we have localized Hmox2 to male autonomic structures that regulate copulatory activity. In male mice lacking functional Hmox2, erectile function was normal, but reflex activity of the bulbospongiosus muscle, which helps to mediate ejaculation, was markedly diminished. Furthermore, Hmox2-deficient males displayed defective sexual behaviors including mounting, intromission, and ejaculation. These findings suggest that CO may help mediate reflex activity involved in ejaculatory process.

Introduction

There is an abundance of evidence suggesting that nitric oxide (NO) acts as a neurotransmitter in the central and peripheral nervous systems (1). More recently, another gas, carbon monoxide(CO), has been implicated in neurotransmission. The majority of physiological CO production is believed to stem from the activity of heme oxygenase (Hmox), which breaks down heme to yield CO, free iron, and biliverdin. A subtype of Hmox, heme oxygenase-2 (Hmox2), is localized to several neuronal populations in the central and peripheral nervous systems (2). Numerous recent observations lend support to the idea that CO generated by Hmox2 may be a biologically functional byproduct in processes such as hippocampal long-term potentiation, olfactory neuronal responses, cerebellar Purkinje cell activity, and vasorelaxation (3-6). First, cerebral expression of Hmox2 closely resembles that of soluble guanylyl cyclase, an in vivo target of NO which can also be stimulated in vitro by CO (4). Second, metalloporphyrin inhibitors of Hmox2 potently block several biological activities (2). Third, the addition of CO to live tissue preparations can increase cGMP levels and affect neuronal or muscular activity (3-6). Despite this, the findings that metalloporphyrins may have pharmacological targets other than Hmox and that mice with targeted disruptions of *Hmox2* gene copies had normal hippocampal long-term potentiation have cast doubts on the idea that CO is a relevant signaling molecule (7, 8).

Recently, it was demonstrated that Hmox2-deficient (*Hmox2*$^{-/-}$) mice have defects in myenteric plexus neurotransmission, providing the first genetic evidence that CO may indeed be an in vivo neuromodulator (9). Here, because of an earlier finding that NO may be essential for erection (10), we hypothesized that CO could also participate in copulatory processes. Therefore, we utilized *Hmox2* $^{-/-}$ mice to examine the role of CO in erectile and ejaculatory physiology. In addition, we closely examined sexual behavior in these mice. We found that *Hmox2* $^{-/-}$ mice display abnormalities in both a bulbiospongiosus reflex representing the ejaculatory process, and in male sexual behaviors such as mounting, intromission, and ejaculation. Our results suggest that Hmox2 and CO play important roles in male copulatory function.

Methods and Materials

Histology

Animals were killed by CO_2 asphyxiation, and the urinary bladder, urethra, and the penis with adjacent bulbospongiosus musculature were removed en bloc. Tissue sections (10μm) were obtained after liquid nitrogen immersion for immunohistochemistry and histology as described in (7).

Affinity-purified rabbit anti-rat Hmox2 antibody was generated against a synthesized peptide corresponding to amino acids 247-258 of rat Hmox2 (11). Immunohistochemical localizations of nerves were verified with rabbit anti-human protein gene product 9.5 antibody (12).

Electrophysiology

Monitoring of urethrogenital reflexes was conducted similarly to the method described by McKenna et al. (13). Briefly, animals were anesthetized with urethane (1.8 mg/kg intraperitoneally), and underwent lower midline abdominal laparotomy and cystotomy for antegrade proximal urethral cannulation with a PE-50 catheter, distal penile urethra ligation, and bipolar electrode placement on the surface of the bulbiospongiosus muscle for electromyographic recordings. Urethral pressures were generated by catheter infusion for 50 sec durations in duplicate at 10 cm H_2O increments from 40-90 cm H_2O, with 200 sec intervals between stimuli. Action potential responses were detected by a window discriminator, and the resultant standardized pulses were averaged by a low pass filter to produce a signal that is proportional to the frequency of the action potentials. This signal was sampled at 25 Hz and recorded on a computer for further processing. Experiments were done with the experimenter blind to the genotype of animals.

Electrophysiologic induction of penile erections was performed as described previously (10).

Behavior

Behavioral testing involved a battery of sensorimotor tasks that appraise capabilities necessary for copulatory success in rodents and mating studies as described previously (14).

Results

Localization of Hmox2 in Male Copulatory Structures

Immunohistochemical staining revealed that Hmox2 protein is localized to the major pelvic ganglion and its nerve distributions to the penis, urethra, bladder neck, vas deferens, and prostate, and to pudendal nerve branches in the penis and urethra , as well as to vascular endothelium and epithelium within genitourinary structures of wild-type mice (Fig. 1). The expression of Hmox2 in petrosal, superior cervical nodose neurons resembles that in myenteric ganglia, while genitourinary endothelial expression of Hmox2 resembles that in other blood vessels (6). Tissues from *Hmox-2*$^{-/-}$ mice showed no immunoreactivity in these experiments (Fig. 1).

Aberrant Ejaculatory Reflexes of *Hmox-2*$^{-/-}$ Mice

To determine whether CO may play a role in erection, we employed a paradigm of physiological erection by electrically stimulating cavernous nerves of *Hmox-2*$^{-/-}$ mice. We found that erection following nerve stimulation is similar in *Hmox-2*$^{-/-}$ mice (n = 3) as that in wild-type mice (n = 18; data not shown).

Since Hmox2 is also localized to neuronal systems that might mediate ejaculation, we monitored reflex activity of the bulbiospongiosus muscle. McKenna and colleagues have demonstrated that bulbiospongiosus electrical activity following increased urethral pressure reflects firing of the pudendal motor neurons that mediate contraction of perineal musculature during ejaculation (13). Progressive increases in urethral pressure produced increasing activity of the bulbiospongiosus muscle in wild-type mice. However, this response was virtually obliterated in *Hmox-2*$^{-/-}$ mice, with no consistent effect of increased urethral pressure (Fig. 2). Importantly, this disparity was observed between two different background strains of *Hmox-2*$^{-/-}$ mice and the appropriate wild-type controls; namely, a (C57BL/6 x 129/SvEv) hybrid strain and a 129/SvEv coisogenic strain were used (coisogenic data not shown). That Hmox2 is required for this reflex suggests that Hmox2 and CO may normally help mediate ejaculatory processes.

Defects in Male Sexual Behavior of *Hmox-2*$^{-/-}$ Mice

We had noticed no gross abnormalities in the fecundity of *Hmox-2*$^{-/-}$ mating pairs in our mouse colony (8). However, because of the striking deficits observed in ejaculatory responses of *Hmox-2*$^{-/-}$ mice, we closely examined *Hmox-2*$^{-/-}$ mice for any behavioral manifestations. We initially studied the mating behavior of two strains of *Hmox-2*$^{-/-}$ and wild-type males paired with estrous females during a 30-minute test period. Results from each strain indicated trends of *Hmox-2*$^{-/-}$ animals toward abnormalities in mounting, intromission, and ejaculation (Table 1). Combined results from analysis of both strains indicated that 60% of wild-type males mounted, compared to only 37% of *Hmox-2*$^{-/-}$ mice ($X^2 = 6.80$, $p < 0.05$). Of these males that mounted, 83% of wild-type males proceeded to intromit, compared to only 54% of *Hmox-2*$^{-/-}$ males ($X^2 = 6.31$, $p < 0.025$). Of the 6 *Hmox-2*$^{-/-}$ mice which intromitted, none ejaculated during the test period, compared to 7 of 20 intromitting wild-type males. Latencies to mount and intromit were similar between wild-type and *Hmox-2*$^{-/-}$ mice. In addition, the mating behavior of female *Hmox-2*$^{-/-}$ mice was normal.

Serum testosterone, which may affect copulatory behavior, was normal in *Hmox-2*$^{-/-}$ males (data not shown). Furthermore, to ascertain that the abnormal sexual behavior in *Hmox-2*$^{-/-}$ males did not derive from defects in sensorimotor activity, we evaluated olfactory ability, motor coordination, motor strength, and visual acuity as well as behavior in an open field arena. *Hmox-2*$^{-/-}$ mice did display increased open field activity

and some decrease in forelimb strength (Table 2). However, the overall sensorimotor behavior of *Hmox-2*$^{-/-}$ males did not seem to be notably impaired and is not likely to account for the deficits in intromission and ejaculation. Therefore, we conclude from our tests that the *Hmox-2*$^{-/-}$ had fairly specific defects in copulatory behavior.

Discussion

Utilizing mice devoid of functional Hmox2, we addressed whether Hmox2-generated CO has a role in mediating erectile and ejaculatory physiological processes. We found that male *Hmox-2*$^{-/-}$ mice had defects in a bulbospongiosus reflex which stimulates ejaculation. Behaviorally, *Hmox-2*$^{-/-}$ mice showed poor performance in mounting, intromission, and ejaculation.

Ejaculation has not been well-characterized in terms of fundamental neuromuscular mechanisms that mediate the response. The ejaculatory reflex itself is thought to be comprised of coordinaed contractions of the bulbospongiosus and ischiocavernosus somatic muscles as well as the smooth musculature of the vas deferens, ejaculatory ducts, proximal urethra, and bladder neck (15). Sympathetic activity is necessary for regulation of ejaculation, since ablations of sympathetic nerves and antisympathetic drugs impair ejaculation. Specifically, a descending serotonergic pathway may inhibit ejaculation, as certain 5,6-dihydroxytryptamine lesions can enhance ejaculation, while antidepressants that augment serotonergic neurotransmission retard it (15-17). Our results indicating a severely reduced bulbiospongiosus response in *Hmox-2*$^{-/-}$ mice suggest that Hmox2, which shows prominent expression in urogenital structures, somehow participates. The fecundity of Hmox2-/- mating pairs is not affected despite this large deficit, however, suggesting that alternative systems that contribute to ejaculation, other than the physiological paradigm described here, function effectively in Hmox2-deficient males.

The abnormalities in sexual behavior of *Hmox-2*$^{-/-}$ mice probably do not reflect a defect in erection, since induced erection by nerve stimulation appeared to be normal. Recent studies indicated that the "coital reflex" comprises closely coordinated systems that mediate both intromission and ejaculation (18). Thus, the same or closely related abnormalities may underlie both the reduced number of intromissions and the defective ejaculation in *Hmox-2*$^{-/-}$ animals. The reduced frequency of mounting in *Hmox-2*$^{-/-}$ mice may be secondary to motivation due to diminished positive feedback from intromission and ejaculation activity.

One paradoxical aspect of these results is that *Hmox2*$^{-/-}$ murine mating pairs show no reduced fecundity, yet males have very little bulbospongiosus response along with abnormal mating behavior in our experiments. This might be best explained by the fact

that bulbiospongiosus muscles of many Hmox2-deficient males occasionally fired when stimulated in our experiments. Although the average responses were very low, perhaps an infrequent response was enough to sustain normal litter numbers. Also, it is not clear that the type of bulbospongiosus muscle reflex during urethral pressure measured here represents the sole or even major component required for ejaculation. Our results only suggest that Hmox2 is important for this physiological component of ejaculation, and that its dysfunction affects male sexual behavior.

Although levels of heme, biliverdin, and free iron are likely affected by the *Hmox-2* mutations, we believe that the ablation of CO production may be primarily responsible for the male sexual defects. Recently, by analyzing *Hmox2*$^{-/-}$ mice, Zakhary et al. showed that Hmox2-generated CO appears to help mediate intestinal non-adrenergic, non-cholinergic neurotransmission by stimulating cGMP production (9). Whether cGMP is an essential second messenger in the paradigms examined here remains to be shown. Attempts to rescue defective physiological responses with CO or cGMP analogues may be useful in addressing these issues. In addition, our study has not clarified the structures in which Hmox2 is important for sexual function. Besides its neuronal localization in the genitourinary tract, Hmox2 is expressed in vascular endothelium and epithelial layers that might have some influence on ejaculatory mechanisms.

In conclusion, our results demonstrate a defect in the ejaculatory response of Hmox2-deficient mice. It is notable that approximately 40% of adult human males suffer from some type of ejaculatory disturbance (19). Except for the recent use of antidepressants that inhibit serotonin reuptake, such as fluoxetine, sertraline, and paroxetine, few treatments are available for premature ejaculation. Remedies for delayed ejaculation are similarly lacking. Therefore, *Hmox-2*$^{-/-}$ mice might be valuable as models for examining the effects of candidate drugs on latency prior to ejaculation. In addition, we speculate that drugs that modulate Hmox activity may be potentially useful for medical care of ejaculatory ailments.

References

1. Jaffrey, S. R. & Snyder, S. H. (1995). *Ann. Rev. Cell. Dev. Biol.* **11**, 417-440.
2. Maines, M. D. (1997). *Annu. Rev. Pharmacol. Toxicol.* **37**, 517-554.
3. Stevens, C. F. & Wang, Y. (1993). Nature **364**, 147-149.
4. Verma, A., Hirsch, D. J., Glatt, C. E., Ronnett, G. V. & Snyder, S. H. (1993). *Science* **259**, 381-384.
5. Nathanson, J. A., Scavone, C., Scanlon, C. & McKee, M. (1995). *Neuron* **14**, 781-794.
6. Zakhary, R., Gaine, S. P., Dinerman, J. L., Ruat, M., Flavahan, N. A. & Snyder, S. H. (1996). *Proc. Natl. Acad. Sci. USA* **93**, 795-798.
7. Meffert, M. K., Haley, J. E., Schuman, E. M., Schulman, H. & Madison, D. V. (1994). *Neuron* **13**, 1225-1233.
8. Poss, K. D., Thomas, M. J., Ebralidze, A. K., O'Dell, T. J. & Tonegawa, S. (1995). *Neuron* **15**, 867-873.
9. Zakhary, R., Poss, K. D., Jaffrey, S. R., Ferris, C. D., Tonegawa, S. & Snyder, S. H. (submitted)
10. Burnett, A. L., Lowenstein, C. J., Bredt, D. S., Chang, T. S. K. & Snyder, S. H. (1992). *Science* **257**, 401-403.
11. Prabhakar, N. R., Dinerman, J. L., Agani, F. H. & Snyder, S. H. (1995). *Proc. Natl. Acad. Sci. USA* **92**, 1994-1997.
12. Gulbenkian, S., Wharton, J., and Polak, J. M. (1987). *J. Auton. Nerv. Sys.* **18**, 235-247.
13. McKenna, K. E., Chung, S. K. & McVary, K. T. (1991). *Am. J. Physiol.* **30**, R1276-R1285.
14. Nelson, R. J., Demas, G. E., Huang, P. L., Fishman, M. C., Dawson, V. L., Dawson, T. M. & Snyder, S. H. (1995). *Nature* **378**, 383-386.
15. Benson, G. M. (1994) in *The Physiology of Reproduction*, eds. Knobil, E. & Neill, J. D. (Raven Press, New York), pp. 1489-1506.
16. Marson, L. & McKenna, K. E. (1994). *Pharmacol. Biochem. Behav.* **47**, 883-888.
17. Janicak, P. G., Davis, J. M., Preskorn, S. H. & Ayd, F. J. (1994) *Principles and Practice of Psychopharmacotherapy.* (Williams and Wilkins, Baltimore).
18. Everitt, B. J. (1990). *Neurosci. Biobehav. Rev.* **14**, 217-232.
19. Spector, I. P. & Carey, M. P. (1990). *Arch. Sex. Behav.* **19**, 389-408.

Table 1. Mating Behavior of *Hmox2*$^{-/-}$ Male Mice

Behavior	*Hmox2*$^{+/+}$			*Hmox2* $^{-/-}$		
	Strain			Strain		
	129	B6/129	Total	129	B6/129	Total
Mounting						
Fraction mounting	14/25	10/15	24/40 (60%)	6/22	5/8	11/30 (37%)*
Latency to mount (s)	681 ± 142	496 ± 128	----	857 ± 172	767 ± 181	----
Intromission						
Fraction Intromitting	12/14	8/10	20/24 (83%)	3/6	3/5	6/11 (54%)*
Latency to intromit (s)	978 ± 140	835 ± 152	----	919 ± 180	868 ± 83	----
Ejaculation	4/12	3/8	7/20 (35%)	0/3	0/3	0/6 (0%)

Data are listed as number of performing animals as the numerator and total number of animals examined as denominator, or as mean ± SD. * $P < 0.05$ by Chi square analysis.

Table 2. Sensimotor Task Performance by *Hmox2*$^{+/+}$ and *Hmox2*$^{-/-}$ Mice

Task	*Hmox2*$^{+/+}$	*Hmox2*$^{-/-}$
Latency to find hidden cookie (s)	386 ± 27	420 ± 41
Latency to turn in blind alley (s)	20.1 ± 2.9	28 ± 4.3
Latency to walk one body length (s)	14.8 ± 5.2	20.7 ± 4.7
Latency to turn on an inclined screen (s)	13.9 ± 2.3	16.5 ± 1.7
Forelimb strength (latency to fall from a suspended wire (s))	76.1 ± 7.0	18.5 ± 6.2*
Latency to fall from a suspended pole (s)	37.7 ± 7.0	50.0 ± 14.0
Open field behavior:		
# of external squares crossed	155 ± 17	210 ± 19*
# of internal squares crossed	10.5 ± 3.2	20.1 ± 6.6
Duration spend in open field (s)	12.5 ± 2.6	18.1 ± 2.6

Data are expressed as mean ± SEM for groups of 14 *Hmox2*$^{+/+}$ and 6 *Hmox2*$^{-/-}$ male mice of the B6/129 strain background. *P < 0.05 by Student's t-test analysis.

Fig. 1. Hmox2 immunostaining of genitourinary tissues from wild-type and *Hmox-2*$^{-/-}$ mice. A-D, In sections of the dorsal aspect of the penis (A) and proximal urethra (C) of wild-type mice, Hmox2 localizes to the nerve trunks of the dorsal nerve of the penis (arrows), the endothelium (arrowheads), and the epithelium of the ejaculatory ducts (labeled as "E") and urethra (labeled as "U"). Corresponding sections from *Hmox-2*$^{-/-}$ mice (B and D) exhibit only non-specific background staining. E, In the major pelvic ganglion of wild-type mice, Hmox2 immunoreactivity is apparent in ganglion cells (arrows) and nerve fibers (arrowheads) as well as in the glandular epithelium of the adjacent prostate (labeled as "P"). F, Preincubation of Hmox2 antiserum with Hmox2 peptide abolishes immunoreactivity. V = dorsal vein of the penis. All magnification bars = 250 μm.

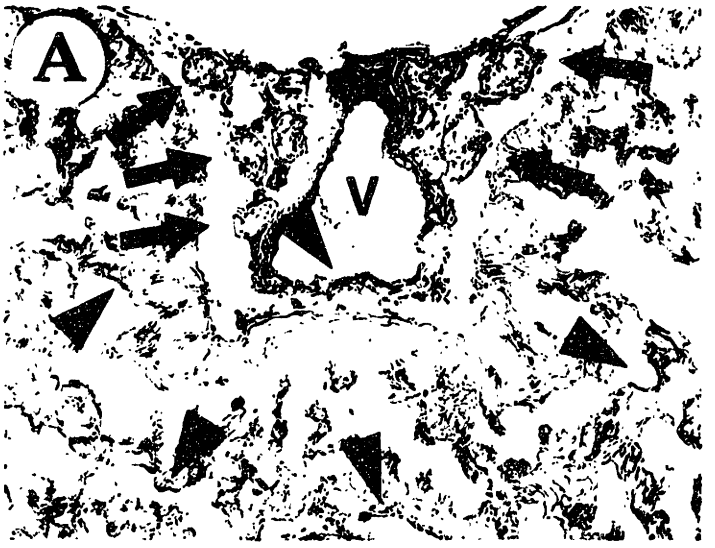
A
V

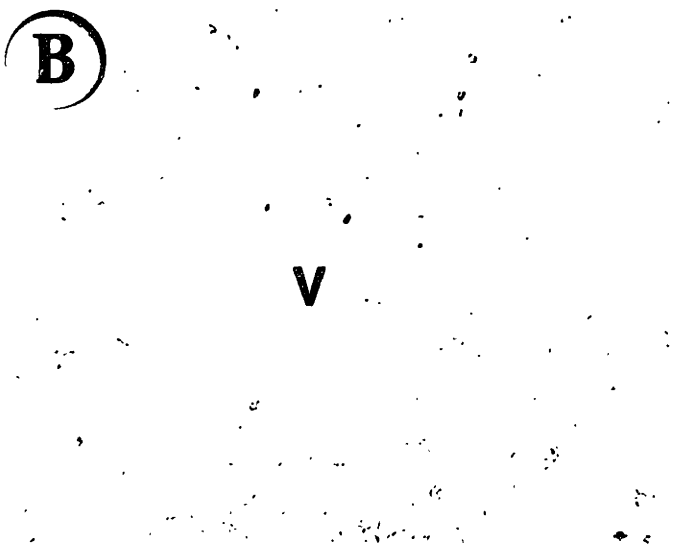
B
V


C
U
E
E

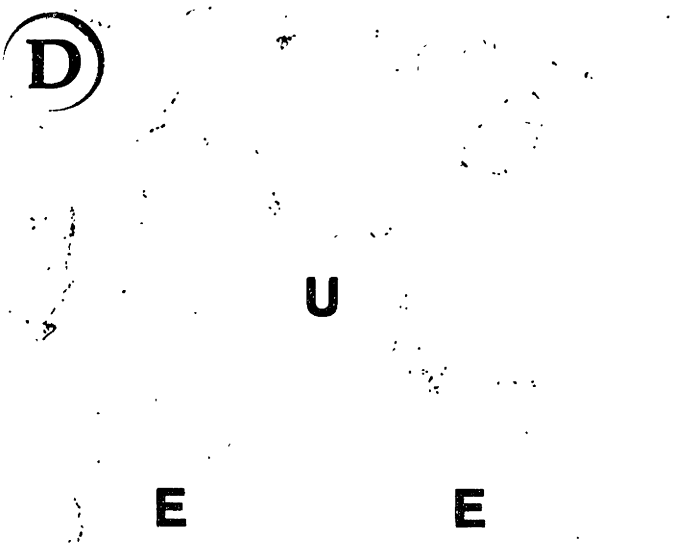
D
U
E
E

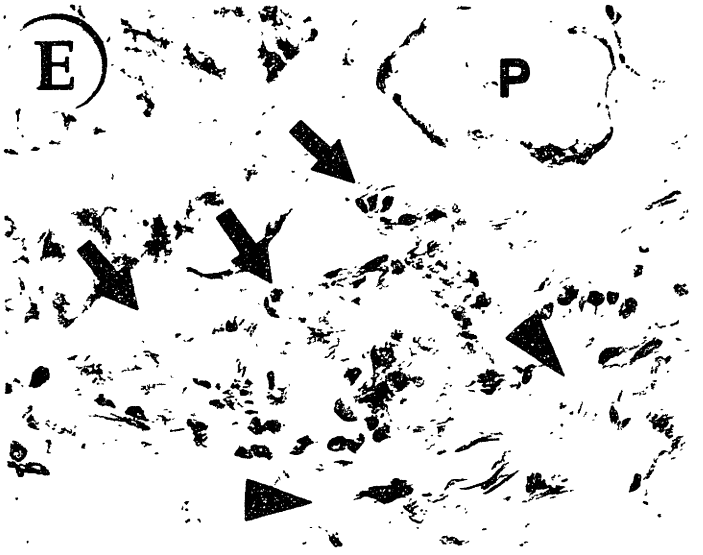
E
P

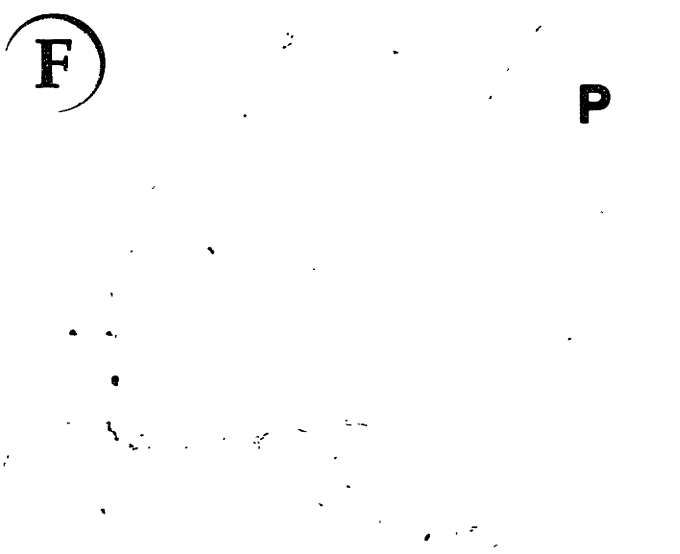
F
P

Fig. 2. Bulbiospongiosus electromyographic activity in response to urethral pressure stimulation in wild-type and *Hmox-2*$^{-/-}$ mice. A, Example of experiment using a urethral pressure stimulus of 80 cm H_2O in which unprocessed and integrated voltage recordings were obtained. B, Bulbiospongiosus firing (arbitrary units) at designated urethral pressures in wild-type and *Hmox-2*$^{-/-}$ mice. Reflex activity is significantly reduced ($p < 0.005$ for all pressure levels) in *Hmox-2*$^{-/-}$ mice ($n = 8$) compared with that of wild-type mice ($n = 7$). Data are shown mean ± SEM.

A

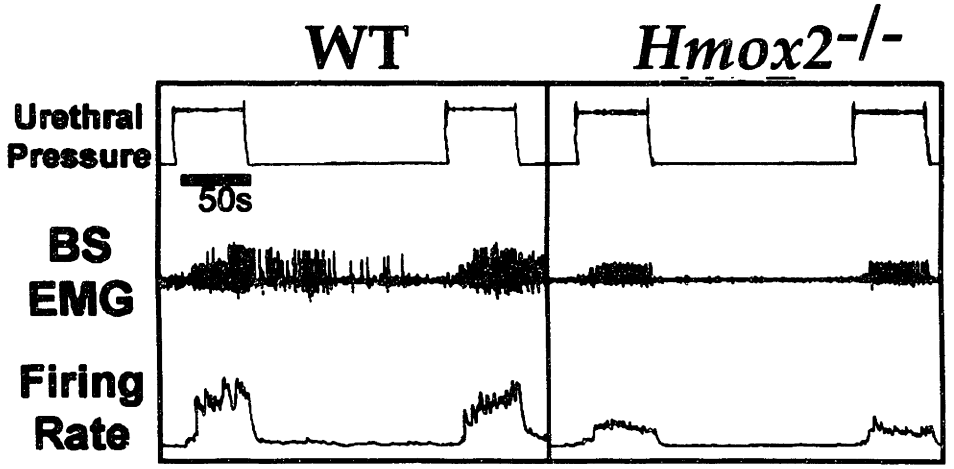
WT
Hmox2-/-
Urethral Pressure
50s
BS EMG
Firing Rate

B

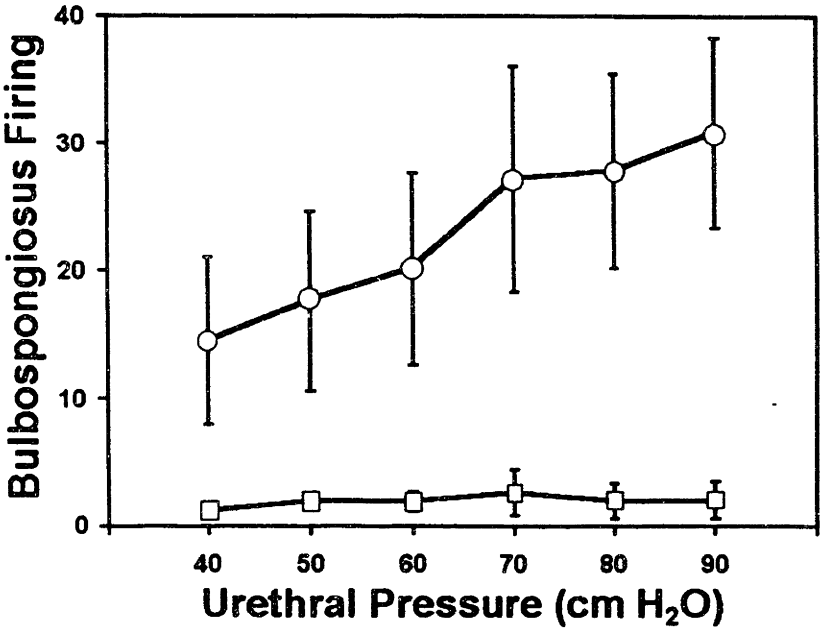
Bulbospongiosus Firing
40
30
20
10
0
40
50
60
70
80
90
Urethral Pressure (cm H2O)

Chapter 7

Perspectives

The findings detailed in the preceding chapters describe my attempts to define roles that Hmox isoforms have in significant mammalian physiological phenomena. Yet, although the genetic approach is often the favored one, there remain additional experiments necessary to solidify inferences made from these studies. I conclude my thesis paper by giving current perspectives of how Hmox isoforms may be involved in each of the physiological systems addressed in the results chapters, namely development, hippocampal LTP, peripheral systems such as intestinal relaxation and the ejaculatory reflex, adult iron metabolism, and cellular antioxidant defense.

Before the availability of mice deficient in Hmox isoforms, the developmental contributions of these enzymes had been unknown. Work described in Chapter 3 indicates that Hmox1 is indeed essential for normal development; however, its exact role remains elusive. Placental defects are observed in *Hmox1*$^{-/-}$ fetuses, and by altering the strain of the maternal placental contribution, *Hmox1*$^{-/-}$ pup survival is enhanced. Therefore, it would appear that Hmox1 is important for placental growth and function. To confirm that developmental requirements of Hmox1 are limited to the placenta, these observations could be furthered by testing the survival of aggregate chimeras of *Hmox1*$^{-/-}$ blastomeres with *Hmox1*$^{+/+}$ tetraploid blastomeres. Since tetraploid cells only contribute to extraembryonic tissues (1), increased survival rates of these aggregation chimeras versus unmanipulated *Hmox1*$^{-/-}$ embryos would indicate that Hmox1 is required in the extraembryonic tissues and not the embryo proper. A supplemental test of *Hmox1*$^{-/-}$ placental function examines maternal substance delivery to *Hmox1*$^{-/-}$ pups. It would be especially interesting to study iron transfer through *Hmox1*$^{-/-}$ placentas, as studied in mice with X-linked anemia (*sla*) (2, 3). Since it has been proposed that fetal iron is partially derived from maternal hemoglobin (4, 5), Hmox1 might be important for supplying iron to the fetus. However, in unpublished experiments not reported in Chapter 3, iron-supplemented or -deficient diets given to gravid *Hmox1*$^{+/-}$ mothers did not affect survival of *Hmox1*$^{-/-}$ pups.

Although the Hmox2 isoform is dispensible for development, the finding that mice lacking both Hmox1 and Hmox2 gene products die at mid-gestation with complete

penetrance suggests that Hmox1 and Hmox2 carry out similar developmental functions, and may compensate for each other. This might suggest that the level of Hmox2 expression in *Hmox1*$^{-/-}$ pups is an important factor determining survival. In any case, examination of doubly mutant early embryos would reveal more clearly the developmental role of Hmox.

The notion that CO acts as a neurotransmitter was abandoned by many neurobiologists in the midst of my thesis projects. Results described in Chapter 2 indicate that LTP is normal in Hmox2-deficient mice and that CO likely does not participate therein. This finding along with work by others have discouraged the use of pharmacology in studying putative functions of Hmox in systems such as LTP (6). Recently, however, strong evidence was demonstrated indicating that a retrograde message may indeed contribute to LTP. In these studies, it was shown that LTP was reduced in mice lacking both the neuronal and endothelial Nos isoforms, and that NO synthesized postsynaptically is required in the presynaptic terminal for LTP in hippocampal neuronal cultures (7, 8). In these ways, the major requirements of a retrograde messenger are fulfilled by NO.

Although LTP appears to rely on NO, but not CO, Chapters 5 and 6 of this thesis are truly supportive of peripheral roles for CO. Both intestinal cGMP generation and neuronal-stimulated relaxation were defective in *Hmox2*$^{-/-}$ animals, while male Hmox2-deficient mice had hypoactive sexual behavior linked to aberrant ejaculatory reflexes. Still, the involvement of Hmox-generated CO in these systems needs to be more closely scrutinized. An important approach will be to combine the use of *Hmox2*$^{-/-}$ mice with "caged CO", or CO that is maintained in a nonreactive complex until being released by UV illumination (9). With these reagents, physiological concentrations of CO may be applied in a tightly controlled manner to cells lacking Hmox2, for a reasonably direct test of whether the defects in *Hmox2*$^{-/-}$ systems originate from reductions in CO generation. Furthermore, it will be important to get a better understanding of CO production in mammalian tissues. In work not reported here, I analyzed CO production from as little as 10 mg of intact cerebral tissue by gas chromatography. No effects of glutamate analogs on CO production in murine cerebral tissue were noted, but I did observe a tremendous influence of pH on CO generation (K. D. P. and H. J. Vreman, unpublished data). This ability to measure minute quantities of CO should be helpful in determining whether CO generation is actually affected by synaptic activity, an observation that is essential to the idea that CO is a neuromodulator.

Chapter 3 describes how Hmox1-deficient mice have excess storage iron in liver and kidneys, along with reduced accessible iron in blood. These symptoms are unusual

among mouse mutants, and suggest that Hmox1 is important for taking iron from heme and releasing it into the extracellular space, while other pathways mainly shuttle heme iron to ferritin (see Fig. 1). Because iron metabolism is normal in mice lacking Hmox2, issues that should be addressed are why Hmox2 is dispensable for iron reutilization, and what accounts for this functional difference between the Hmox isoforms. Additional studies in the future should focus on the pathway of iron within cells. Specifically, through what cellular compartments and molecular players does iron move in its journey from heme to Hmox to the extracellular space? Furthermore, the *Hmox1*$^{-/-}$ mice might be useful for the study of the regulation of iron absorption. It is difficult to predict whether intestinal iron absorption will be normal, reduced, or enhanced in these mutant mice. By comparison with other murine iron metabolism mutants demonstrating either iron deficiency or increased storage, it will be possible to deduce whether levels of storage iron or levels of accessible iron have the greater effect on homeostatic mechanisms of absorption. Notwithstanding, the *Hmox1*$^{-/-}$ phenotypes would be best attributed to a recycling defect if labeled iron were followed in the mutant animals and shown to accumulate in liver and kidneys.

The field of iron metabolism has in fact had some extremely important findings during the tenure of my thesis work. A recent study indicated that a mutation in an HLA-type gene is responsible for hereditary hemochromatosis (10). Further links of iron metabolism with the immune system arose when it was shown that mice deficient in β_2-microglobulin display iron-loading (11). Finally, a putative iron transporter was cloned in mice via refined mapping of the mutation responsible for microcytic anemia (*mk*), and by expression-cloning studies in *Xenopus* oocytes (12, 13). This protein, Nramp2, is a homologue of a protein named Nramp1, which controls murine resistance to infection by intracellular parasites (14). Interestingly, Hmox1 is strongly upregulated during inflammation, and constitutes the fourth gene product recently implicated in both immune and iron metabolic mechanisms. In addition to the several models suggested by previous investigators mentioned in Chapter 4, studies described here may point to two novel ideas whereby upregulation of Hmox1 gives stressed cells an adaptive advantage (Fig. 1). First, reduction of cellular iron levels by extrusion of heme iron might lower free radical generative capacity. Secondly, these reductions in iron during infection might decrease intracellular pathogenesis by limiting bacterial growth. As discussed below, the hypersensitivity of Hmox1-deficient cells to oxidants is consistent with the first idea; however, whether Hmox1-deficient cells such as macrophages are defective in bacteriocidal activity remains to be examined.

The research described in Chapter 4 gives genetic evidence that upregulation of Hmox1 is important for cellular protection against oxidative damage during stress. Cells lacking Hmox1 were sensitive to stress induced by direct oxidant challenges to embryonic fibroblasts, or by endotoxic challenges to young adult mice. Endotoxemia in mice is a model for sepsis in humans. That Hmox1 may play a protective role during sepsis has clinical implications, especially because its activity can be easily increased in mammalian organs by addition of drugs such as hemoglobin (15, 16). However, endotoxin has widespread, systemic effects in mammals. To study functions of Hmox1 in "cleaner" stress paradigms, the role of Hmox1 in disease is currently being pursued by using models of other common human disorders. For instance, collaborating investigators plan to administer fatty diets and score atherogenesis in mice lacking Hmox1. Finding sensitivity of Hmox1-deficient vascular tissue would suggest that Hmox1 has a protective role against the formation of atherosclerosis. Furthermore, another group will examine the effects of cerebral ischemia in *Hmox1*$^{-/-}$ mice, while others will examine the effects of rhabdomyolysis, hypoxia, and hyperoxia on mutant tissues. These experimental conditions all model frequent human disorders, and all result in local increases in Hmox1 expression. Whether Hmox1 has important roles in protecting against oxidative damage during these diseases can be assessed in *Hmox1*$^{-/-}$ mice, given that paradigms are implemented before characteristic mutant iron metabolic symptoms arise.

In conclusion, I point out that analyses of Hmox-deficient mice must be considered differently than those of mice lacking a given receptor or ligand. The former lack metabolic enzymes that normally carry out a ubiquitious biochemical reaction: the depletion of heme to yield CO, iron, and biliverdin. Therefore, metabolism of four potentially influential and potentially toxic biomolecules is disturbed in virtually all cell types. In this way, Hmox-deficient mice can be valuable reagents for the study of a variety of mammalian systems; however, it is implicit that a high level of precaution must be taken in interpreting results of their analysis.

References

1. Kubiak, J. Z. & Tarkowski, A. K. (1985). *Exp. Cell. Res.* **157**, 561-566.
2. Bannerman, R. M. (1976). *Fed. Proc.* **35**, 2281-2285.
3. Kingston, P. J., Bannerman, C. E. & Bannerman, R. M. (1978). *Br. J. Haematol.* **40**, 265-276.
4. Dumartin, B. & Canivenc, R. (1992). *Anat. Embryol.* **185**, 175-179.
5. Kaufman, M. H. (1992) in *The Atlas of Mouse Development*, (Academic Press Limited, Cambridge), pp. 469-477.
6. Meffert, M. K., Haley, J. E., Schuman, E. M., Schulman, H. & Madison, D. V. (1994). *Neuron* **13**, 1225-1233.
7. Son, H., Hawkins, R. D., Martin, K., Kiebler, M., Huang, P. L., Fishman, M. C. & Kandel, E. R. (1996). *Cell* **87**, 1015-1123.
8. Arancio, O., Kiebler, M., Lee, C. J., Lev-Ram, V., Tsien, R. Y., Kandel, E. R. & Hawkins, R. D. (1996). *Cell* **87**, 1025-1035.
9. Lev-Ram, V., Makings, L. R., Keitz, P. F., Kao, J. P. & Tsien, R. Y. (1995). *Neuron* **15**, 407-415.
10. Feder, J. N., Gnirke, A., Thomas, W., Tsuchihashi, Z., Ruddy, D. A. et al. (1996). *Nature Genet.* **13**, 399-408.
11. Rothenberg, B. E. & Voland, J. R. (1996). *Proc. Natl. Acad. Sci. USA* **93**, 1529-1534.
12. Fleming, M. D., Trenor, C. C., Su, M. A., Foernzler, D., Beier, D. R., Dietrich, W. D. & Andrews, N. C. (1997). *Nature Genet.* **16**, 383-386.
13. Gunshin, H., Mackenzie, B., Berger, U. V., Gunshin, Y., Romero, M. R., Boron, W. F., Nussberger, S., Gollan, J. L., Hediger, M. A. (1997). *Nature* **388**, 482-488.
14. Vidal, S. M., Malo, D., Vogan, K., Skamene, E. & Gros, P. (1993). *Cell* **73**, 469-485.
15. Otterbein, L., Sylvester, S. L. & Choi, A. M. (1995). *Am. J. Respir. Cell. Mol. Biol.* **13**, 595-601.
16. Nath, K. A., Balla, G., Vercellotti, G. M., Balla, J., Jacob, H. S., Levitt, M. D., & Rosenberg, M. E. (1992). *J. Clin. Invest.* **90**, 267-270.

Fig. 1. Hypothetical scheme for functions of Hmox1 in normal iron metabolism and in the stress response within hepatocytes or macrophages. Heme is synthesized within the cell or is taken up by the cell. Here, Hmox1 primarily releases iron from heme to the extracellular space, while a Hmox1-independent pathway catalyzed by hypothetical enzyme X mainly retains iron within the cell, stored in ferritin. Under normal conditions, these pathways are balanced. During stress or inflammation, Hmox1 is upregulated and the equilibrium is shifted so that iron from heme is predominantly shuttled out of the cell. This might reduce iron-catalyzed free radical generation, or it might thwart hemophilic bacteria. In cells from Hmox1-deficient mice, equilibrium is shifted so that enzyme X predominates and less heme iron is released; rather, iron stores accumulate, leading to oxidative damage and hypersusceptibility to oxidative challenges. Cells from mice lacking Hmox1 may even be unusually vulnerable to infection, although this remains to be determined.

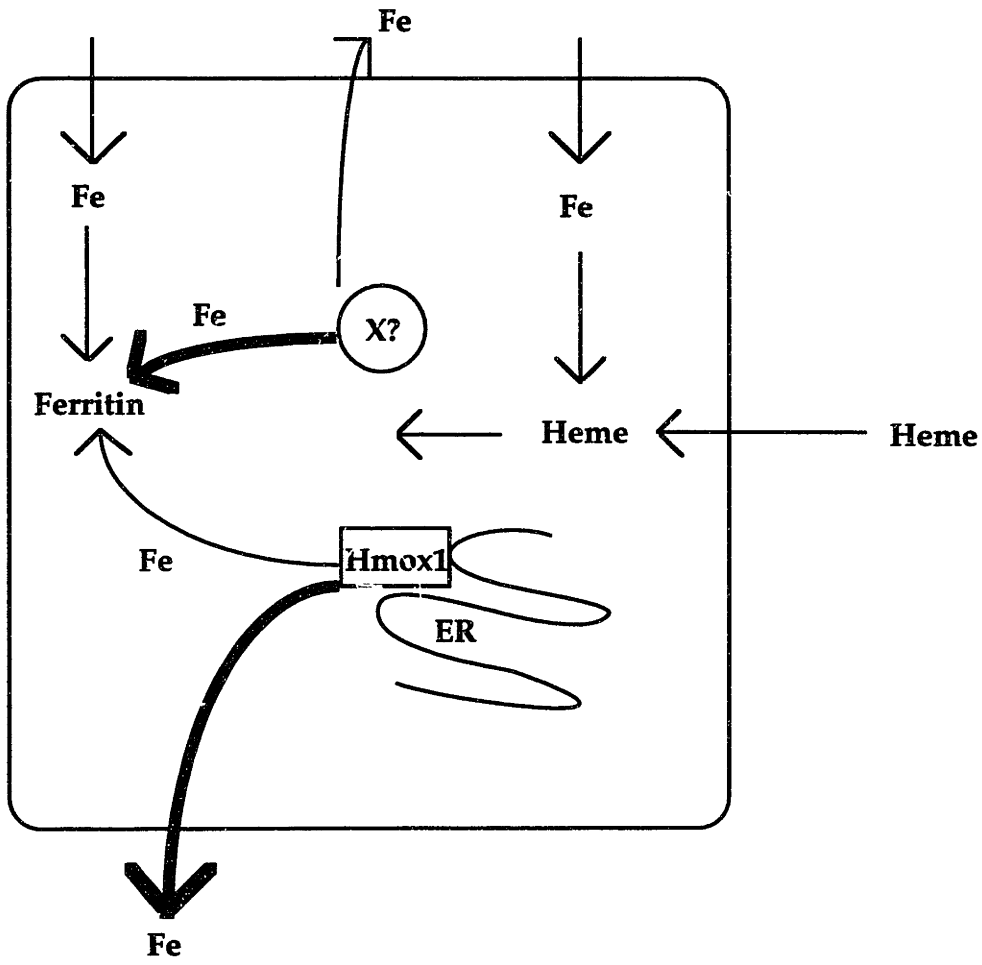

	Effects on Fe dissociated from heme	
	Stored Fe	**Released Fe**
Normal conditions:		
Hmox1 activity = enzyme X activity	**normal**	**normal**
Stress or infection:		
Hmox1 activity > enzyme X activity	**low**	**normal or high**
***Hmox1*$^{-/-}$ cells:**		
enzyme X >> Hmox1 activity	**high**	**low**

THESIS PROCESSING SLIP

FIXED FIELD: ill. _____ name _____

index _____ biblio _____

▶ **COPIES:** (Archives) Aero Dewey Eng Hum

Lindgren Music Rotch (Science)

TITLE VARIES: ▶ ☐ _____

_____

_____

NAME VARIES: ▶ ☑ See degree book

_____

IMPRINT: (COPYRIGHT) _____

_____

▶ **COLLATION:** 139 l

_____

▶ **ADD: DEGREE:** _____ ▶ **DEPT.:** _____

SUPERVISORS: _____

_____

_____ _____ _____

_____ _____ _____

_____ _____ _____

_____ _____ _____

_____ _____ _____

_____ _____ _____

_____ _____ _____

NOTES:

cat'r: date:

page:

▶ **DEPT:** Biol ▶ F66

▶ **YEAR:** _____ ▶ **DEGREE:** Ph.D.

▶ **NAME:** POSS Kenneth D.

_____